Post-Transcriptional Regulatory Mechanisms in the Control of Cell Identity

Post-transcriptional Regulatory Mechanisms in the Control of Cell Identity

A dissertation presented

by

Kaloyan M. Tsanov

to

The Division of Medical Sciences

in partial fulfillment of the requirements

for the degree of

Doctor of Philosophy

in the subject of

Biological and Biomedical Sciences

Harvard University

Cambridge, Massachusetts

April 2017

Dissertation Advisor: Professor George Q. Daley Kaloyan M. Tsanov

Post-transcriptional Regulatory Mechanisms in the Control of Cell Identity

Abstract

Cell identity is shaped by complex gene expression programs, at the core of which lies the set of messenger RNAs (mRNAs) expressed in a given cell. While there is considerable knowledge about the involvement of mRNA transcription in cell fate control, the role of post-transcriptional mechanisms – which are governed by various RNA-binding proteins (RBPs) – is less well understood. By focusing on specific RBPs, the stem cell factor LIN28 and the terminal uridylyltransferases (TUTases) ZCCHC6/11, this dissertation explores novel post-transcriptional regulatory mechanisms that contribute to the control of cell identity.

Chapter 2 addresses the question of how signaling and post-transcriptional regulation are integrated to influence cell fate. In particular, we investigated the role of LIN28 phosphorylation in pluripotent stem cells (PSCs). We found that MAPK/ERK, a central signaling regulator of pluripotency, phosphorylates LIN28 to increase its protein stability and thereby enhance LIN28's translational regulation of its mRNA targets, which contributes to the control of pluripotency transitions. These findings establish a novel link between extracellular cues, mRNA translation, and cell fate regulation.

Chapter 3 examines the role of ZCCHC6/11-mediated mRNA uridylation, a recently appreciated mechanism for promoting global mRNA decay, in the control of cell identity. In particular, we explored the functions of these TUTases in cancer cells, PSCs and muscle progenitors. We found that ZCCHC6/11 contribute to oncogenic transformation and support the growth and tumorigenicity of cancer cell lines. Mechanistically, these effects were associated

with altered mRNA uridylation and turnover, including dysregulation of cell cycle factors and concomitant cell cycle impairment. Interestingly, we also report that ZCCHC6/11 promote a less differentiated cell state in both PSCs and lineage-restricted muscle progenitors. Our results reveal novel functions for ZCCHC6/11 and implicate uridylation-mediated mRNA turnover as a mechanism of oncogenesis.

Collectively, our work uncovers new post-transcriptional regulatory mechanisms in the control of cell identity, with implications for stem cell and cancer biology.

TABLE OF CONTENTS

ACKNOWLEDGEMENTS

The work presented in this dissertation – and my graduate school journey in general – would have been impossible without the help of many people.

First of all, I am profoundly grateful to my advisor, Prof. George Q. Daley, for his unwavering generosity and support throughout my graduate training. I cannot thank him enough for giving me the opportunity to pursue questions that I find interesting, believing in my ability to lead projects stemming from these questions, and, most importantly, the freedom to fail and learn from my mistakes. This is a rare privilege for a graduate student, which I deeply appreciate. George has taught me invaluable lessons, some of which I did not even anticipate learning in graduate school: about science, people, mentoring, and even karaoke and good wine. His infectious enthusiasm, broad engagement in science, and vigorous passion for life are extraordinary and inspiring.

In addition, I am greatly thankful to Dan Pearson, who has become not only my lab partner-in-crime but also a close and trusted friend. Dan's scientific rigor, drive for self-improvement, and love of protein bars have all been inspiring and, in the latter case, essential to survival during late nights in the lab. His patient and consistent support, in and out of the lab, has made a great difference in my life and I feel fortunate to have met him in graduate school.

I am also truly grateful to John Powers for his mentorship and friendship. John's out-of-the-box scientific thinking, contagious positivity, and exceptional interpersonal skills have all been a source of inspiration. From brainstorming experiments to talking politics over tacos, it has been a genuine pleasure to interact with him and learn from him.

I also want to thank Yu-Chung "Harry" Huang, whom I have had the pleasure to mentor and work with as he has become an integral part of our "Team TUT." His patience and persistence are matched only by his kindness, and I am very grateful for his contributions and friendship. Additionally, I have had the privilege to mentor a number of other students and technicians, who not only helped my research but also taught me so much about mentorship. To Jess Barragan, Asher Bohmer, Grace LaPier, Wei-Ting Ng and Marc Seligson: thank you all.

Furthermore, I am thankful to the whole Daley Lab for their support and friendship over the years. Special thanks to the “Lin28 sub-group,” which attracted me to the lab and has remained an important core of support: from early members Shyh-Chang Ng, Hao Zhu, Sutheera “Mam” Ratanasirintrawoot, Zhaoting Wu and Yvanka de Soysa to more recent ones Pavlos Missios, Jihan Osborne, Areum Han, Ho-Chou Tu and Alena Yermalovich. Many thanks also to Mike Morse, Beth Kaleta, Aimee Dixon, Kathryn Entner, Judit Totth, Patricia Sousa and Sam Ross for keeping the lab running, and to Willy Lensch, Marcella Cesana, Sergei Doulatov, Linda Vo, Deepak Jha, Sam Morris, Anne Cherry, Patrick Cahan and everyone else for their camaraderie.

I also wish to deeply thank my Dissertation Advisory Committee, Profs. Gary Ruvkun, Phil Sharp, Lew Cantley and Chris T. Walsh, for their invaluable guidance and support throughout my graduate training. In addition, I have greatly benefited from the advice and contributions of a number of collaborators from other labs, whom I highly appreciate: Steve Gygi, Robinson Triboulet, Richard Gregory, Lorena Pantano, Oliver Hofmann, Matt Jones and Dónal O’Carroll. For creating a wonderful community and funding my studies, my special thanks also go to the BBS and LHB Programs, and the Herchel Smith and HHMI Fellowships. And a big “thank you” to Trista North for critically reading the draft versions of this dissertation.

In one way or another, many people outside of the lab have also contributed to the completion of this dissertation. I am truly grateful to my classmates, roommates and college friends, who all provided critical moral support and distractions from research when they were needed, especially Stéphane Ricoult, Laura Smith, Niroshi Senaratne, Mary Haas and all the BBStars, Curtis Chan, Iain Kaplan, Julian De Freitas, Patricia Pepper, Toma Halkina, Patricia Machado, Tony Chiu, Francisco Martinez, Paula Popescu and Ayfer Ali.

Last but definitely not least, I wish to thank my family. The older I get, the more I realize how difficult it must have been for them to let me go thousands of miles away from home to pursue my dreams. I am forever indebted to my parents and sister for their unconditional love and support, which are behind everything I have achieved.

LIST OF FIGURES

CHAPTER 1

Background

1.1. Cell Identity in Development and Cancer: A Historical Perspective.

Embryonic development, stem cells and pluripotency

In 1665, Robert Hooke made the groundbreaking observation that organisms are comprised of smaller building blocks he termed “cells” [2]. Over 350 years later, we know that the adult human organism contains more than 200 different types of cells with specialized functions [3], all of which originate from a single cell – the zygote. But how does this single cell give rise to a myriad of specialized cell types?

As a framework for understanding this question, McCulloch and Till proposed the model of developmental hierarchies of cells [4, 5]. In these hierarchies, a powerful type of cell – called a stem cell – sits on top, as it can produce an offspring of increasingly specialized cell types. The stem cell is characterized by two unique properties: the ability to self-renew and the capacity, through the process of differentiation, to form more specialized cell types. Depending on its differentiation capacity, also known as potency, a stem cell can be further defined as uni- or oligopotent (able to produce one or a few specialized cell types), multipotent (able to produce many specialized cell types), or pluripotent (able to produce all adult cell types).

As the zygote develops into a blastocyst, it gives rise to two lineages: the inner cell mass (ICM), which harbors the founder pluripotent stem cell (PSC) population, and the trophectoderm, which forms an epithelial layer that surrounds and supports the ICM [6]. At the late epiblast stage (embryonic day 3.5-4.5 [E3.5-4.5] in the mouse), the ICM segregates into epiblast and hypoblast (primitive endoderm) lineages. Each epiblast cell is capable of generating all embryonic lineages and therefore constitutes a developmentally “naïve” state of pluripotency (Figure 1.1). As development proceeds (mouse E4.5 to E6.5), naïve epiblast cells transition to a “primed” state of pluripotency, which is bound to initiate lineage-specification programs and ultimately yield the many specialized cells of the adult organism [7]. Therefore, the switch from the naïve to the primed pluripotent state represents one of the earliest and most fundamental cell fate transitions during embryogenesis.

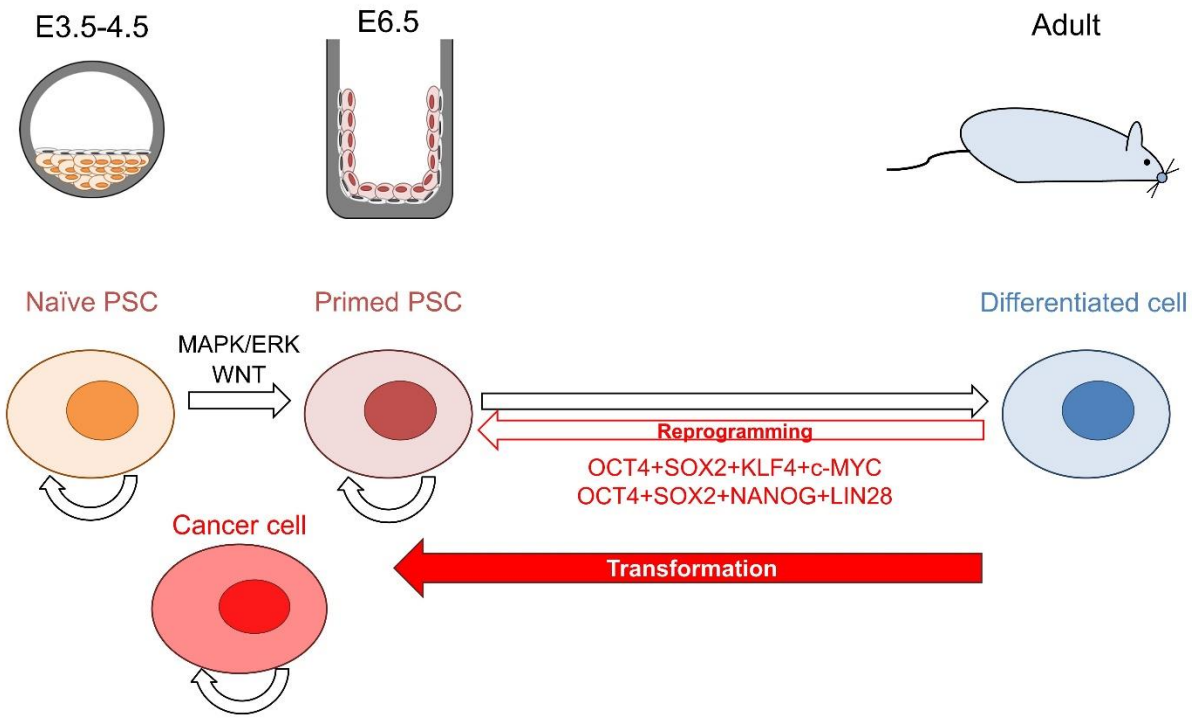

Figure 1.1. Cell identity transitions in development and cancer. During embryogenesis, naïve PSCs become primed upon stimulation by MAPK/ERK and WNT signaling, and can then take different paths to ultimately acquire various differentiated cell identities. Schematic on top indicates the corresponding stages during mouse development. In somatic cell reprogramming, overexpression of four pluripotency factors (two commonly used cocktails are shown) is sufficient to revert a differentiated cell back to pluripotency. In oncogenic transformation, these and other genes and signaling pathways involved in embryogenesis are often aberrantly activated to transform a normal cell into a cancer cell, highlighting the molecular commonalities between development and oncogenesis. Curved arrows designate self-renewal and straight arrows represent cell fate transitions.

Given that these processes occur on a rapid time scale *in vivo*, the ability to capture and propagate the pluripotent state in the dish was critical to the study of pluripotency. In 1981, Evans and Martin derived PSC lines directly from mouse blastocysts and could maintain these mouse embryonic stem cells (mESCs) *in vitro* without losing their hallmark properties of self-renewal and pluripotent differentiation potential [8, 9]. Subsequent studies improved mESC culture conditions, identifying critical factors that regulate the balance between self-renewal and differentiation. In 1988, one such factor, the cytokine leukemia inhibitory factor (LIF), was identified as a key differentiation inhibitor and became part of routine mESC culture [10, 11]. Further work revealed that the principal mESC differentiation trigger is fibroblast growth factor (FGF), which activates

the mitogen-activated protein kinase/extracellular signal-regulated kinase (MAPK/ERK) pathway [12]. A similar role was discovered for glycogen synthase kinase 3 (GSK3), a core member of the WNT/β-catenin pathway [13, 14]. These findings led to the development of a new chemically defined culture protocol, which combined selective inhibitors of MEK/ERK and GSK3, PD0325901 and CH99021 respectively [15]. These two-inhibitor ("2i") conditions enabled for the first time the robust maintenance of naïve mESCs, thereby allowing for deeper mechanistic interrogation of this distinct pluripotent state and the critical decision to transition from naïve to primed pluripotency [16-18].

Dedifferentiation, stem cells and cancer

As naïve PSCs become primed and proceed through later differentiation steps, their developmental potency becomes increasingly restricted. This is not because the more specialized cells harbor different sets of genes but instead because they selectively express some of these same genes, in accordance with the dedicated function of a given cell type. This "nuclear equivalence" concept was demonstrated through the seminal work of Spemann, Briggs and King, and Gurdon, who ultimately showed that a nucleus from a fully differentiated cell was capable of sustaining the complete development of an adult organism [19-21]. These studies also indicated that the progressive restriction of cell identity is reversible through a process of "dedifferentiation." However, the nature of the instructive cues that drive dedifferentiation remained enigmatic until Takahashi and Yamanaka found that the ectopic expression of only four pluripotency-associated genes – *Oct4*, *Sox2*, *Klf4*, and *c-Myc* – was sufficient to reprogram mouse fibroblasts back to the pluripotent state [22] (Figure 1.1). A year later, the same cocktail of factors [23, 24], as well as a different version featuring *NANOG* and *LIN28* [25], was shown to similarly reprogram human cells.

The identity of the reprogramming factors, all of which have been implicated in cancer [26], also revived a century-old idea: that dedifferentiation and oncogenesis share common mechanisms [27]. Indeed, early work on tumors called teratocarcinomas revealed that they

contain a mixture of adult tissue types, as if representing a caricature of normal development [6, 28-31]. German pathologist Rudolf Virchow further noted that teratocarcinomas contain embryonic-like tissue [32], which led Durante and Cohnheim to propose the “embryonal rest theory” of cancer [33, 34]. According to this theory, cancers arise from remnants of embryonic tissue present in the adult body, which normally lie dormant but could be reactivated upon certain environmental changes [35]. Ribbert revised the theory to include the possibility that these embryonic cells could originate from dedifferentiated adult cells [36], a mechanism that Virchow himself had suggested [32]. In a similar vein, David von Hansemann, a mentee of Cohnheim and Virchow, described the theory of “anaplasia” (from Greek, *ana* [backward] + *plasis* [formation]), which stipulated that cancer cells exhibit loss of differentiation [37, 38].

The embryonic and dedifferentiation theories – with further updates and revisions – have remained the major models for the developmental origin of cancer ever since. In the 1950s, teratocarcinomas were shown to contain PSCs called embryonal carcinoma cells (ECCs) [39-42], which led to the proposal that cancers are fueled by stem cells that have undergone a maturation arrest [43-46]. This concept was further supported by work on leukemia, which ultimately demonstrated that a rare subpopulation of cancer cells could self-renew and propagate the tumor [47-53]. These findings stimulated the development of a “cancer stem cell” (CSC) model, which can be seen as the modern-day version of the developmental theories of cancer [54, 55].

At the same time, the concurrent revolution in cancer genetics led to the proposal that tumorigenesis is driven by the stepwise acquisition of mutations in “proto-oncogenes” and “tumor-suppressor genes,” and their Darwinian natural selection [56-59]. In 1990, Fearon and Vogelstein documented the step-wise acquisition of specific mutations during colorectal cancer progression, thus providing molecular genetic evidence for this evolutionary model [60]. The advent of powerful genomics tools has since enabled global interrogation of cancer-associated mutations, which has offered ample support for the complex Darwinian nature of tumorigenesis [61, 62]. Importantly, this evolutionary model yields a system of heterogeneous clonal populations that differs from the

hierarchically structured scenario described by the CSC model, thus providing an alternative theory for the cellular origin and progression of cancer. Because of this key difference, the clonal evolution and the CSC models are commonly seen as mutually exclusive and have generated much controversy and debate as to whether different tumors follow one model or the other, or a hybrid version [54, 55, 63, 64].

Molecular commonalities of stem cells and cancer cells

Regardless of which model more accurately explains a given cancer type, there is an observation that holds true for a majority of tumors: because of their capacity for indefinite self-renewal, cancer cells appear to often hijack molecular mechanisms normally employed by stem cells during embryonic development [65] (Figure 1.1). As noted earlier, all of the Yamanaka factors have been implicated in oncogenesis [26, 66-71]. In addition, the major signaling pathways governing pluripotency, including MAPK/ERK and WNT, are commonly subjected to aberrant activation in cancer through epigenetic or genetic lesions affecting key pathway members [72]. Likewise, pathways acting during later developmental stages or operative in tissue stem cells are often co-opted by cancer cells, with excellent examples being WNT, Hedgehog and Notch signaling [73-75]. Of note, all of the above genes and pathways have been implicated in the regulation of CSCs, further highlighting the shared mechanisms between normal stem cells and their malignant counterparts [76].

Thus, the “cancer state” can be seen a distinct cell identity – or rather a set of identities – much like those arising during the normal process of embryonic development. The striking parallels between oncogenesis and embryogenesis indicate that stem cells and cancer share common molecular mechanisms. Elucidating these mechanisms is thus of paramount importance to solving the fundamental puzzle of cell identity acquisition and maintenance, with implications for regenerative and cancer therapies alike. This dissertation explores a particular class of

molecular mechanisms – post-transcriptional regulation – which has emerged as a central player in cell fate control but remains poorly understood, as discussed next.

1.2. Post-transcriptional Control of Cell Identity.

Post-transcriptional regulation and RNA-binding proteins

In 1958, Francis Crick hypothesized that DNA encodes the information for protein production and proposed the existence of an RNA intermediate between DNA and protein [77]. This idea, which he termed “the Central Dogma” of molecular biology, was soon experimentally proven and the intermediate was appropriately named “messenger RNA” (mRNA) [78]. In the decades since, we have learned that, rather than being simple templates for protein synthesis, mRNAs have complex lives involving multiple events following their “birth” via transcription [79] (Figure 1.2). Each of these post-transcriptional events is subject to tight regulation, which can ultimately affect when, where and how much protein is synthesized from a given mRNA, thus constituting an essential layer of gene regulation.

At the core of post-transcriptional mechanisms are numerous RNA-binding proteins (RBPs), which control the various steps in mRNA’s complex life cycles, from their maturation through their degradation [80, 81] (Figure 1.2). RBPs account for ~7.5% of the coding genome, or an estimated 1,500 genes, highlighting their extensive functional relevance and diverse regulatory roles [80]. They can protect or expose mRNAs to the influence of other proteins or RNAs, sequester or recruit mRNAs to specific complexes or locations, and even alter mRNA composition or structure. Through these functions, RBPs facilitate the generation of cell fate diversity from similar primary transcriptomes, enforce transcriptional programs that maintain a given cell identity, and guide the timely transitions between different cell fates [82].

Indeed, RBP-governed post-transcriptional mechanisms dominate the earliest steps of embryogenesis, when transcription of the zygotic genome has not yet commenced [83, 84]. They are also instrumental to the control of pluripotency [85] and in guiding later stages of development

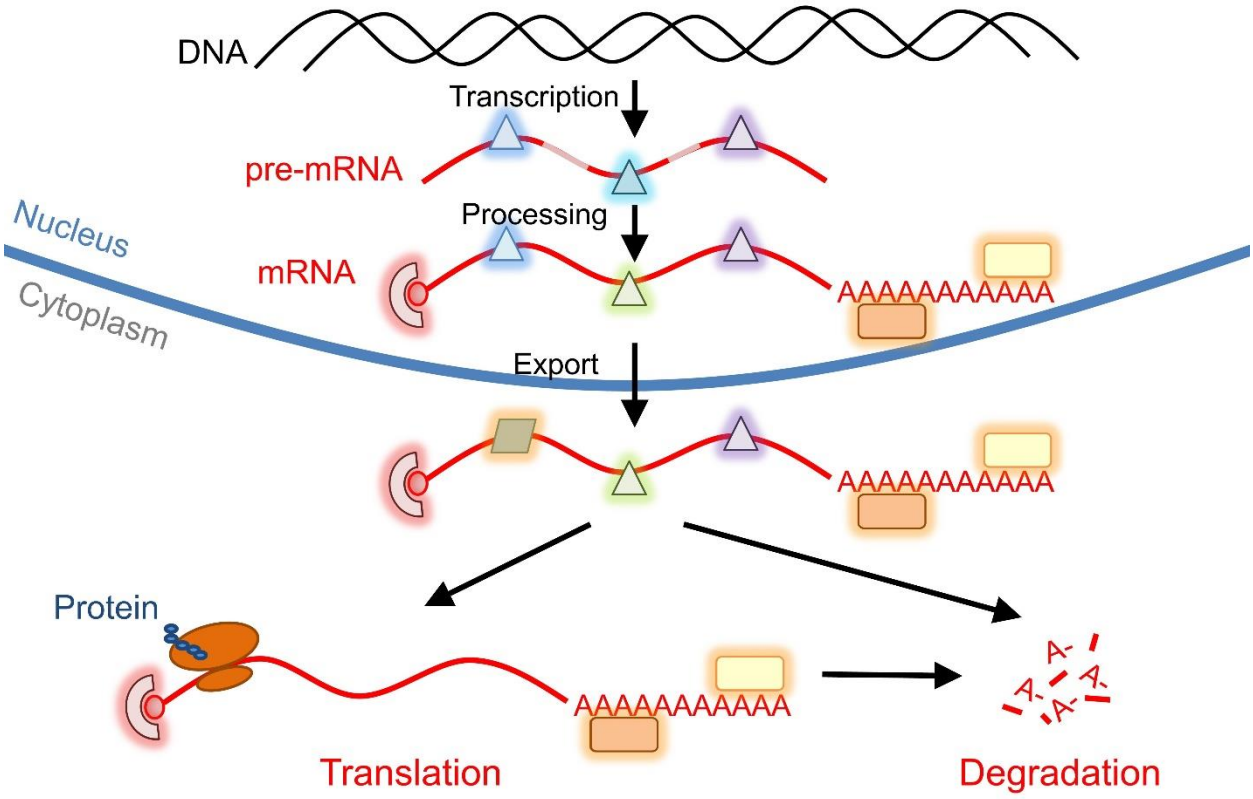

Figure 1.2. The mRNA life cycle. After their transcription, mRNAs commonly undergo nuclear processing, export, translation and degradation (the last two being the focus of this dissertation). The variously colored shapes designate the many RBPs that associate with mRNAs and govern their regulation.

[86]. Similarly, oncogenesis relies heavily on post-transcriptional mechanisms, whose dysregulation promotes tumor initiation and progression [87]. The significant impact of these mechanisms is highlighted by the reported poor correlation between mRNA and protein abundance in global integrative analyses of differentiating ESCs [88, 89], somatic cells undergoing reprogramming [90], and proliferating cancer cell lines [91-93], which – save for protein stability changes – can only be explained through post-transcriptional regulation.

In the following sections, we review three major post-transcriptional events with particular relevance to the work presented herein: mRNA translation, mRNA decay, and microRNA (miRNA) regulation. As these processes are at the end of the mRNA life cycle (Figure 1.2), they provide critical last opportunities for gene regulation and are therefore under the intricate control of

complex RBP machineries. We specifically highlight key RBPs that have been implicated in the control of normal development and cancer.

mRNA translation in the control of cell identity

Translation involves the recruitment of mRNAs to ribosomes, which catalyze the linking of amino acids to form a protein based on the sequence of the mRNA template. An actively translated mRNA typically associates with multiple ribosomes to form so-called “polysomes” [94]. Translation includes three phases – initiation, elongation and termination – of which initiation is the main point of regulation [95]. For most mRNAs, their 5’-end “cap” binds initiation factors that recruit the ribosome. These factors include eIF4E, eIF4A and eIF4G, with eIF4G being the protein that interacts with a pre-initiation complex comprised of the small (40S) ribosomal subunit, the initiator transfer RNA, and additional initiation factors (eIF1, 1A, 2, 3 and 5) [96]. The 3’-end poly(A) tail of the mRNA also plays an important role, as poly(A)-binding protein (PABP) binds eIF4G to further facilitate ribosome recruitment [96]. Once this complex is formed, the 40S subunit scans the mRNA sequence 5’ to 3’ until it locates an initiation codon. Then, the large (60S) ribosome subunit is recruited with the aid of an additional initiation factor (eIF5B), and elongation begins.

Multiple mechanisms have been shown to exert control at the initiation step and beyond, which entails the interaction of specific RBPs and mRNA regulatory elements [97]. One group of RBPs includes eIF4E-binding protein (4EBP) and eIF4E-homologous protein (4EHP), which can prevent the formation of the initiation complex and block translation [97-99]. Another involves deadenylases (e.g. CCR4) and poly(A) polymerases (e.g. GLD2), which shorten or lengthen the poly(A) tail to inhibit or enhance translational efficiency, respectively [100]. On the mRNA side, the interaction is mediated via structural and sequence-specific regulatory elements that are commonly found in the 5’ untranslated region (UTR) but also appear in other parts of the mRNA.

They include 5'UTR elements that confer sensitivity to eIF4A, as well as elements across the mRNA sequence that recruit distinct RBPs with positive or negative impact on translation [101].

Translational control plays an essential role in the regulation of cell identity. As mentioned earlier, the initial stages of embryogenesis lack active transcription and are instead driven by the mRNAs deposited by the oocyte, thus relying heavily on translational regulation [102-104]. Global increase in translation is also a hallmark of ESC differentiation [89, 105], as well as tissue stem cell differentiation into more restricted progenitors [106-108]. Similarly, cancer cells almost invariably exhibit enhanced translation [109]. Increase in the size and number of nucleoli, organelles instrumental to ribosome production and thereby translation, has long been recognized as a marker of oncogenic transformation [110, 111]. Initiation factors are overexpressed across various tumors [109], and genetic studies have directly implicated components of the initiation machinery [112-115] and ribosomal proteins [116, 117] in tumorigenesis. Lastly, major oncofetal signaling pathways directly or indirectly impact translation, mainly through the initiation complex. MYC increases eIF4E levels through transcriptional upregulation, the RAS-MAPK pathway hyperactivates eIF4E via phosphorylation, and PI3K-mTOR signaling inactivates 4EBP [101].

While these changes have a global impact on translation, there is a growing appreciation of transcript-specific alterations that affect distinct translational programs [115, 118, 119]. In support of this idea, a number of more specialized RBPs control the translation of distinct mRNAs to shape cell identity. These include several RBPs, such as RBM351, PTBP1, PUM1 and LIN28, which act as positive or negative regulators of pluripotency [85], as well as various RBPs with oncogenic and tumor-suppressive functions [120]. Importantly, some of these RBPs have been implicated in both normal development and oncogenesis, further emphasizing the post-transcriptional regulatory commonalities between these two processes. While some core principles have been established, we are only beginning to unravel these intricate translational regulatory networks and their impact on cell fate control.

mRNA decay in the control of cell identity

mRNA decay fulfills two general functions: to alter the half-life of mRNAs and thereby their protein output, which will be the focus of this discussion, or to eliminate defective mRNAs that would lead to the production of aberrant proteins [121]. mRNAs are normally protected from degradation by their caps, poly(A) tails, and associated proteins. Thus, mRNA decay is typically initiated by poly(A) tail shortening, which is reversible and carried out by the deadenylases PAN2-PAN3, CCR4-NOT and PARN [122]. Then, two irreversible pathways can be followed: (i) the multiprotein complex LSM1-7 binds the 3' end and induces removal of the cap via decapping enzymes DCP1/2, followed by 5'→ 3' decay by the exonuclease XRN1, or (ii) the exosome, a multiprotein complex with exonuclease activity, degrades the mRNA in a 3'→ 5' direction [123, 124]. For some mRNAs, decay can also be initiated by endonuclease-mediated internal cleavage, followed by XRN1- or exosome-mediated degradation [125]. All of these processes occur in dedicated ribonucleoprotein complexes, at least some of which form structures called "processing bodies" (P-bodies) [126].

Akin to translation, mRNA decay is regulated by various RBPs that recognize specific *cis*-regulatory elements in the mRNAs, typically located in the 3'UTRs [122]. Among these RBPs, the most studied family are the AU-rich element (ARE)-binding proteins, which recognize an AUUUA pentameric motif [127]. Prominent examples include AUF1, TTP, CUGBP, KSRP, RHAU and ELAV [122]. With the exception of ELAV proteins, such as HuR and HuD, the rest generally have a destabilizing function through the recruitment of the decay machinery [128-132]. On the other hand, HuR can compete for mRNA binding with several of the above factors, as well as remove mRNAs from P-bodies, thereby inhibiting mRNA decay and leading to mRNA stabilization [133-135]. In addition to these ARE-binding proteins, there is a growing number of other RBPs that control mRNA stability, including GU-rich element-binding proteins (e.g. CELF1), PUF proteins (e.g. PUM1/2), and hnRNPE1/2 proteins, which have been reviewed elsewhere [136-138].

The regulation of mRNA decay has a profound impact on cell identity. Indeed, it has been proposed that developmental gene expression is shaped by an “mRNA degradation code” [139]. Similarly to translation, decay control is critical at the earliest stages of embryogenesis, particularly the maternal-to-zygotic transition when oocyte-provided mRNAs need to be rapidly cleared [84, 140]. Global analyses in pluripotent versus differentiated cells have also revealed differential regulation of mRNA stability and coordinated control of specific mRNAs [141]. A few specific RBPs have been studied in more detail in embryonic development. One group includes the ARE-binding protein BRF1 [142, 143] and the PUF protein PUM1 [144], which promote differentiation through destabilization of pluripotency transcripts. Another group includes TRIM71 [145-147], LARP7 [148], and UNR [149], which destabilize pro-differentiation transcripts and thus promote the pluripotent state. Lineage-restricted cell fate transitions are also governed by mRNA decay pathways, with relevant examples being AUF1, KSRP and HuR in muscle specification [150-152], and ELAV proteins in neurogenesis [153, 154].

Dysregulation of mRNA stability has also been linked to oncogenesis. Tumor initiation and progression are characterized by abnormal overexpression of ARE-containing transcripts for pro-tumorigenic genes, which is often due to aberrations in decay-regulating RBPs [155]. A prominent example is TTP, which is downregulated in a number of tumor types and appears to serve a tumor-suppressive role by promoting degradation of oncogenic transcripts [156]. On the other hand, HuR – a stabilizing factor – is overexpressed and correlates with tumor grade in breast [157], ovarian [158, 159], and colon cancer [160]. And, more recently, TRBP, a protein with canonical functions in the miRNA biogenesis pathway (reviewed in the next section) has been shown to destabilize metastasis-suppressing transcripts in breast cancer cells and thereby promote tumor progression [161].

Finally, major oncofetal signaling pathways, including p38 MAPK, PI3K/AKT, MAPK/ERK and WNT/β-catenin, directly regulate the functions of ARE-binding proteins [150, 162-164], providing another potential link to cell fate control. Likewise, a growing number of RNA modifications that

affect mRNA turnover have been implicated in development and cancer [165, 166]. Together, the above-mentioned examples are beginning to uncover the contribution of mRNA decay to cell identity regulation, yet they only scratch the surface of what is likely a much more extensive regulatory network.

miRNAs in the control of cell identity

Both mRNA translation and mRNA decay are impacted by miRNAs. miRNAs are short non-coding RNAs that bind complementary sequences in the 3'UTRs of mRNAs to silence their expression [167]. miRNAs are synthesized as long primary transcripts (pri-miRNAs), which are trimmed in the nucleus by the Microprocessor complex, comprised of the RNase III enzyme DROSHA and its co-factor DGCR8 [168-171]. A stem-loop structure in the pri-miRNA is cleaved by DROSHA to release a ~60-70-nucleotide hairpin-shaped precursor miRNA (pre-miRNA) [168-170, 172], which is then exported from the nucleus [173-175]. In the cytoplasm, the pre-miRNA is further processed by DICER1, another RNase III enzyme, which cleaves the stem asymmetrically and generate a mature ~22-nucleotide miRNA duplex [176, 177]. DICER1 associates with a co-factor, TRBP, which can alter miRNA processing [178], enhance the fidelity of DICER1 [179], and recruit the Argonaute proteins (AGO1-4) of the miRNA-induced silencing complex (miRISC) [180]. One strand of the miRNA duplex, termed the "guide" strand, is bound by an AGO protein and incorporated in miRISC to guide the complex to the 3'UTRs of mRNA targets [181]. This is achieved through base-pairing between the guide and complementary sequences in the 3'UTR, with nucleotides 2 to 7 of the miRNA (termed the "seed" sequence) forming the critical region for target recognition [167]. miRNAs that share the same seed are grouped into the same family as they target the same pool of mRNAs [167]. Silencing is accomplished by promoting mRNA decay and/or inhibiting mRNA translation [182], typically involving relocation to P-bodies [183, 184]. Through this mechanism, a given miRNA can regulate many mRNAs that contain its cognate recognition site and, due to the presence of several miRNA sites in many 3'UTRs, a given mRNA

can be under the simultaneous control of multiple miRNAs [167]. As the human genome is estimated to encode hundreds of miRNAs [185] and over 60% of protein-coding genes contain miRNA sites in their 3'UTRs [186, 187], these miRNA-mRNA interactions create elaborate networks with an immense regulatory impact.

miRNAs and their associated mechanisms play a central role in the control of cell identity. Originally discovered in *C. elegans* as regulators of developmental timing [188, 189], miRNAs have since been shown to have evolutionarily conserved roles in normal development and stem cell biology [190, 191]. Global loss of miRNAs, achieved by *Dicer1* or *Dgcr8* knockout, disrupts embryogenesis in mice [192-194]. Studies in mESCs have further implicated miRNAs in the regulation of pluripotency, as both *Dicer1* and *Dgcr8* knockout mESCs show decreased proliferation and impaired differentiation capacities [195-197]. Importantly, specific miRNA families have been linked to these phenomena. The *miR-290-295* family, which are the predominant miRNAs in PSCs, promote cell cycle transitions in mESCs and contribute to embryogenesis [198-201]. On the contrary, *let-7* family members are generally the highest expressed miRNAs in somatic tissues and facilitate the switch from self-renewal to differentiation [202, 203]. Consistent with these functions, *miR-290* overexpression or *let-7* inhibition promote reprogramming to pluripotency [203-206]. Further, these and other miRNAs also play important roles during later development and in tissue stem cell homeostasis [207-209].

miRNA dysregulation is also a major player in oncogenesis [210]. Large-scale profiling studies have shown that miRNA expression signatures can classify tumors according to their developmental lineage and differentiation status with remarkable accuracy [211-213], suggesting parallels to development. Additionally, miRNA expression is globally suppressed in tumors relative to normal tissue counterparts [212], and genetic depletion of *DICER1* enhances tumorigenesis in cancer models [214]. Decreased DROSHA and DICER1 levels are seen in a number of cancers and correlate with poor prognosis [215-217]. *DROSHA*, *DGCR8* and *DICER1* mutations have been identified in multiple tumors, further implicating the involvement of aberrant

miRNA regulation [218-224]. In addition, dysregulation of specific miRNA families has been functionally linked to various cancer types, with either oncogenic or tumor-suppressive effects. Among many others [225], the *miR-17~92* family, also known as *oncomiR-1*, are prominent oncogenic miRNAs [226], while *miR-15/16* [227] and *let-7* [228-232] function as tumor-suppressors. At least for *let-7*, this activity mirrors its functions in promoting stem cell differentiation, in a powerful example of the molecular commonalities between embryogenesis and oncogenesis.

Lastly, signaling pathways can also regulate miRNA biogenesis [233]. GSK3β phosphorylates DROSHA to promote its nuclear localization [234, 235], ERK phosphorylates DGCR8 [236] and TRBP [237] to increase their stability, and MAPKAPK2, AKT3, and EGFR phosphorylate AGO with various downstream effects [238-240]. In light of the oncofetal nature of these pathways, these examples further highlight shared molecular mechanisms between development and cancer.

RBPs as lenses into post-transcriptional control

The processes and players described above illustrate the incredible complexity of post-transcriptional mechanisms and their crucial roles in guiding cell identity. While they were presented separately for clarity, there is extensive crosstalk between these regulatory steps [81, 241]. In line with this interconnectedness, an increasing number of RBPs have been found to affect multiple aspects of mRNA metabolism [81, 85]. This extends the originally proposed concept of the “RNA regulon,” where a single RBP regulates many mRNAs through a given functionality [242], by adding a multifunctional dimension [85]. Altogether, the combination of possible mRNA targets and potential regulatory steps creates numerous opportunities for an RBP to exert an extensive level of mRNA control and thereby influence cell identity. Given the large number of RBPs and broad range of cell types that express them, these relationships create intricate post-transcriptional regulatory networks with an essential role in cell fate control, which

has remained largely unexplored. Thus, individual RBPs can serve as powerful lenses for gaining insights into this biology and revealing core regulatory principles. In the remainder of this chapter, we focus on two such RBP families – LIN28 and TUTases – which are the specific focus of this dissertation.

1.3. The LIN28 Pathway: Mechanisms, Functions, and Regulation.

LIN28: Major post-transcriptional regulator of cell identity

In 1984, Ambros and Horvitz reported the results of a genetic screen for regulators of developmental timing – or "heterochronic" genes – in the nematode *C. elegans*, and arranged these regulators in an elegant pathway that governs key cell fate specification events [243-245]. At the center of this heterochronic pathway was the *lin-28* (cell *lin*eage abnormal *28*) gene [246], which was further shown to be an evolutionarily conserved RBP that is highly expressed in embryonic tissues and rapidly downregulated during development [247, 248]. Its mechanism of action remained unclear until several groups found that LIN28 (also referred to as LIN28A) and its paralog LIN28B inhibit the biogenesis of the *let-7* miRNAs [249-252], downstream members of the heterochronic pathway and potent regulators of development, stem cells and cancer [253]. These findings, along with the discoveries that LIN28 can promote the reprogramming of somatic cells to pluripotency [25] and drive oncogenic transformation [254], generated intense interest that has fueled a growing body of research and established the LIN28 pathway as a major post-transcriptional regulator of cell identity. In the following sections, we review molecular mechanisms, cellular- and organismal-level functions, and regulation of the LIN28 pathway, highlighting open questions in the field.

Molecular mechanisms of the LIN28 pathway

The LIN28 proteins are known to directly regulate two classes of RNAs: the *let-7* miRNAs and numerous mRNAs (Figure 1.3). As mentioned above, LIN28A/B block the maturation of *let-7*,

which is achieved at both the DROSHA and DICER processing steps [249-252]. In the nucleus, LIN28B binds the terminal loop of pri-*let-7* to sequester it in the nucleolus away from DROSHA, thereby interfering with its processing [255, 256]. In the cytoplasm, LIN28 binds the terminal loop of pre-*let-7*, which prevents association with DICER [255, 256]. LIN28 also recruits a TUTase, ZCCHC6/TUT7 or ZCCHC11/TUT4, which catalyzes the addition of an oligo(U) tail to the 3' end of pre-*let-7* [257-260] (see section 1.4 for a detailed review of the TUTases). This oligouridylation has two consequences: (i) it makes pre-*let-7* a less favorable substrate for DICER, further inhibiting DICER-mediated processing [257, 259]; and (ii) it serves as a signal for the recruitment of an exonuclease, DIS3L2, which catalyzes the degradation of pre-*let-7*, thereby preventing downstream processing [261, 262]. X-ray crystallography studies have solved the structure of the LIN28::pre-*let-7* complex, confirming an association with the terminal loop of pre-*let-7* at a conserved GGAG motif near the site of DICER cleavage [263, 264]. Consistent with this finding, multiple studies using crosslinking and immunoprecipitation coupled with RNA-sequencing (RNA-seq) have independently retrieved the GGAG sequence as a consensus motif for LIN28 binding [265-268].

These observations suggested a division of labor between LIN28 and LIN28B with reference to the nuclear versus cytoplasmic *let-7* processing steps [255]. This mechanistic difference, coupled with the reported nucleolar versus cytoplasmic localization of LIN28B and LIN28, respectively, was proposed to be a key distinction between the two paralogs [255], but this model has since been challenged. Both LIN28 proteins contain a putative nucleolar localization signal and multiple studies have demonstrated that both paralogs can localize to the nucleolus and cytoplasm [269-274]. Additionally, both LIN28 and LIN28B can bind pri- and pre-*let-7* [249-252, 275, 276], and utilize the TUTase/DIS3L2 pathway to degrade pre-*let-7* [257, 259, 277]. It is thus likely that the two paralogs have similar functions with respect to *let-7*, which has also been

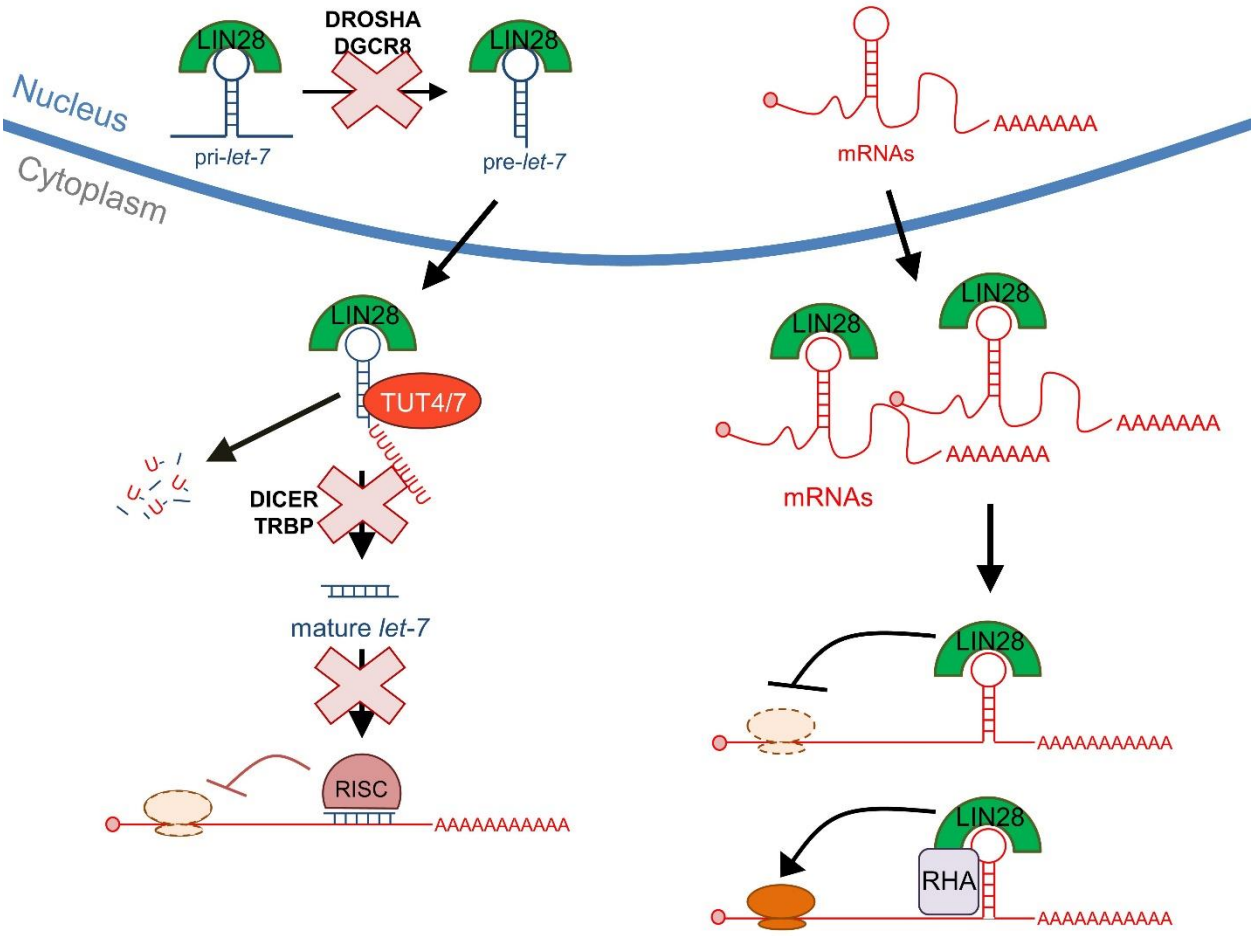

Figure 1.3. The LIN28 pathway. *let-7*- and mRNA-dependent effects are shown. See text for details.

supported by a recent side-by-side comparison of their effects on *let-7* [278]. In any case, the ultimate effect of LIN28A/B activity is depletion of mature *let-7*, which leads to the derepression of *let-7*'s numerous mRNA targets [70]. Of note, a few studies have suggested LIN28-mediated regulation of other miRNAs [279-283], although *let-7* appears to be the functionally dominant miRNA target.

Apart from *let-7*, LIN28 proteins associate with numerous mRNAs to directly modulate their translation (Figure 1.3). One of the earliest mechanistic insights into LIN28 biology was that LIN28 can bind *IGF2* mRNA and enhance its translation by facilitating its recruitment to polysomes [284]. Over the past few years, new methods have enabled transcriptome-wide characterization of LIN28's targets, which has expanded this translational regulatory concept. A number of studies

have reported that LIN28A/B bind mRNAs corresponding to hundreds of genes and estimated that mRNAs are LIN28A/B's predominant physical targets [265, 266, 268, 271, 285]. Consistent with the LIN28::pre-*let-7* interaction, a GGAG sequence has been identified as a common mRNA recognition motif, possibly situated in loop structures [265, 268]. Further analyses have demonstrated altered translation of many mRNA targets and supported the model whereby LIN28 modulates association with polysomes [265, 285-287]. Intriguingly, in some cases the outcome is translational enhancement [268, 271, 285-289], while in others it is the opposite [265, 268, 290].

The molecular determinants underlying these translational effects have remained largely elusive [291]. An exception is an RNA helicase, RHA/DHX9, which has been implicated as a LIN28 co-factor that may promote secondary structure remodeling to facilitate mRNA translatability [286, 287]. It remains to be seen whether this is a widespread mechanism of translational enhancement. Likewise, it is still unknown how LIN28 mediates translational repression. One possibility is that LIN28 promotes mRNA sequestration away from the polysomes, as it is known to localize to P-bodies [269]. At least one study has shown that LIN28 can enhance and suppress different mRNA targets in the same cellular context [268], suggesting that the respective mechanisms may involve formation of distinct protein complexes. In addition, the identity of the mRNA targets has also been controversial. While most studies agree that LIN28 is a translational regulator, they have provided largely non-overlapping lists of mRNA targets, except for some prominent ribosomal protein and metabolic enzyme transcripts [265, 268, 271, 285]. A possible reason for these discrepancies is the use of different target mapping methods and the varied cellular contexts examined. Further exploration is warranted, as the *let-7*-independent contribution to LIN28's functions is significant, as discussed below.

It should be noted that LIN28 has been suggested to operate through additional mechanisms as well, including mRNA stability [271], splicing [292], and even transcription [293]. Overall, a model is emerging where LIN28 may act as a multi-functional RBP that affects several events in

the mRNA life cycle, although the relevance of its non-translational activities remains to be determined.

Biological functions of the LIN28 pathway

As a core heterochronic gene in *C. elegans*, *lin-28* regulates developmental transitions between larval stages, which involve specific patterns of cell division and differentiation [294]. It does so at two mechanistically distinct steps: (i) a *let-7*-independent step that promotes cell fates of the second larval stage; and (ii) a *let-7*-dependent step that controls cell fates of the third larval stage and subsequent differentiation [243, 246, 295]. At the cellular level, this involves changes in both the proliferative and differentiation capacities of stem cell populations called hypodermal seam cells and vulval precursor cells [243, 246, 296]. At the molecular level, *lin-41* (*Trim71* in mammals) is a key *let-7* target, while *hbl-1* has been identified as a major *let-7*-independent effector, although the specific details of the *let-7*-independent mechanism remain unclear [295].

Remarkably, these developmental roles are highly conserved in evolution, as LIN28A/B are expressed early and downregulated later during embryogenesis and cell differentiation in *Drosophila*, *Xenopus,* zebrafish, mouse and human [247, 248, 274, 297, 298]. Moreover, LIN28A/B have been implicated in cell fate specification in the early embryo and in more tissue-restricted lineages [70]. LIN28 depletion impairs the maternal-to-zygotic transition in zebrafish [298] and the two- to four-cell stage transition in *Xenopus* [274]. Further, LIN28 promotes germ cell development and fertility in *Drosophila* [299] and the mouse [300, 301], which in the latter case has been linked to *let-7*-dependent regulation of the germ cell factor *Blimp1* [301]. In the ectodermal lineage, a series of studies have implicated LIN28 in neural development and differentiation [251, 302, 303], including the decision to acquire neuronal versus glial cell fates, which was attributed to both *let-7*-dependent and -independent functions [304]. In the mesoderm, a study in *Xenopus* indicated a requirement for LIN28 during early specification [274], and multiple mammalian studies have linked LIN28 proteins to the development of specific hematopoietic

lineages [305-310] and muscle progenitor differentiation [284]. While the downstream mechanism in the blood lineage was suggested to involve the *let-7* target *Hmga2* [305, 308], the *Xenopus* and myoblast studies implicated *let-7*-independent mechanisms [274, 284] In the endodermal lineages, LIN28A/B expression has been detected in fetal lung, intestines, liver and kidney, with evidence for functional roles in the latter two tissues [248, 282, 311]. Lastly, whole-body overexpression and knockout mouse models have indicated a broader growth-promoting function of LIN28 paralogs [312-314], as well as a regulatory impact on the timing of puberty [313, 315]. Importantly, *Lin28a/b* double-knockout mice are embryonic lethal at mid-gestation, demonstrating that LIN28 proteins are indispensable for the completion of embryonic development [312]. In sum, these studies suggest broad-ranging roles for LIN28A/B across developmental stages and lineages, which involve both proliferative and differentiation processes as well as *let-7*-dependent and -independent mechanisms, closely mirroring its functions in *C. elegans*.

These functions also hold true in PSCs. LIN28 is upregulated during mESC derivation from the ICM, which correlates with the acquisition of indefinite self-renewal [200]. LIN28 proteins are dispensable for pluripotency *per se*, given that *Lin28a/b* double-knockout mouse embryos do not die until E10.5-12.5 [312], but LIN28A/B promote self-renewal by supporting the proliferative and metabolic properties of PSCs [285, 290, 316]. Further, LIN28 expression is low in the naïve but high in the primed pluripotent state, and LIN28 has been shown to promote priming [196, 290, 317]. LIN28's role in the exit from pluripotency is less clear, as *let-7* facilitates differentiation only in the absence of other miRNAs [203], but this warrants further investigation in light of its priming activity. On the other hand, LIN28 proteins promote the induction of pluripotency during somatic cell reprogramming. LIN28A is among the strongest markers of deterministic reprogramming; overexpression of either LIN28 paralog along with OCT4, SOX2 and NANOG dramatically enhances reprogramming; and LIN28A/B depletion drastically reduces reprogramming efficiency [25, 290, 318-320]. Intriguingly, ectopic overexpression of LIN28 alone in adult mice enhances tissue repair in several lineages, likely reflecting a similar reversion toward a more embryonic-like

state [288]. This function appears to be evolutionarily conserved, as LIN28 is required for retinal regeneration in the fish [321]. Mechanistically, all of these effects have been linked to both *let-7*-dependent and -independent mechanisms, further demonstrating the important contribution of each of these LIN28 functionalities [285, 288, 290, 317].

Consistent with their functions in promoting less mature cell fates, LIN28 proteins also act as oncogenes. In a classic oncofetal fashion, LIN28A/B expression, which is normally low or absent in differentiated tissues, is reactivated in ~15% of human cancers across different tumor types [254]. Further, LIN28A/B overexpression promotes oncogenic transformation *in vitro* and can drive tumorigenesis *in vivo* [254, 322]. The growing list of cancer types that can be initiated by LIN28A/B overexpression in mouse models includes neuroblastoma [323], T-cell lymphoma [324], Wilms tumor [311], colon [325, 326], and liver cancer [327]. The requirement of LIN28A/B for tumor initiation and maintenance has also been tested by RNAi-based strategies in cancer cell lines (reviewed in [328]), reversal of LIN28A/B induction in doxycycline-inducible transgenic mouse models [311, 326], or RNAi-based and genetic LIN28A/B depletion in established tumors *in vivo* [327]. Additionally, LIN28A/B have been shown to promote invasiveness and metastasis [326, 329-333], consistent with the reported correlation between LIN28A/B expression and tumor grade in patient samples (reviewed in [322]). Nonetheless, the exact contributions of LIN28 proteins to different stages of oncogenesis remain to be elucidated. Finally, at least in one case, LIN28's tumorigenic functions have been specifically linked to CSC maintenance [334], which might represent a more general phenomenon and thus requires further exploration.

Mechanistically, most cancer studies have focused on *let-7*, given its powerful tumor-suppressive roles [228, 229, 231, 232, 253, 335-340]. Indeed, *let-7* is often downregulated in cancer and the mechanism for coordinate inhibition of the many *let-7* species remained elusive until the discovery that LIN28A/B block *let-7* processing [209, 328, 341]. *Let-7*-independent mechanisms have also been implicated [325-327], although the extent of their contribution to LIN28A/B's oncogenic function remains unclear. The recognition of LIN28A/B's oncogenic role

has stimulated efforts to develop strategies for LIN28A/B inhibition, with the goal of therapeutic applications, but the reported effects of such inhibitors on *let-7* have been mild in cell-based assays and their ability to affect oncogenic phenotypes has not been tested [342-345].

How does LIN28A/B impact such a broad range of biological phenomena? While multiple molecular targets and cellular mechanisms have been uncovered, a common theme has emerged whereby LIN28 proteins coordinate a core program of growth regulators to influence cell fate [70]. This is achieved both via control of specific cell cycle, metabolic and translation factors, and through broader modulation of major growth regulatory pathways. LIN28 upregulates various cyclins and cyclin-dependent kinases through *let-7*-dependent and -independent mechanisms to facilitate cell cycle progression [285, 316, 336, 346]. LIN28 proteins upregulate the *let-7* target PDK1 [347] and can translationally enhance or suppress numerous metabolic enzymes, which leads to modulation of glycolysis, amino acid metabolism, and oxidative phosphorylation in a context-dependent manner [285, 288, 290, 348]. Intriguingly, LIN28A/B also bind and translationally regulate many ribosomal protein mRNAs [285], and regulate nucleolar-based processes [271, 273, 274], suggesting that they may further enhance ribosome biogenesis and translation. In addition, through *let-7*-dependent and -independent mechanisms, LIN28A/B separately stimulate central pro-growth pathways, namely RAS/MAPK [229], PI3K/mTOR [284, 314, 349], c-MYC [340], and HMGA2 [337, 338], all of which promote proliferation, metabolism, ribosome biogenesis and translation.

Importantly, LIN28's cell cycle and metabolic effects have been linked to the control of cell identity. From the early *C. elegans* work to recent pluripotency studies, the ability of LIN28 to stimulate proliferation has been shown to affect cell fate decisions [337, 338]. In light of the reported deterministic role of cell cycle regulators in pluripotency [350], it would be interesting to explore if any specific LIN28 targets are directly responsible for cell fate control. Similarly, cellular metabolism is increasingly recognized as more than a "housekeeping" program, with extensive downstream impact on the epigenetic control of cell identity [351]. In line with this idea, LIN28's

regulation of amino acid metabolism has been shown to affect histone methylation and thereby contribute to pluripotency control [290, 348]. Given recent appreciation that the ribosome can exert specialized control over gene expression and cell identity [352, 353], it is tantalizing to speculate that LIN28A/B's modulation of ribosomal regulators may similarly promote more specific cell fate programs. The relevance of these pro-growth mechanisms to tumorigenesis is also becoming clear, as the control of proliferation and metabolism appear to be central to LIN28A/B's oncogenic functions (reviewed in [354]), although the extent of the parallels to pluripotency remains to be determined.

Upstream regulation of the LIN28 pathway

Despite LIN28A/B's major functional roles and many mechanistic insights, the understanding of its upstream regulation is relatively limited. In *C. elegans*, the transcription factor *daf-12*, a nuclear receptor, transduces extrinsic signals from steroid hormones to *lin-28* and *let-7* [355-357], with homologous receptors regulating *let-7* in other systems [358-360], although a direct connection to LIN28A/B is missing. On the other hand, LIN28A/B have been extensively linked to the pluripotency transcriptional network, as OCT4, SOX2, NANOG, KLF4, c-MYC and TCF3 have all been shown to regulate *Lin28a/b* transcription in PSCs [361, 362]. Interestingly, *LIN28B* is upregulated earlier than *LIN28A* during reprogramming [290], suggesting differential transcriptional regulation of the two paralogs that might contribute to their distinct tissue-specific expression patterns. Consistent with this model, NFκB and c-MYC have been reported to specifically transactivate *LIN28B* in cancer cells [363, 364].

Beyond transcription, LIN28A/B are also regulated post-transcriptionally by miRNAs and RBPs. Seminal studies in *C. elegans* identified *lin-4*, the first miRNA to be discovered, as a regulator of *lin-28* in the heterochronic pathway [246]. This regulatory interaction has been conserved in evolution, since the mammalian *lin-4* homologs, *miR-125a/b*, also target the *LIN28A/B* 3'UTRs, along with *miR-9* and *let-7* [365]. At least two RBPs, TTP and LIN28 itself,

have also been shown to destabilize and stabilize *LIN28*, respectively, through direct mRNA binding [268, 366]. Of note, both post-transcriptional mechanisms involve *LIN28A/B* auto-regulation, which creates a positive-feedback mechanism that is thought to play a critical role in developmental progression [70].

Finally, recent studies have begun to uncover post-translational regulatory mechanisms that control LIN28A/B. The RBP MSI1 was identified as a LIN28 interaction partner that recruits LIN28 to the nucleus to facilitate blockade of the DROSHA *let-7* processing step [272]. Two other proteins, the zinc-finger protein LEP-2/Makorin [367] and the ubiquitin ligase TRIM71 [368], have been shown to promote protein degradation of *C. elegans* LIN-28 and mammalian LIN28B, respectively. PCAF-mediated acetylation [369] and SET7/9-mediated methylation [273] have also been implicated in the regulation of LIN28A/B stability and nucleocytoplasmic distribution, with reported downstream effects on *let-7*. Overall, the expanding picture of LIN28A/B's regulation supports its central place as a cell fate modulator, with a key outstanding question being how these inputs are governed by the critical signaling pathways that shape cell identity, which will be explored in part in this dissertation.

1.4. TUTases and Terminal RNA Uridylation.

Terminal RNA uridylation: An emerging post-transcriptional regulatory mechanism

Besides the canonical mRNA cap and poly(A) tail, RNAs contain over 100 different modifications [166, 370]. Recent technological developments have enabled their global interrogation, which has uncovered key regulatory roles and led to the concept of a distinct "epitranscriptomic" layer of gene regulation [166, 371]. Among these modifications, the 3' terminal addition of non-templated nucleotides ("tailing"), such as adenylation, uridylation and guanylation, has emerged as a surprisingly widespread phenomenon [372, 373]. From pioneering studies in yeast and plants to recent work in mammalian cells, uridylation in particular has been recognized as a pervasive mark that controls the fate of mRNAs and non-coding RNAs, revealing an ancient

yet mostly unexplored mechanism of post-transcriptional gene regulation [374]. In the following sections, we review accumulating knowledge about the RNA uridylation pathway, including key protein factors, known RNA substrates and uridylation's effects on them, as well as emerging links to biological processes.

Terminal uridylyltransferases

Terminal RNA uridylation is catalyzed by a class of enzymes called terminal uridylyl-transferases (TUTases). They belong to the DNA polymerase β-like nucleotidyltransferase superfamily, which were originally described as poly(A) polymerases due to the ability of some members to carry out mRNA adenylation [375-377]. The recognition that other members have uridylation activity led to their categorization as poly(U) polymerases or TUTases [378, 379].

Humans have seven predicted TUTases: the nuclear TUT3/PAPD5, TUT5/PAPD7 and TUT6/U6TUT, the mitochondrial TUT1/PAPD1, and the cytoplasmic TUT2/GLD2, TUT4/ZCCHC11 and TUT7/ZCCHC6 [373]. All of them share a core catalytic region comprised of two domains: (i) a nucleotidyltransferase domain (NTD) that chelates divalent metal ions critical for catalytic activity; and (ii) a poly(A) polymerase (PAP)-associated domain that contains a nucleotide recognition motif [374, 375]. In addition, some TUTases, including the human TUT4/7, contain one C2H2-type and two C2HC-type zinc finger domains, as well as multiple intrinsically disordered regions, all of which may allow for interaction with various protein co-factors and RNA targets [374, 380, 381]. TUT4/7 also harbors duplicated but inactive catalytic regions, which are also thought to fulfill regulatory functions [374, 375, 378].

The catalytic region and uridylation activity have ancient evolutionary origins, having been found in viruses, archaea, prokaryotes and eukaryotes, with the notable exception of the budding yeast *S. cerevisiae* [373, 382]. However, the remaining regions and overall domain organization of TUTases exhibit little conservation between species, possibly reflecting an expanding capacity to associate with a variety of co-factors and targets during evolutionary progression [373]. Indeed,

different TUTases have been shown to regulate various types of RNA substrates in several cellular compartments, from small RNAs in the nucleus and mitochondria to many mRNAs and miRNAs in the cytoplasm [374]. Below, we focus specifically on the cytoplasmic substrates (Figure 1.4), whose regulation is relatively better understood and most relevant to the work in this dissertation.

Uridylation of cleaved and histone mRNAs

The first insight into cytoplasmic RNA uridylation came from the finding that 5' products of miRNA-mediated cleavage can be modified at the 3' end by non-templated addition of U-tails, which was originally observed in *Arabidopsis* and the mouse [383] and later in human cells [384]. In *Arabidopsis*, the U-tailing is catalyzed by the TUTase HESO1 [385], while in humans TUT2 uridylates the 5' cleavage products and other TUTases may further uridylate secondary degradation fragments [384]. Importantly, the presence of uridylation on degradation intermediates [384], as well as the correlation between uridylation, decapping and 5' mRNA shortening [383], were an early indication that the addition of a U-tail may promote mRNA degradation.

Another major insight came from studies of replication-dependent histone mRNA decay (Figure 1.4a, left). Unlike other mRNAs, these histone mRNAs lack a poly(A) tail and instead terminate with a 3' stem-loop structure bound by the stem-loop binding protein (SLBP), which governs mRNA metabolic steps [386, 387]. These mRNAs are degraded in a cell-cycle-dependent manner to prevent toxic histone accumulation when DNA replication is completed or inhibited [386, 388]. Hence, at the end of S-phase or upon inhibition of replication, they are rapidly degraded, which is stimulated by uridylation [389]. Oligouridylation of the stem-loop's 3' end facilitates recruitment of the LSM1-7 complex, which in turn interacts with the exonuclease ERI1 (3'hExo) [390, 391]. ERI1 "nibbles" 2-4 nucleotides, which is followed by multiple rounds of uridylation/nibbling, eventually leading to degradation of the stem-loop [391]. The RNA exosome

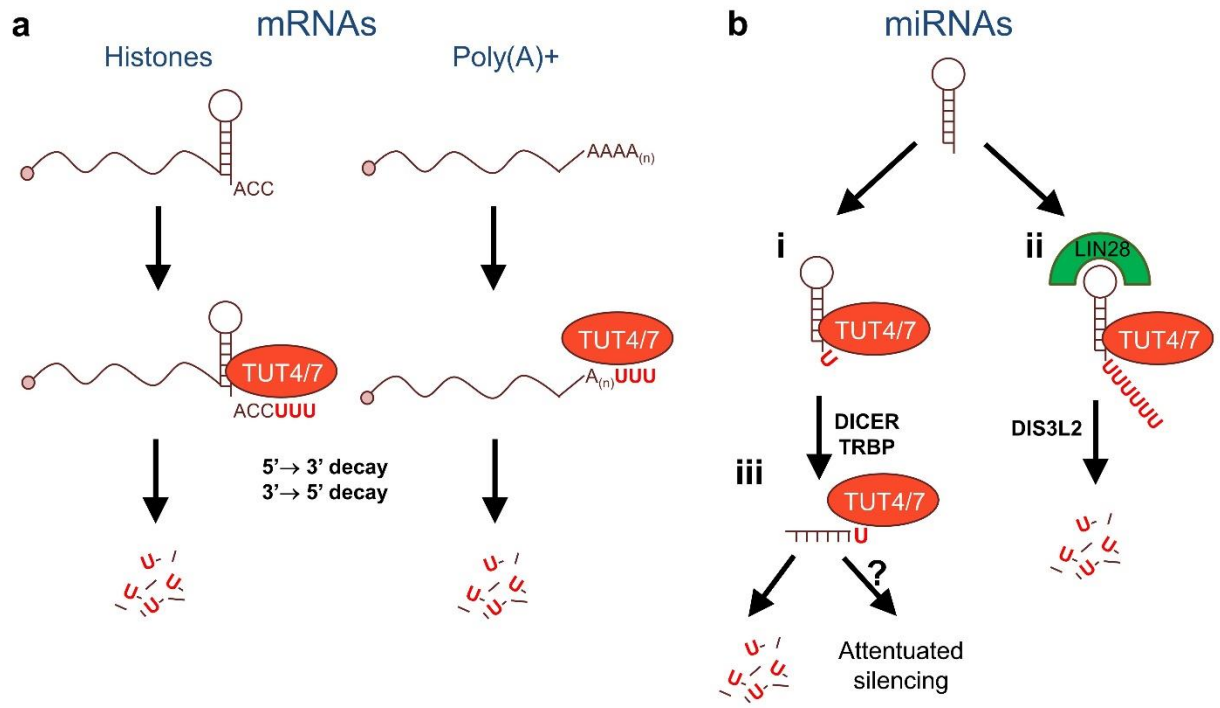

Figure 1.4. Major substrates and functions of TUT4/7 in mammalian cells. (a) TUT4/7 oligouridylate histone mRNAs or poly(A)+ mRNAs, in both cases to promote their decay. (b) TUT4/7 have three miRNA-directed modes of action: (i) in the absence of LIN28, they monouridylate a subset of pre-*let-7* miRNAs to promote their processing by DICER/TRBP; (ii) in the presence of LIN28, they oligouridylate pre-*let-7* miRNAs to promote their degradation by the exonuclease DIS3L2; (iii) TUT4/7 can also monouridylate mature miRNAs to modulate their abundance and/or activity. Of note, the pri-miRNA activities have also been reported for a broad range of miRNAs, independently of LIN28. See text for further details.

is then recruited and its exonucleolytic component RRP6 (PM/Scl-100) catalyzes the decay of the remaining mRNA fragment [391]. While this 3'→ 5' degradation pathway appears to be predominant, LSM1-7 can also stimulate decapping and subsequent 5'→ 3' decay by the XRN1 exonuclease [389, 391-393]. Of note, it has recently been proposed that uridylation also repairs unwanted 3'-end nibbling during S-phase, suggesting a more complex model for the role of uridylation in histone mRNA turnover [394]. Several TUTases have been proposed to uridylate histone mRNAs, with earlier studies implicating TUT1, TUT3 and TUT4 [389, 393, 395], and recent work pointing to TUT7 as the major enzyme uridylating the 3' end of the stem and subsequent degradation intermediates [396].

Overall, these seminal studies provided glimpses into a novel mechanism of uridylation-dependent mRNA decay, whose scope was not fully appreciated until groundbreaking work demonstrated its integral role in the turnover of polyadenylated mRNAs.

Uridylation of polyadenylated mRNAs

The uridylation of polyadenylated mRNAs was first appreciated in *S. pombe* and shortly after in another fungus, *A. nidulans*, where mRNAs were found to contain short U-tails or longer C/U-mixed tails, respectively [379, 397-399]. A subsequent study reported mRNA uridylation in *Arabidopsis*, indicating conservation in higher eukaryotes [400]. Two observations suggested that these modifications promote mRNA degradation. First, mutation of the *S. pombe* deadenylation (Ccr4) or decapping factors (Dcp1 and Lsm1) led to accumulation of uridylated mRNAs [399]. Second, deletion of the TUTases Cid1 (in *S. pombe*) and CutA/B (in *A. nidulans*) resulted in increased mRNA stability for several model genes [397-399]. However, while *Arabidopsis* U-tails occur predominantly on deadenylated mRNAs, consistent with a role in mRNA decay, mutation of the respective TUTase, URT1, did not increase mRNA half-lives [400]. These data led to the suggestion that uridylation determines the directionality rather than rate of mRNA decay in this context [400]. Together, these pioneering studies implicated a role for uridylation in the decay of polyadenylated mRNAs; however, as they only analyzed a handful of genes, questions remained as to whether or not this was a more general regulatory mechanism.

This problem was addressed by the development of a novel high-throughput technique for deep sequencing of the 3' mRNA termini called TAIL-seq, which allows for simultaneous measurement of poly(A) tail length and 3' tailing at a transcriptome-wide scale [372]. TAIL-seq analysis of human and mouse cell lines demonstrated that uridylation is a pervasive phenomenon, with over 85% of mRNA species being uridylated at a higher than 1% frequency [372]. Further, uridylation was predominantly found on mRNAs with shortened poly(A) tails (<~25 nt) and negatively correlated with mRNA half-life, suggesting a role in global mRNA decay [372]. A follow-

up study provided compelling evidence that this is indeed the case and specifically implicated TUT4 and TUT7 as the responsible TUTases [401] (Figure 1.4a, right). TUT4/7 depletion dramatically reduced mRNA uridylation and stabilized mRNAs on a global scale [401]. Additionally, depletion of 5'→ 3' decay factors XRN1, DCP1 and LSM1, or 3'→ 5' decay factors RRP41 (exosome component) and DIS3L2 led to accumulation of uridylated mRNAs, demonstrating that TUT4/7-mediated uridylation is an integral part of the global mRNA decay pathway [401].

These findings have been corroborated by additional studies of the DIS3L2 exonuclease. Use of X-ray crystallography to solve DIS3L2 structure in complex with an oligo(U) RNA revealed an extensive network of uracil-specific interactions [402]. Further, DIS3L2 depletion in cultured human cells led to increased mRNA half-lives [403], in agreement with the above study [401], and its deletion in *S. pombe* similarly resulted in accumulated transcripts with enhanced uridylation [404]. Likewise, yet another study showed that apoptosis-induced mRNA decay involves TUT4/7-mediated uridylation and subsequent clearance by DIS3L2 [405].

In addition to its major functions in mRNA decay, uridylation has also been linked to other effects on polyadenylated mRNAs. First, TAIL-seq analysis in *Arabidopsis* indicated that URT1-mediated uridylation acts to repair mRNAs' deadenylated tails [406], akin to the recently suggested role for histone mRNA uridylation during S-phase [394], thereby preventing rather than promoting deadenylation. Second, uridylation has been shown to influence translation. Long A/U-tails, synthesized by the poly(A) polymerase KPAP1 and TUTase RET1, recruit mitochondrial mRNAs to mitochondrial ribosomes to enhance their translation [407]. Conversely, uridylation has been proposed to suppress translation in *A. nidulans* (via ribosome dissociation) [397], *Xenopus* (using a reporter mRNA) [408], and starfish oocytes (for maternal mRNAs) [409]. Thus, it is possible that mRNA uridylation may have different functions depending on the specific target or context, although its contribution to mRNA decay remains the most established one so far.

miRNA uridylation

Apart from mRNAs, uridylation has also been shown to regulate miRNAs in multiple ways [410] (Figure 1.4b). First, mono-uridylation of Group II *let-7* pre-miRNAs by TUT2/4/7 promotes their processing, as it extends the 3' overhang and thereby creates an optimal substrate for DICER processing [258, 411] (Figure 1.4b, i). However, in the presence of LIN28, the TUTase::pre-*let-7* interaction is stabilized, thus enhancing processivity of the uridylation reaction [412]. As a result, pre-*let-7* species are oligouridylated instead, which inhibits DICER processing and stimulates degradation by DIS3L2, in a second mode of regulation that is similar to the mRNA decay mechanism [249, 257-259, 261, 262, 275, 411, 413] (Figure 1.4b, ii). Oligouridylation has also been described on truncated pre-miRNAs with a 5' overhang, independently of LIN28, which likely promotes the turnover of degradation intermediates [411]. Furthermore, in *Drosophila*, oligouridylation of intron-derived pre-miRNAs (mirtrons) promotes their degradation [414, 415]. Importantly, the dual roles of mono- versus oligouridylation of pre-miRNAs are an integral part of a global pre-miRNA surveillance pathway for quality control of miRNA biogenesis [416]. Thus, TUTases can sense overhang structure to either repair pre-miRNAs or promote their degradation [411], analogously to their emerging dual functionality on mRNA substrates described earlier.

In a third mode of action, uridylation also occurs on mature miRNAs and regulates their abundance and/or function (Figure 1.4b, iii). This was first observed in *Arabidopsis*, where uridylation of miRNAs and siRNAs is associated with their degradation [417]. Follow-up studies implicated HESO1 and URT1 as the responsible TUTases, and confirmed their regulatory effects on miRNA stability [418-420]. A number of studies have further identified widespread uridylation of mature miRNAs in viruses [421], *Chlamydomonas* [422], *Drosophila* [423], mouse [424] and human cells [425-427]. In mouse and human cells, this finding has been attributed to TUT4/7, whose activity does not appear to affect miRNA abundance but attenuates miRNA-mediated silencing instead [424-426]. Interestingly, the mRNA target itself can induce miRNA uridylation and degradation in mammalian cells, which at least in one case involves DIS3L2 [428-430].

Hence, further studies are needed to determine if and when uridylation promotes miRNA decay in mammals and to explore the mechanism of abrogating mRNA silencing.

Biological functions of uridylation

As the molecular consequences of RNA uridylation are becoming elucidated, there is a growing interest in its functional effects at the cellular and organismal level. Thus far, important clues have been provided by a number of studies spanning diverse model organisms and biological processes.

The *S. pombe* TUTase Cid1 was originally identified as a regulator of the S-to-M cell cycle transition, in line with its histone mRNA regulatory function [379, 431-433]. Cid1 knockout cells were specifically sensitive to the combination of hydroxyurea, which inhibits DNA synthesis, and caffeine, which overrides the *S. pombe* S/M checkpoint [433], suggesting that TUTases may participate in an ancient cell-cycle regulatory mechanism. Consistent with this idea, TUT4 expression is regulated in a cell-cycle-dependent manner [395] and TUT4 overexpression can promote proliferation, albeit through a reportedly catalytically-independent mechanism [434].

Evidence for a pro-growth function of TUTase-mediated uridylation has also come from mouse and human genetic studies. TUT4 knockout mice show decreased neonatal survival and growth, which has been linked to abrogated miRNA uridylation and concomitant upregulation of IGF1 [424]. In addition, loss-of-function mutations in DIS3L2 have been identified as the cause of Perlman syndrome, a fetal overgrowth and cancer predisposition condition [435]. The identity of the specific targets responsible for these phenotypes remains unclear, as DIS3L2 can recognize both uridylated mRNAs and non-coding RNAs [261, 262, 403, 404, 415, 436-438]. In agreement with these observations, DIS3L2 has also been suggested to act as tumor-suppressor. Perlman syndrome involves susceptibility to Wilms tumor [435] and DIS3L2 mutations have been mapped in Wilms tumor patients [224]. The fact that LIN28 overexpression can also induce Wilms tumor by repressing *let-7* suggests that DIS3L2's tumor-suppressive activity may be attributed to *let-7*

regulation, although this model remains to be tested [311]. In another cancer-relevant setting, TUT4/7-driven mRNA uridylation followed by DIS3L2-mediated decay appears to be an integral part of apoptosis, implying that TUTase activity may also be tumor-suppressive by supporting cell death in certain settings [405]. However, TUT4 has also been shown to have oncogenic roles as a co-factor of LIN28 in suppressing *let-7* biogenesis in several cancers [255, 439]. Thus, the role of the TUTase pathway in cancer remains to be fully elucidated.

Lastly, other studies have linked uridylation to additional processes. TUT4-mediated uridylation of *miR-26* attenuates its ability to silence *IL-6* mRNA, thereby leading to increased cytokine expression and enhanced immune response in human cells [425]. The *Drosophila* TUTase Tailor and Dis3L2 have recently been linked to gametogenesis, as mutations of either gene lead to fertility defects [440]. And inhibition of TUT4/7 in zebrafish leads to embryonic arrest and dysregulation of *hox* gene expression, suggesting an even broader developmental role [426]. Overall, these functional analyses offer first glimpses into what is likely a complex and extensive involvement of RNA uridylation in regulating cell identity in normal and pathological settings, which is explored further in this dissertation.

1.5. Summary of Dissertation Work.

The work presented in this dissertation is motivated by two key factors: (i) the commonalities between development and oncogenesis, and (ii) our limited understanding of the post-transcriptional regulation of cell identity. As such, it aims to explore novel mRNA regulatory mechanisms that contribute to the control of cell identity in pluripotency and cancer. We have focused on specific RBPs – LIN28 and the TUTases ZCCHC6/11 – which serve as valuable lenses into this problem.

Chapter 2 addresses the broad question of how signaling and post-transcriptional regulation are integrated to influence cell fate. In particular, we investigated the role of LIN28 phosphorylation in PSCs. We found that MAPK/ERK, a central signaling regulator of pluripotency,

phosphorylates LIN28 to increase its protein stability and thereby enhance LIN28's translational regulation of its mRNA targets, which contributed to the control of pluripotency transitions. These findings establish a novel link between extracellular cues, mRNA translation, and cell fate control.

Chapter 3 examines the role of TUTase-mediated mRNA uridylation in the control of cell identity. In particular, we explored the functions of ZCCHC6/11 in cancer cells, PSCs and muscle progenitors. We found that these TUTases contribute to oncogenic transformation and support the growth and tumorigenicity of cancer cell lines. Mechanistically, these effects were associated with altered mRNA uridylation and turnover, including dysregulation of cell cycle factors and concomitant cell cycle impairment. Interestingly, we also report that ZCCHC6/11 promote a less differentiated cell state in both PSCs and lineage-restricted muscle progenitors. These results reveal novel functions for ZCCHC6/11 and implicate uridylation-mediated mRNA turnover as a mechanism of oncogenesis.

Collectively, the work presented herein illuminates the role of extrinsic and intrinsic signals in post-transcriptional gene regulation and uncovers new mRNA regulatory mechanisms in the control of cell identity, with implications for stem cell and cancer biology.

AUTHOR CONTRIBUTIONS

This chapter has not been published, except for a minor portion of section 1.2 that was partially adapted from [441]. K.M. Tsanov wrote the text and generated the figures, with edits from T.E. North and G.Q. Daley.

CHAPTER 2

LIN28 Phosphorylation by MAPK/ERK Couples Signaling to the Post-transcriptional Control of Pluripotency

2.1. Introduction.

The control of pluripotency requires precise coordination of multiple gene regulatory mechanisms, yet how this is orchestrated at the molecular level remains incompletely understood. Signaling has a key role in this network [442], with the MAPK/ERK pathway holding a particularly prominent place, since its activity primes PSCs for lineage commitment [443] whereas its inhibition is essential for the maintenance of a "naïve" state of pluripotency [15]. The effects of MAPK – and signaling pathways in general – are typically associated with downstream transcriptional mechanisms, while less is known about their integration with the post-transcriptional gene regulatory machinery [85, 442]. Gaining insights into the latter is critical, as post-transcriptional mechanisms play a major role in the control of cell identity, especially in guiding transitions between cell fates [85] (see Chapter 1.2).

LIN28, a highly conserved RBP, is a master post-transcriptional regulator of cell fate that controls embryonic development from *C. elegans* to mammals [70, 246] (see Chapter 1.3). It supports the proliferative and metabolic capacities of PSCs, promotes reprogramming to pluripotency, and facilitates the transition from naïve to primed pluripotency [25, 70, 196, 290]. Its effects are mediated through blockade of the biogenesis of the *let-7* miRNA family [249-252], and through direct translational enhancement or suppression of select mRNAs [265, 268, 284, 285, 288, 290]. Hence, how LIN28 is integrated with the pluripotency signaling network is a question of fundamental significance to the understanding of cell fate control.

Here we show that LIN28 is phosphorylated by MAPK/ERK in PSCs, which increases its levels via post-translational stabilization. LIN28 phosphorylation had little impact on *let-7* but enhanced LIN28's effect on its direct mRNA targets, revealing a mechanism that uncouples LIN28's *let-7*-dependent and -independent activities. We have linked this mechanism to the induction of pluripotency by somatic cell reprogramming and the transition from naïve to primed pluripotency. Collectively, our findings indicate that MAPK/ERK directly impacts LIN28, defining an axis that connects signaling, post-transcriptional gene control, and cell fate regulation.

2.2. Results.

MAPK/ERK phosphorylates LIN28 on S200

Global phosphoproteomic studies of human embryonic stem cells (hESCs) had identified several putative phosphosites in LIN28 [444, 445]. To validate their conservation between human and mouse, we employed a targeted phosphoproteomics strategy in mESCs (Supplementary Figure 2.1a-c). We were able to map four phosphosites, two of which, S184 and S200, were confidently assigned to specific serine residues (Supplementary Table 2.1). Combining our data and prior results [444, 445], we generated a comprehensive profile of LIN28 phosphorylation in PSCs (Figure 2.1a).

To identify kinases that phosphorylate LIN28, we interrogated the LIN28 amino acid sequence for conserved kinase recognition motifs (Supplementary Figure 2.1d). Since we noticed members of the MAPK family as predicted kinases for S200, we decided to further investigate this phosphorylation event (Figure 2.1b). We generated an antibody reactive against phospho-S200 and validated its specificity with a phospho-null LIN28 mutant, in which S200 is mutated to alanine (S200A) (Figure 2.1c). Using this antibody, we profiled a panel of human PSCs, all of which exhibited LIN28 (S200) phosphorylation, suggesting that this phosphorylation is a common molecular feature of PSCs (Supplementary Figure 2.1e).

To identify the particular MAPK responsible for S200 phosphorylation, we performed a targeted inhibitor screen in human embryonal carcinoma cells (hECCs). We used selective inhibitors of the major MAPKs, including MEK/ERK, p38 MAPK, JNKs, CDKs, and GSK3β, as well as mTOR, an unrelated proline-directed kinase. Of those, only the MEK/ERK inhibitor, PD0325901, consistently reduced S200 phosphorylation under the tested conditions (Figure 2.1d). We then serum-starved hECCs and subjected them to short-term treatment with phorbol myristate acetate (PMA), which activates MAPK/ERK signaling. S200 phosphorylation was induced, corroborating the inhibitor data (Figure 2.1e). Pre-treatment with the MEK/ERK inhibitor

Figure 2.1. MAPK/ERK phosphorylates LIN28A on S200. (a) Schematic of the LIN28A domain structure with indicated phosphorylation sites, as mapped by mass spectrometry. Respective motifs and homologous sequences across several mammalian species are shown below each site. CSD = cold-shock domain; NLS = nuclear localization signal; CCHC = zinc finger domains. (b) Representative phosphopeptide MS/MS spectrum for S200. (c) Western blot analysis of LIN28A (S200) phosphorylation in HeLa cells stably expressing wild-type (WT) or phospho-null (S200A) FLAG-LIN28A. A representative image of three independent experiments is shown. (d) Western blot analysis of LIN28A (S200) phosphorylation in PA1 hECCs after 60-min treatment with a panel of inhibitors of proline-directed kinases. Tn1 = Torin1 (100 nM); PD = PD0325901 (1 μM); SB = SB203580 (2 μM); SP = SP600125 (20 μM); Ken = Kenpaullone (5 μM). Quantification of Western blot data is shown on top. n=3 independent experiments. Error bars represent s.e.m. *P<0.05 (two-tailed Student's *t*-test). (e) Western blot analysis of LIN28A (S200) phosphorylation in PA1 cells after 30-min pre-treatment with DMSO, PD0325901 (1 μM), or SB203580 (2 μM), followed by 30-min treatment with DMSO or PMA (200 nM). Cells were serum-starved for 16-20 h prior to addition of inhibitors. A representative image of two independent experiments is shown. (f) Western blot analysis of LIN28A (S200) phosphorylation in 293T cells stably expressing wild-type FLAG-LIN28A after transfection with RFP, wild-type (WT), constitutively active (R4F), or kinase-dead (K97M) MEK1. Cells were transfected, incubated for 48 h, and then serum-starved for 16-20 h prior to analysis. A representative image of two independent experiments is shown. (g) Western blot analysis of LIN28A (S200) phosphorylation in PA1 cells after 30-min stimulation with serum (10%), fibroblast growth factor (FGF) (100 ng/ul), or epidermal growth factor (EGF) (100 ng/ul). Cells were serum-starved for 16-20 h prior to stimulation. A representative image of two independent experiments is shown.

Figure 2.1 (Continued)

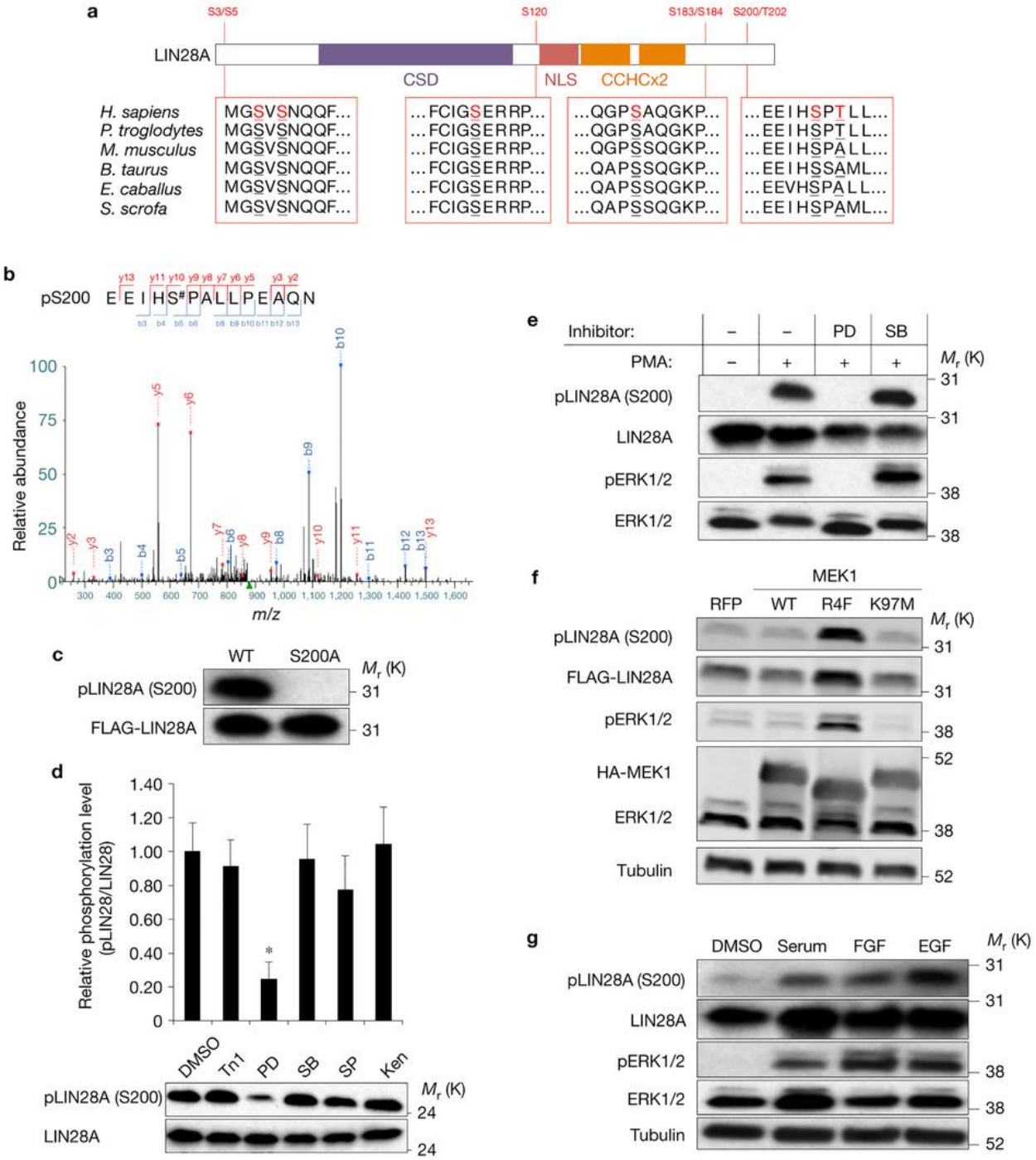

but not with an inhibitor of a different MAPK, p38 MAPK, abrogated the PMA-induced phosphorylation of LIN28, indicating that the PMA effects are mediated via ERK (Figure 2.1e).

To confirm this conclusion, we also expressed wild-type, constitutively active (R4F), or kinase-dead (K97M) versions of MEK1 [446] in 293T cells stably expressing a LIN28 ORF and subjected them to serum starvation. As expected, only the R4F mutant was able to activate ERK and maintain LIN28 phosphorylation under these conditions (Figure 2.1f). Lastly, we serum-starved hECCs and added back serum or treated them with fibroblast growth factor (FGF) or epidermal growth factor (EGF), physiologically relevant cues that induce ERK signaling. All three treatments led to increased LIN28 phosphorylation (Figure 2.1g). Collectively, our results demonstrate that ERK phosphorylates LIN28 on S200 in response to mitogenic stimuli.

LIN28 phosphorylation increases its protein stability

Next, we explored whether S200 phosphorylation affects LIN28 function. Intriguingly, we noticed that pre-treatment with the phosphatase inhibitor Calyculin A led to increased LIN28 abundance in our mass spectrometry samples (Supplementary Figure 2.1b). Western blot analysis confirmed an approximately 30% increase of LIN28 protein (Figure 2.2a). A similar effect was observed in the MEK1 overexpression experiments (Figure 2.1f), suggesting that ERK-mediated phosphorylation may stabilize LIN28 protein. To test this hypothesis, we treated hECCs with PMA for three hours, which led to a 30% increase in LIN28 protein, without concordant mRNA changes (Figure 2.2b). Conversely, a 48-hour treatment with the MEK/ERK inhibitor resulted in a one-third decrease of LIN28 at the protein but not mRNA level (Figure 2.2c and Supplementary Figure 2.2a), overall supporting our hypothesis.

To further explore this question, we generated stable isogenic 293T and HeLa cell lines expressing wild-type, phospho-mimetic (S200D or S200E), or phospho-null (S200A) LIN28, in which serine phosphorylation is mimicked or abrogated by substitution with aspartate/glutamate or alanine, respectively. While the phospho-mimetics showed 50-100% increase in protein levels, the phospho-null exhibited 40-50% decrease, without corresponding mRNA changes (Figure

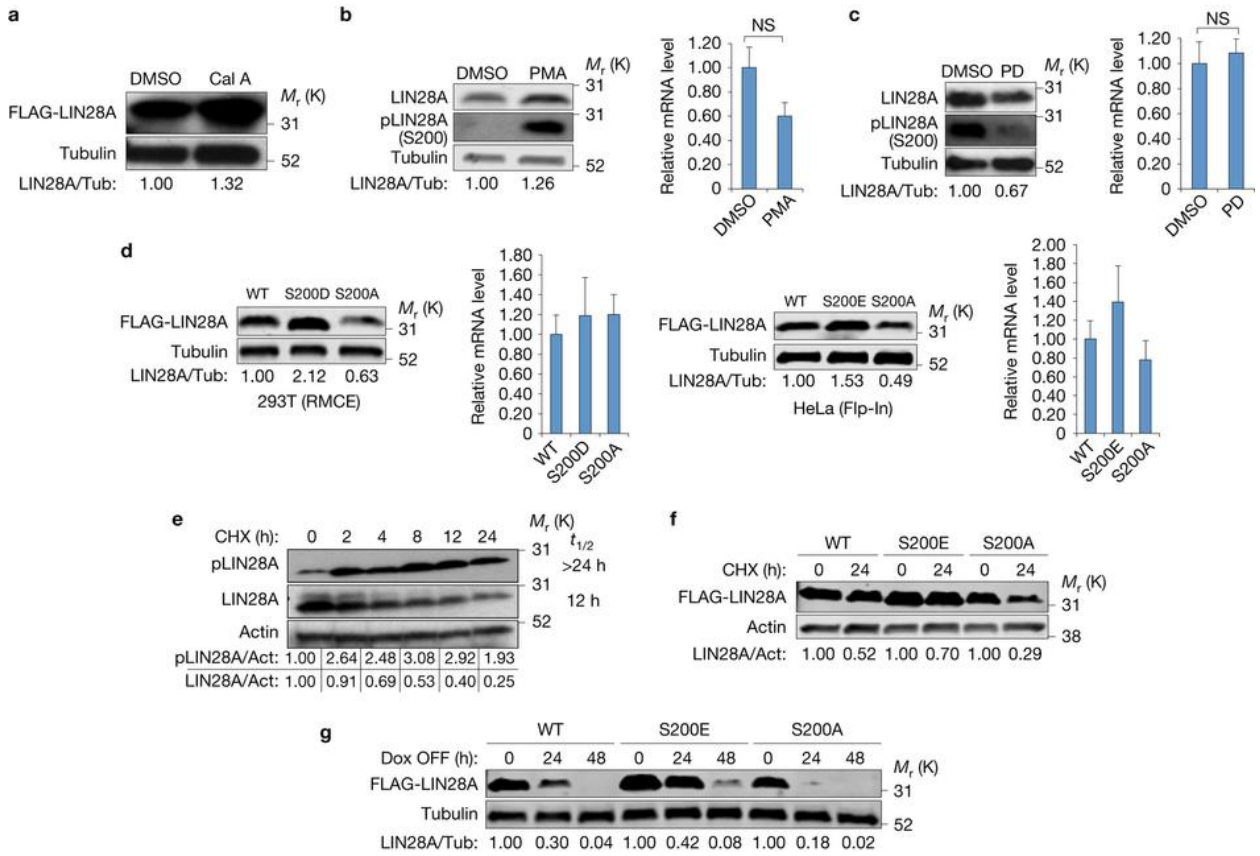

Figure 2.2. LIN28A phosphorylation increases its protein stability. (a) Western blot analysis of transgenic FLAG-LIN28A in iLIN28A mESCs after 30-min treatment with DMSO or Calyculin A (100 nM). A representative image of three independent experiments is shown. (b) Western blot (left) and qRT-PCR (right) analysis of endogenous LIN28A in PA1 cells after three-hour treatment with DMSO or PMA (200 nM). Cells were serum-starved for 16-20 h prior to addition of drugs. n=3 independent experiments. Error bars represent s.e.m. NS = non-significant; P=0.09 (two-tailed Student's *t*-test). (c) Western blot (left) and qRT-PCR (right) analysis of endogenous LIN28A in PA1 cells after 48-hour treatment with DMSO or PD0325901 (1 μM). n=3 independent experiments. Error bars represent s.e.m. NS = non-significant; P=0.79 (two-tailed Student's *t*-test). (d) Western blot (left) and qRT-PCR (right) analysis of transgenic FLAG-LIN28A in isogenic 293T (RMCE) or HeLa (Flp-In) cells. Cells were engineered to stably express a single copy of the respective LIN28A variant: wild-type (WT), phospho-mimetic (S200D or S200E), or phospho-null (S200A). n=3 independent experiments. Error bars represent s.e.m. P=0.77 (S200D) and P=0.70 (S200A) for 293T; P=0.42 (S200E) and P=0.48 (S200A) for HeLa (two-tailed Student's *t*-test). (e) Cycloheximide chase of endogenous phospho- and total LIN28A in PA1 cells. CHX = cycloheximide (100 μg/ml). A representative image of two independent experiments is shown. (f) Cycloheximide chase of transgenic FLAG-LIN28A variants in HeLa (Flp-In) cells. CHX = cycloheximide (100 μg/ml). A representative image of two independent experiments is shown. (g) Chase of transgenic FLAG-LIN28A variants after Dox withdrawal (Dox OFF) in HeLa (Flp-In) cells. Dox = doxycycline (100 ng/ml). A representative image of two independent experiments is shown.

2.2d). These data indicate that the observed effects on the LIN28 protein levels are post-translational and specifically mediated through the ERK target site in LIN28.

Lastly, we performed cycloheximide chase experiments in hECCs to track the decay kinetics of endogenous pLIN28 (S200) and total LIN28. While the total protein decayed with an estimated half-life of 12 hours, the phosphoprotein remained stable for the 24-hour course of the experiment (after an initial treatment-induced phosphorylation spike), suggesting that pLIN28 has a longer half-life and is thus relatively more stable (Figure 2.2e). We then conducted analogous experiments using the isogenic HeLa cells expressing LIN28 phosphorylation mutants, which showed that the mimetic (S200E) and null (S200A) mutants decay slower and faster, respectively, compared to wild-type LIN28 (Figure 2.2f). As these LIN28 variants are under doxycycline-control, we also withdrew doxycycline and tracked their decay kinetics in an unperturbed way, which confirmed the cycloheximide chase results (Figure 2.2g). Taken together, the above data indicate that ERK-mediated phosphorylation stabilizes LIN28 post-translationally by increasing its protein half-life.

LIN28 phosphorylation can uncouple its let-7-dependent and -independent activities

We then examined the effects of LIN28 phosphorylation on its downstream targets. First, we assessed *let-7* regulation. We performed *let-7* measurements in hECCs after a 48-hour treatment with the MEK/ERK inhibitor, which revealed a lack of statistically significant change in *let-7* levels (Supplementary Figure 2.2b). These data suggested that the ~30% reduction of LIN28 abundance due to loss of phosphorylation was insufficient to consistently affect *let-7* processing. In support of this observation, ~30% knockdown of LIN28 protein yielded similar results (Supplementary Figure 2.3a). To further address this question, we derived individual clones of HeLa cells stably expressing wild-type LIN28 at different levels. LIN28 protein expression equivalent to about 50% of its native level in hECCs achieved saturation of *let-7* suppression, confirming our earlier conclusion (Supplementary Figure 2.4a). To specifically assess the role of S200 phosphorylation,

we also measured *let-7* levels in the isogenic HeLa cells expressing wild-type or phospho-null (S200A) LIN28. As expected, the two LIN28 variants achieved comparable *let-7* suppression despite the consistently lower protein levels of the S200A mutant (Supplementary Figure 2.4b,c).

We then performed RNA immunoprecipitation (RIP) experiments in hECCs stably overexpressing wild-type or phospho-mimetic (S200D) LIN28 (Figure 2.3a), followed by qRT-PCR measurement of pri/pre-*let-7* association. The two proteins precipitated comparable amounts of most pri/pre-*let-7* miRNAs analyzed, consistent with lack of effect on *let-7* processing (Figure 2.3b). In line with these results, mature *let-7* levels were also unchanged in the mimetic relative to the wild-type cells (Figure 2.3c). Overall, our data from multiple assays demonstrate that LIN28 phosphorylation does not have a significant impact on *let-7*.

Next, we explored the effect of LIN28 phosphorylation on its mRNA targets. To do this on a transcriptome-wide scale, we performed RNA immunoprecipitation coupled with mRNA-seq (RIP-seq) of the wild-type and phospho-mimetic (S200D) LIN28 in hECCs. When normalized to the amount of immunoprecipitated LIN28, the two proteins showed highly similar mRNA binding profiles, indicating that they have comparable affinities to their mRNA targets (Figure 2.3d). However, when normalized to cell number, a follow-up qRT-PCR analysis of representative mRNAs revealed a stoichiometric increase in mRNA association that was specific to the LIN28 targets (Figure 2.3e). Of note, similar results were obtained with the S200E mutant in the isogenic HeLa cells (Supplementary Figure 2.4f,g). Overall, these data suggest that the phospho-mimetic mutants have comparable mRNA binding affinities to the wild-type protein but, due to their higher abundance per cell, associate with a greater amount of the same targets.

To further support this conclusion, we also performed complementary analysis in the isogenic HeLa cells expressing wild-type or phospho-null (S200A) LIN28. Consistent with its reduced protein abundance, the phospho-null LIN28 reproducibly precipitated lower amount of RNA per cell relative to the wild-type construct, which was proportional to their respective protein levels

Figure 2.3. LIN28A phosphorylation can uncouple its *let-7*-dependent and -independent activities. (a) Western blot analysis of RNA immunoprecipitation in PA1 cells overexpressing wild-type (WT) or phospho-mimetic (S200D) FLAG-LIN28A. A representative image of four independent experiments is shown. (b) qRT-PCR analysis of pri/pre-*let-7* species immunoprecipitated by wild-type (WT) or phospho-mimetic (S200D) FLAG-LIN28A in PA1 cells. n=4 independent experiments. Data were normalized to cell number prior to RT. Error bars represent s.e.m. *P<0.05 (two-tailed Student's *t*-test, S200D vs. WT). (c) qRT-PCR analysis of mature *let-7* species in PA1 cells stably overexpressing wild-type (WT) or phospho-mimetic (S200D) FLAG-LIN28A. n=3 independent experiments. Error bars represent s.e.m. P>0.05 (two-tailed Student's *t*-test, S200D vs. WT). (d) RNA-seq analysis of mRNAs immunoprecipitated by wild-type (WT) or phospho-mimetic (S200D) FLAG-LIN28A in PA1 cells. Each dot represents an average enrichment value for transcripts from a given gene. n=3 independent experiments. Data were normalized to the amount of immunoprecipitated LIN28A prior to sequencing. Detailed description of the analysis is provided in the Methods section. (e) qRT-PCR analysis of representative mRNA targets immunoprecipitated by wild-type (WT) or phospho-mimetic (S200D) FLAG-LIN28A in PA1 cells. n=4 independent experiments. Data were normalized to cell number prior to RT. Error bars represent s.e.m. *P<0.05 (two-tailed Student's *t*-test, S200D vs. WT). (f) qRT-PCR analysis of representative mRNA targets in PA1 cells stably expressing wild-type (WT) or phospho-mimetic (S200D) FLAG-LIN28A. n=3 independent experiments. Error bars represent s.e.m. P>0.05 (two-tailed Student's *t*-test, S200D vs. WT). (g) Western blot analysis of representative mRNA targets in PA1 cells stably expressing wild-type (WT) or phospho-mimetic (S200D) FLAG-LIN28A. A representative image of three independent experiments is shown.

Figure 2.3 (Continued)

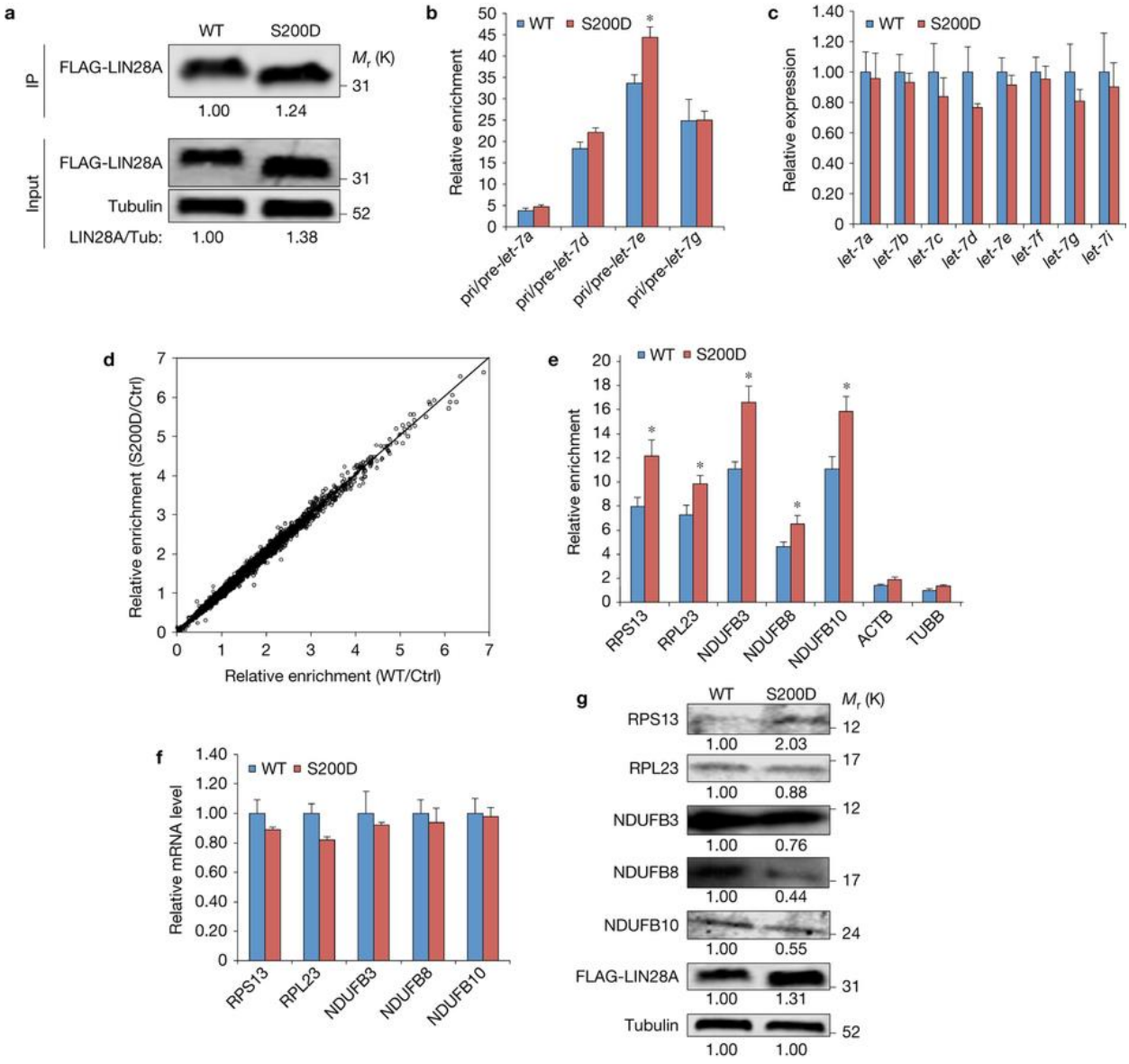

(Supplementary Figure 2.4d). However, when normalized to the amount of immunoprecipitated LIN28, the two constructs showed aligned mRNA binding profiles, corroborating the hECC data (Supplementary Figure 2.4e).

Lastly, we wanted to confirm that the changes in mRNA binding per cell affect their cognate protein expression, as LIN28 is known to modulate mRNA translation [265, 268, 284, 285, 288,

290]. We validated a set of previously established LIN28 mRNA targets by assessing their mRNA and protein levels after ~30% LIN28 knockdown in hECCs. As expected, mRNA levels were unaffected while protein levels decreased (for RPS13) or increased (for RPL23, NDUFB3, NDUFB8, and NDUFB10), in agreement with their reported LIN28-dependent translational enhancement and suppression, respectively (Supplementary Figure 2.3b,c) [265, 285, 290]. We then performed qRT-PCR and Western blot analyses of these targets in the hECCs expressing wild-type or phospho-mimetic (S200D) LIN28. While the mRNA levels were unchanged, protein levels were altered in the mimetic relative to the wild-type construct, consistent with stronger translational activity of LIN28 (Figure 2.3f,g). Importantly, these protein changes were in the opposite direction to the ones observed after LIN28 depletion and involved both positively and negatively regulated targets, suggesting that they reflect LIN28's overall translational activity rather than only its translation-promoting or suppressing function. Together, our results indicate that ERK-mediated LIN28 phosphorylation has little impact on *let-7* but enhances LIN28's regulation of its mRNA targets, thereby acting as a mechanism for uncoupling of LIN28's *let-7*-dependent and -independent activities.

LIN28 phosphorylation contributes to the regulation of pluripotency transitions

Given these molecular findings, we wondered if this mechanism regulates LIN28's function in guiding cell fate transitions. As LIN28 potently promotes the induction of pluripotency via somatic cell reprogramming [25], we performed factor-based reprogramming using wild-type, phospho-null (S200A), or phospho-mimetic (S200D) LIN28 in combination with OCT4, SOX2 and NANOG. Consistent with our earlier data, the S200A and S200D mutants showed lower and higher protein expression than the wild-type, respectively, without concordant mRNA changes (Figure 2.4a). The altered LIN28 protein abundance further appeared insufficient to differentially affect *let-7* (Figure 2.4b). Importantly, however, the S200A and S200D LIN28 led to approximately 50% decreased or increased reprogramming efficiency, respectively, indicating that S200

phosphorylation and its effect on LIN28 have a substantial role in the induction of pluripotency (Figure 2.4c).

We then addressed LIN28's function in ESCs. Since ERK [15] and LIN28 [196, 290] control the transition from naïve to primed pluripotency, we explored the regulation of LIN28 levels in mESCs cultured in serum/LIF versus dual-inhibitor/LIF (2i/LIF) conditions. Consistent with previous reports [196, 290], LIN28 levels were reduced both at the protein and mRNA level in the 2i/LIF culture (Figure 2.4d). To examine whether ERK-dependent post-translational control contributes to this reduction, we performed inhibitor dropout experiments. Short-term removal of the MEK/ERK inhibitor – but not the GSK3β inhibitor – led to a ~30% increase in LIN28 protein but not mRNA, supporting an ERK-mediated protein stabilization model (Figure 2.4e). To confirm that S200 phosphorylation is involved, we replaced endogenous LIN28 with wild-type, phospho-mimetic (S200D), or phospho-null (S200A) LIN28 by expressing respective ORF constructs in mESCs with knocked out LIN28A/B loci. Consistent with our earlier data, the mimetic and null maintained higher and lower protein levels (when cultured in serum), respectively, without analogous mRNA changes (Figure 2.4f). We then performed clonogenic assays upon transfer from 2i/LIF to serum/LIF and assessed the alkaline phosphatase (AP) staining pattern of colonies emerging in the serum/LIF culture, which is characterized by a mix of compact, uniformly AP-positive, naïve-like ("solid") colonies and larger, heterogeneously AP-stained, more primed ("mixed") colonies [196]. The S200D mutant showed a reproducibly lower fraction of solid colonies while the S200A exhibited a higher fraction relative to wild-type LIN28, demonstrating that the higher LIN28 protein level mediated by S200 phosphorylation enhances LIN28's function in promoting the transition from naïve to primed pluripotency (Figure 2.4g). Together, our reprogramming and ESC data demonstrate that LIN28 phosphorylation contributes to the regulation of pluripotency transitions.

Figure 2.4. LIN28A phosphorylation contributes to the regulation of pluripotency transitions. (a) Western blot (left) and qRT-PCR (right) analysis of wild-type (WT), phospho-null (S200A), and phospho-mimetic (S200D) FLAG-LIN28A at day 6 of reprogramming. n=4 independent experiments. Error bars represent s.e.m. P=0.10 (S200A) and P=0.52 (S200D) (two-tailed Student's *t*-test vs. WT). (b) Levels of mature *let-7* miRNAs at day 6 of reprogramming using respective LIN28A constructs. EV = empty vector. n=4 independent experiments. Error bars represent s.e.m. P>0.05 (two-tailed Student's *t*-test vs. WT). (c) TRA-1-60 staining of iPSCs harboring empty vector (EV), wild-type (WT), phospho-null (S200A), or phospho-mimetic (S200D) FLAG-LIN28A (day 21 of reprogramming). Quantification of reprogramming efficiency based on the number of TRA-1-60^{+} colonies is shown on the right. n=4 independent experiments. Error bars represent s.e.m. *P<0.05 (two-tailed Student's *t*-test vs. WT). (d) Western blot (left) and qRT-PCR (right) analysis of endogenous LIN28A in v6.5 mESCs cultured in serum/LIF or 2i/LIF. n=3 independent experiments. Error bars represent s.e.m. *P<0.05 (two-tailed Student's *t*-test). (e) Western blot (left) and qRT-PCR (right) analysis of endogenous LIN28A in v6.5 mESCs after a four-hour dropout of PD0325901 (PD) or CHIR99021 (CH). n=3 independent experiments. Error bars represent s.e.m. P=0.99 (PD) and P=0.89 (CH) (two-tailed Student's *t*-test vs. PD+CH). (f) Western blot (left) and qRT-PCR (right) analysis of transgenic wild-type (WT), phospho-mimetic (S200D), or phospho-null (S200A) FLAG-LIN28A added back in LIN28A/B KO mESCs. n=3 independent experiments. Error bars represent s.e.m. P=0.63 (S200D) and P=0.60 (S200A) (two-tailed Student's *t*-test vs. WT). (g) Alkaline Phosphatase (AP) analysis of mESCs from panel (f) grown at clonal density upon transfer from 2i/LIF to serum/LIF. Representative images of colonies with solid and mixed staining patterns are shown on the left. Scale bar = 100 μm. Quantification of the fraction of solid colonies is shown on the right. n=4 independent experiments. Error bars represent s.e.m. **P<0.01 (two-tailed Student's *t*-test).

Figure 2.4 (Continued)

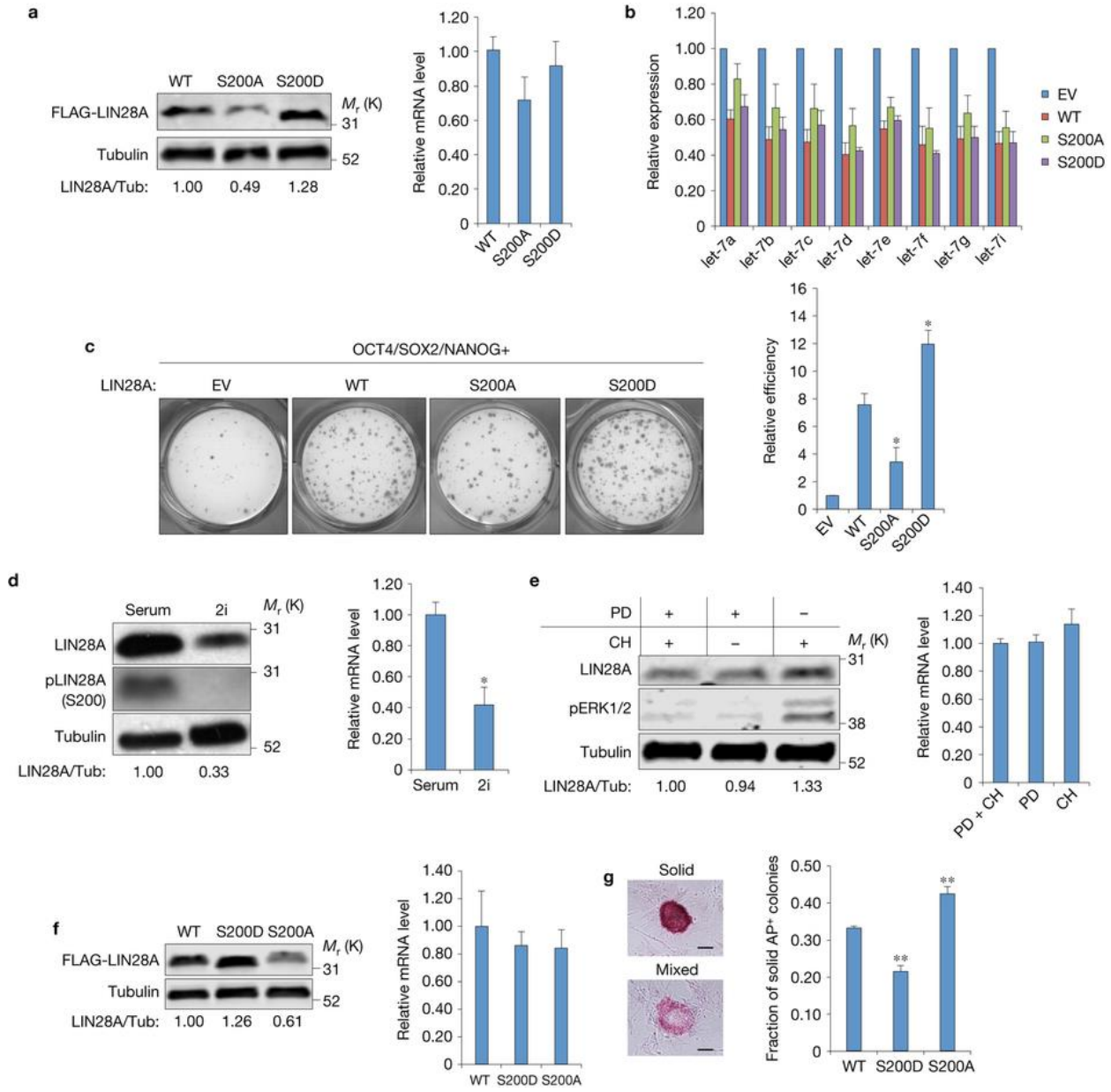

2.3. Discussion.

In sum, our results indicate that LIN28 phosphorylation by MAPK/ERK serves as a molecular link between signaling, post-transcriptional gene regulation, and cell fate control (Figure 2.5). While

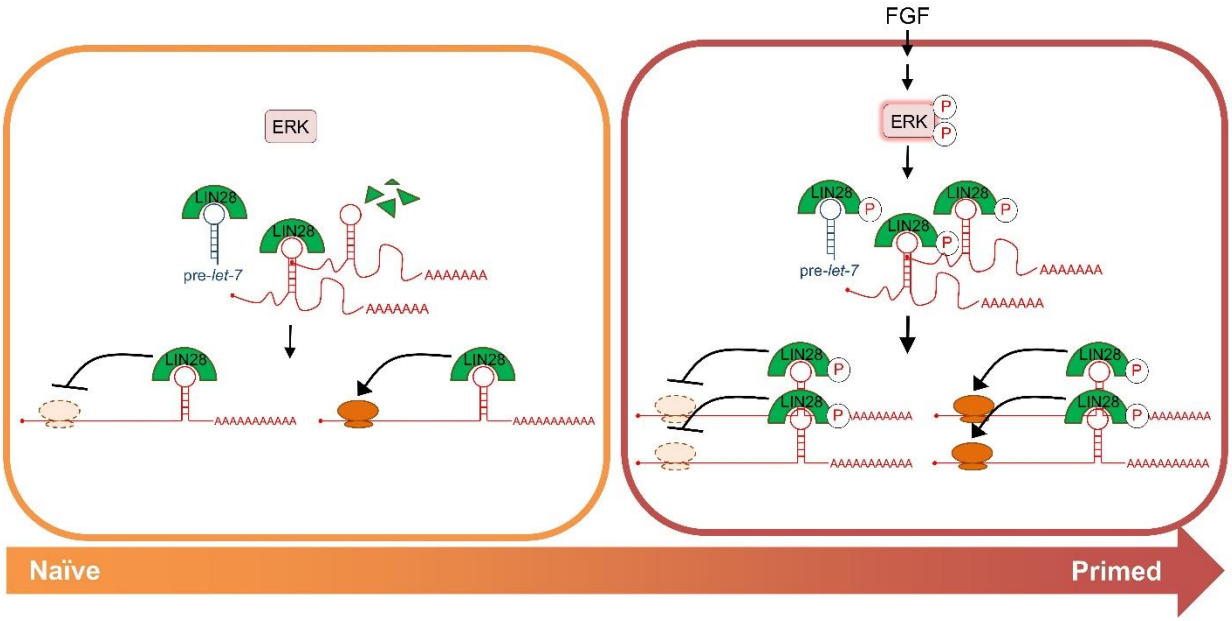

Figure 2.5. Model of the coupling between signaling, post-transcriptional regulation, and cell fate control by the ERK-LIN28 axis. Left: In the absence of fibroblast growth factor (FGF), ERK is inactive, LIN28 is not phosphorylated and thus expressed at a lower level, whereby it can bind and inhibit the processing of *let-7* precursors (pre-*let-7*) and engage with some of its direct mRNA targets to modulate their translation. Right: Upon FGF stimulation, ERK is activated and phosphorylates LIN28, which increases LIN28's protein levels, allowing it to engage with more mRNA targets and enhancing its effect on translation. As indicated on the bottom, this mechanism facilitates the transition from naïve to primed pluripotency.

ERK is known to impact numerous pluripotency transcription factors [447], LIN28 is an RBP and thus represents a distinct mechanism by which ERK signaling regulates gene expression and cell identity. Of note, ERK has also been suggested to regulate LIN28 transcriptionally [196, 330], so it may exert dual regulation on LIN28 to ensure timely and robust control of LIN28 levels. Given the repertoire of pluripotency-associated RBPs [448] and a recent link between ERK and the RBP BRF1 in mESCs [143], other RBPs may be similarly regulated by ERK to modulate cell fate.

Adding to prior findings [196, 290], the ERK-LIN28 coupling reported here further implicates LIN28 as a "priming" factor and suggests that its activity is particularly relevant in guiding transitions between cell states, closely matching its primordial function in *C. elegans* [246]. Given the critical role of timing for these transitions, post-translational mechanisms are well-suited to control LIN28 function. As we and others have mapped multiple phosphorylation sites on LIN28

(Figure 2.1a), additional kinase pathways may also regulate LIN28. Other post-translational modifications, namely acetylation [369] and methylation [273], have also been reported to control LIN28, so LIN28 appears to integrate both extrinsic and intrinsic signals, in line with its role as a key hub of post-transcriptional gene regulation.

Finally, the mechanism described herein highlights the role of LIN28's *let-7*-independent activities in cell fate regulation and may also explain the intriguing observation that LIN28's *let-7*-independent functions precede its *let-7*-mediated ones during cell differentiation and organismal development [295, 304]. A gradual, controlled decrease in LIN28 levels, initiated by protein destabilization, may allow for disengagement of its mRNA targets prior to effects on *let-7*.

2.4. Methods.

Plasmids

For stable expression, FLAG-LIN28A was subcloned in the pBabe-Puro (retroviral) or pSin-Puro (lentiviral) vectors. pBabe-Puro (Addgene plasmid #1764) was a gift from H. Land, J. Morgenstern, and R. Weinberg (Whitehead Institute, USA) [449], and pSin (Addgene plasmid #16578) was a gift from J. Thomson (University of Wisconsin Madison, USA) [25]. Phospho-mimetic and phospho-null mutants were generated using the QuikChange Lightning site-directed mutagenesis kit (Agilent Technologies), as per manufacturer's protocol. pMCL-HA-MEK1 wild-type, constitutively active (R4F), and kinase-dead (K97M) plasmids (Addgene plasmids #40808, 40810, 40811) were gifts from N. Ahn (University of Colorado Boulder, USA) [446].

Cell Culture

iLIN28A [313], v6.5 [450], and LIN28A/B KO [312] mESCs were maintained on irradiated CF1 MEFs (GlobalStem) in mESC medium (DMEM, 15% FBS, 1 U/ml Penicillin, 1 µg/ml Streptomycin, 2 mM L-glutamine, 0.1 mM NEAA, 0.1 mM BME, 1,000 U/ml LIF). hESCs (CHB6, NIH#0006), MSC-iPSCs [23], and BJ1-iPSCs [23] were maintained in hESC medium (DMEM/F12, 20%

KOSR, 1 U/ml Penicillin, 1 µg/ml Streptomycin, 2 mM L-glutamine, 0.1 mM NEAA, 0.1 mM BME, 4 ng/ml FGF). PA1 (ATCC# CRL-1572), NCCIT (ATCC# CRL-2073), HeLa (ATCC# CCL-2), and 293T cells were maintained in DMEM/10% FBS. 293T(RMCE) cells were a gift from E. Makeyev (Nanyang Technological University, Singapore); LIN28-expressing lines were generated following published protocols [451]. HeLa Flp-In cell lines were generated as described previously [278]. 2i/LIF culture was performed following published protocols [15]. No cell lines used in this study were found in the database of commonly misidentified cell lines that is maintained by ICLAC and NCBI Biosample. The cell lines were not authenticated. The cell lines were tested mycoplasma-negative.

Transfections

For plasmid transfections, 293T cells were seeded at 4 x 10^5 cells/well in 6-well plates, transfected with 2 ug respective plasmid 16-20 hours later using X-tremeGENE 9 (Roche), and analyzed after another 48 hours. For siRNA transfections, PA1 cells were seeded at 3 x 10^5 cells/well in 6-well plates, transfected with 0.25 pmol siRNA 16-20 hours later using Lipofectamine RNAiMAX (Invitrogen), and harvested by trypsinization after another 96 hours. The following siRNAs were used: siNC (Ambion #4390843); siLIN28A (Ambion #4392420-s36195).

Viral Production and Stable Cell Line Generation

Viral production was carried out as described previously [290]. Transgenic PA1 and HeLa cells were generated by transduction with unconcentrated viral supernatant and selection with 1 ug/ml Puromycin. HeLa-LIN28A clones were derived by isolation and expansion of single cells from a heterogeneous pool of stable transductants. For transgenic mESC generation, lentivirus was concentrated using the Lenti-X Concentrator (Clontech) and used for transduction in 2i/LIF medium, followed by selection with 1 ug/ml Puromycin.

Drug Treatments

Drugs used were: Calyculin A (Cell Signaling), Torin1 (Tocris), PD0325901 (Stemgent), SB203580 (Invivogen), SP600125 (Sigma), Kenpaullone (Sigma), LY294002 (Cell Signaling), bFGF (Gemini), EGF (Peprotech), PMA (Cell Signaling), CHX (Sigma), and Doxycycline (Sigma). Treatment conditions are described in detail in the text.

Affinity Purification

For mass spectrometry analysis, iLIN28A mESCs were treated with: (i) 1 μg/ml Doxycycline (Sigma) for 48 hours to induce FLAG-LIN28A expression, and (ii) 100 nM Calyculin A (Cell Signaling) for 30 minutes immediately prior to harvest to enrich for phosphorylation events. Cells were harvested in cold PBS and immediately lysed in M2 lysis buffer (50 mM Tris-HCl pH 7.5, 150 mM NaCl, 1 mM EDTA, 1% Triton X-100) containing 2X protease and phosphatase inhibitors (Pierce). FLAG-tagged LIN28 variants were purified using the anti-FLAG M2 affinity gel following the manufacturer's specifications (Sigma).

Mass Spectrometry

Affinity purified proteins were separated on a 4-20% polyacrylamide gel (Bio-Rad) and visualized using the Bio-Safe Coomassie Stain (Bio-Rad). The band containing FLAG-LIN28A was excised and treated with dithiotriethol to reduce disulfide bonds and iodoacetamide to alkylate cysteines. In-gel digestion of the protein was performed with trypsin or chymotrypsin. The resulting peptides were extracted from the gel and analyzed by liquid chromatography tandem mass spectrometry (LC-MS/MS), as described previously [452]. All peptide matches were filtered based on mass accuracy, tryptic state (for trypsin), and XCorr, and confirmed by manual inspection. The reliability of site-localization of phosphorylation events was evaluated using the Ascore algorithm [453].

Antibody Generation

Human and mouse-reactive pLIN28(S200) rabbit polyclonal antibodies were produced by immunizing animals with a synthetic phosphopeptide corresponding to residues surrounding S200 of human or mouse LIN28A, respectively. Antibodies were purified by protein A and peptide affinity chromatography. The human-reactive antibody was generated by Cell Signaling (Danvers, MA) and the mouse-reactive antibody by GenScript (Piscataway, NJ).

Western Blot

Cells were lysed in RIPA buffer containing protease and phosphatase inhibitors (Pierce). Proteins were separated on a 4-20% polyacrylamide gel (Bio-Rad) and transferred to a methanol-activated PVDF membrane (Millipore). The membrane was blocked for 30-60 minutes in 3%BSA/PBST (chemiluminescent blots) or 3%BSA/PBS (fluorescent blots), and probed with primary antibodies at 4°C overnight. Secondary antibody incubation was performed at room temperature for 1-2 hours. Protein levels were detected using the SuperSignal West Pico and Femto Luminol reagents (Thermo Scientific) or the Odyssey CLx near-infrared fluorescence imaging system (LI-COR). Primary antibodies used were: anti-pLIN28(S200) (generated as described above; 1:1,000), anti-LIN28A (Cell Signaling #3978; 1:1,000), anti-α/β-tubulin (Cell Signaling #2148; 1:1,000), anti-pERK1/2 (Sigma E7028; 1:1,000), anti-ERK1/2 (Cell Signaling #4695, clone 137F5; 1:1,000), anti-FLAG (Sigma F3165, clone M2; 1:1,000), anti-Actin (Santa Cruz sc-1616; 1:2,000), anti-HA (Sigma H6533, clone HA-7; 1:1,000), anti-RPS13 (Abcam ab104862; 1:1,000), anti-RPL23 (Proteintech #16086-1-AP; 1:1,000), anti-NDUFB3 (Abcam ab55526; 1:1,000), anti-NDUFB8 (Abcam ab110242, clone 20E9DH10C12; 1:1,000), anti-NDUFB10 (Proteintech #15589-1-AP; 1:1,000). Secondary antibodies used were: for chemiluminescence, HRP-conjugated anti-rabbit IgG (GE Healthcare NA934, 1:2,000), anti-mouse IgG (GE Healthcare NA931; 1:2,000), and anti-goat IgG (Santa Cruz sc-2020; 1:2,000); for fluorescence, IRDye 680RD anti-rabbit IgG (LI-COR #925-68071; 1:20,000), IRDye 800CW anti-mouse IgG (LI-COR

#925-32210; 1:20,000), and IRDye 680RD anti-goat IgG (LI-COR #925-68074; 1:20,000). Quantifications were performed using ImageJ (chemiluminescent blots) or Image Studio for Odyssey CLx (fluorescent blots) (LI-COR).

Quantitative RT-PCR

Total RNA was isolated using Trizol (Invitrogen) combined with miRNeasy columns (Qiagen). 100-250 ng RNA were reverse-transcribed using the miScript II RT kit (Qiagen) and subjected to miScript miRNA assays (Qiagen) or standard mRNA assays. miRNA and mRNA expression was measured by SYBR Green quantitative PCR using the ΔΔCt method. U6 and β-actin were used for normalization of miRNA and mRNA measurements, respectively. Primers used were: hLIN28A (F: GAGCATGCAGAAGCGCAGATCAAA; R: TATGGCTGATGCTCTGGCAGAAGT); FLAG-hLIN28A (F: ATGACGACAAGGGCTCCG; R: CGCACGTTGAACCACTTACA); hACTB (F: AGAAGGATTCCTATGTGGGCG; R: CATGTCGTCCCAGTTGGTGAC); mLin28a (F: AGGCGGTGGAGTTCACCTTTAAGA; R: AGCTTGCATTCCTTGGCATGATGG); mActB (F: CAGAAGGAGATTACTGCTCTGGCT; R: TACTCCTGCTTGCTGATCCACATC); hRPS13 (F: TCCCAGTCGGCTTTACCCTAT; R: CAGGATTACACCGATCTGTGAAG); hRPL23 (F: TCCTCTGGTGCGAAATTCCG; R: CGTCCCTTGATCCCCTTCAC); hNDUFB3 (F: GCTGGCTGCAAAAGGGCTA; R: CTCCTACAGCTACCACAAATGC); hNDUFB8 (F: CCGCCAAGAAGTATAATATGCGT; R: TATCCACACGGTTCCTGTTGT); hNDUFB10 (F: AGCCCAATCCCATCGTCTACA; R: GCTGCCGCTCTATAAATTCTCT); pri/pre-let-7a (F: TGAGGTAGTAGGTTGTATAGTTTTAGGG; R: GGAAAGACAGTAGATTGTATAGTTATC); pri/pre-let-7b (Qiagen #MP00000028); pri/pre-let-7c (Qiagen #MP00000035); pri/pre-let-7d (Qiagen #MP00000042); pri/pre-let-7e (Qiagen #MP00000049); pri/pre-let-7g (Qiagen #MP00000070); pri/pre-let-7i (Qiagen #MP00000077); let-7a (Qiagen #MS00032179); let-7b (Qiagen #MS00001225); let-7c (Qiagen #MS00005852); let-7d (Qiagen #MS00001232); let-7e

(Qiagen #MS00032186); let-7f (Qiagen #MS00005866); let-7g (Qiagen #MS00010983); let-7i (Qiagen #MS00001253); U6 (Qiagen #MS00033740).

RNA Immunoprecipitation

FLAG-tagged LIN28A variants were purified using the protocol described earlier, with the following modifications: (i) Calyculin A was omitted; (ii) 100 U/ml RNasin (Promega) was included in the lysis and wash buffers; (iii) RNA was isolated from the beads by resuspension in Trizol (Invitrogen). Parental PA1 or HeLa Flp-In cells (no FLAG) were used as controls for antibody specificity. RNA purification and qRT-PCR were performed as described earlier. The ΔΔCt method was used to calculate enrichment, whereby RIP Ct values were normalized to the corresponding input and no-FLAG control Ct values. RNA-seq was performed as described below.

RNA Sequencing

Total RNA >200 nt was isolated using Trizol (Invitrogen) combined with RNeasy columns (Qiagen). 50 ng purified RNA was subjected to poly(A) selection using the NEBNext Poly(A) mRNA Magnetic Isolation Module (NEB) and subsequently used for library preparation with the NEBNext Ultra RNA Library Prep Kit (NEB). Libraries were analyzed on a Bioanalyzer (Agilent) for quality control, quantified using the Qubit dsDNA HS Assay (Invitrogen) and qRT-PCR (Kapa Biosystems), and equimolar pools were sequenced on HiSeq 2500 or NextSeq 500 instruments (Illumina) using 50-bp or 76-bp single-end protocols, respectively. Expression values (RPKM) were estimated using the TopHat [454] and HTSeq-count tools [455], and lowly expressed genes (RPKM≤10) were filtered out. Enrichment scores for each gene were calculated by dividing the RPKM value of the target protein RIP by the RPKM value of the no-FLAG control RIP after normalization of each RIP value to its respective input value.

Reprogramming

Reprogramming assays were performed essentially as described previously [290]. Briefly, dH1f fibroblasts were seeded at 2.5 x 10^5 cells/well in a 12-well plate and transduced overnight with a pool of lentiviral (OCT4, SOX2, NANOG) and retroviral (LIN28A variants) particles. Six days later, cells were trypsinized and 1-2 x 10^5 cells/well were re-plated onto MEF-coated 12-well plates. Medium was switched to hESC medium and changed daily until day 21 when reprogramming efficiency was measured. To do so, cells were fixed with 4% paraformaldehyde and stained with biotin-anti-TRA-1-60 (eBioscience #13-8863-82; 1:250) and streptavidin-HRP (Biolegend #405210; 1:500) primary and secondary antibodies, respectively. Staining was developed with the DAB Peroxidase kit (Vector Labs), and the number of iPSC colonies was quantified using ImageJ. Experiments were carried out and analyzed in a blinded manner.

Clonal Assay

mESCs maintained in 2i/LIF were seeded on MEF-coated 6-well plates at clonal density (500 cells/well) and allowed to grow for 5 days. At this point, cells were stained using the Leukocyte Alkaline Phosphatase kit (Sigma) and classified as showing either solid or mixed alkaline phosphatase staining by visual inspection, as described previously [196].

Statistics and Reproducibility

All experiments were performed at least three independent times (unless noted otherwise) and respective data used for statistical analyses. Differences between groups were assessed using a two-tailed Student's *t*-test in Microsoft Excel, with data assumed to fulfill *t*-test requirements. For RIP-seq analysis, differences were assessed using paired *t*-tests and the Benjamini-Hochberg correction for multiple hypotheses testing. Statistical significance is displayed as $P<0.05$ (one asterisk) or $P<0.01$ (two asterisks). Error bars indicate s.e.m. Sample sizes and reproducibility for each experiment are described in the respective figure legends.

Data Availability

RNA-sequencing data that support the findings of this study have been deposited in the Gene Expression Omnibus (GEO) under accession code GSE83906. Proteomics data have been deposited in the Mass spectrometry Interactive Virtual Environment (MassIVE) under ID# MSV000080302. All other data supporting the findings of this study are available from the corresponding author upon reasonable request.

AUTHOR CONTRIBUTIONS

This chapter was partially adapted from [456] (text and all figures except Figure 2.5) and [441] (Figure 2.5). K.M. Tsanov designed and performed most experiments, and wrote the manuscript. D.S. Pearson prepared RNA-seq libraries (for Figure 2.4d and Supplementary Figure 2.4e), generated and analyzed HeLa clonal series (Supplementary Figure 2.4a). Z. Wu performed reprogramming experiments (Figure 2.4c). A. Han performed RNA-seq bioinformatics analysis. R. Triboulet and R.I. Gregory shared unpublished results and generated the isogenic HeLa (Flp-In) cells. M.T. Seligson helped with qRT-PCR expression analysis. J.T. Powers and J.K. Osborne helped with experimental design. S. Kane generated the human pLIN28A antibody. S.P. Gygi supervised the proteomics experiments. G.Q. Daley designed and supervised experiments, and edited the manuscript.

ACKNOWLEDGMENTS

We thank P. Sharp, L. Cantley, G. Ruvkun, and members of the Daley lab for invaluable discussions, A. De Los Angeles for critical feedback on the manuscript, X. Wu/Yi Zhang's lab and R. Rubio/DFCI CCCB for assistance with RNA-seq, and R. Tomaino at the Taplin Biological Mass Spectrometry Core for assistance with mass spectrometry. Bioanalyzer analysis was performed in the BCH IDDRC Molecular Genetics Core, which is supported by NIH (NIH-P30-HD 18655).

Sequencing analysis was conducted on the Orchestra High Performance Computing Cluster at Harvard Medical School. K.M. Tsanov was an HHMI International Student Research Fellow and a Herchel Smith Graduate Fellow. D.S. Pearson was supported by a grant from NIGMS (T32GM007753). R.I. Gregory was supported by a grant from NIGMS (R01GM086386). G.Q. Daley was an investigator of the Howard Hughes Medical Institute and the Manton Center for Orphan Disease Research, and was supported by a grant from NIGMS (R01GM107536).

CHAPTER 3

A Novel Role for the Terminal RNA Uridylyltransferases ZCCHC6/TUT7 and ZCCHC11/TUT4 in Oncogenesis

3.1. Introduction.

Oncogenesis is governed by complex gene expression programs, at the core of which lies the cellular transcriptome: the set of mRNA transcripts expressed in the cell [457]. The transcriptome is shaped by the dynamic balance of mRNA transcription and decay. While there is substantial knowledge about the role of transcription in cancer [457], much less is known about the contribution of mRNA turnover mechanisms [155, 458, 459] (see Chapter 1.2).

Non-templated 3' uridylation of mRNAs, carried out by the TUTases ZCCHC6/TUT7 and ZCCHC11/TUT4, has recently been recognized as a mechanism that promotes global mRNA decay [401] (see Chapter 1.4). It has further been implicated in mRNA regulation through multi-faceted effects on miRNA biogenesis and function [233]. Although these mechanisms are deeply conserved in evolution, the functional roles of ZCCHC6/11 and their homologs in normal and pathological processes are only beginning to be unraveled [374]. A number of studies have linked these TUTases to the cell cycle [379, 431, 433, 434], apoptosis [405], organismal growth [424], immunity [425], development [426, 440], and cancer [255, 439]. In cancer, ZCCHC6/11 have been studied in the context of the LIN28 pathway, where they participate in the inhibition of the *let-7* miRNA family [255, 439] (see Chapter 1.3). Apart from this particular setting, the role of these TUTases in oncogenesis is currently unknown.

Here, we show that ZCCHC6/11 are highly expressed in diverse types of cancer, extending beyond contexts with LIN28A/B expression. ZCCHC6/11 further contribute to the oncogenic transformation of normal fibroblasts and support the growth and tumorigenicity of established cancer cell lines in a LIN28A/B- and miRNA-independent manner. Mechanistically, these effects were associated with altered mRNA uridylation and turnover, including dysregulation of cell cycle factors and concomitant cell cycle impairment. Interestingly, we also report that these TUTases promote a less differentiated cell state in both mESCs and lineage-restricted muscle progenitors. Together, our results reveal novel functions for ZCCHC6/11 and implicate uridylation-mediated mRNA turnover as a mechanism of oncogenesis.

3.2. Results.

ZCCHC6/11 are expressed in select normal tissues and diverse types of cancer

To gain insight into the involvement of ZCCHC6/11 in cancer, we profiled their expression across a range of normal and malignant contexts. First, we performed Western blot analysis of 14 normal human tissues, which indicated that these TUTases – and especially ZCCHC6 – are expressed only in a subset of adult tissues (Figure 3.1a). Of note, human ZCCHC6/11 have multiple predicted isoforms, only the largest of which (171 kD for ZCCHC6 and 185 kD for ZCCHC11) are known to be catalytically active [379], so the protein analysis focused on these isoforms. Second, we surveyed mRNA expression data from diverse types of human tumor tissues, which revealed that about 30% of tumors across cancer types express high levels of ZCCHC6/11 (Figure 3.1b; Supplementary Figure 3.1a). Western blot analysis was then conducted for a small set of normal and tumor tissue samples from colorectal cancer patients. Intriguingly, we observed strong re-activation of ZCCHC6/11 protein expression in about half of the tumors (relative to normal mucosa), suggesting that the mRNA data may underestimate the extent of ZCCHC6/11 protein upregulation in cancer (Supplementary Figure 3.1b). Of note, a survey of available genomic data revealed low frequency of ZCCHC6/11 mutations, deletions and amplifications in human tumors, indicating that the changes in TUTase expression are unlikely to be due to genetic alterations (Supplementary Figure 3.2). Finally, we assembled a panel of 30 cancer cell lines representing six different cancer types and performed Western blot analysis. Strikingly, the majority of cell lines expressed ZCCHC6 and/or ZCCHC11, typically at much higher levels relative to normal fibroblasts (Figure 3.1c). Comparison between the normal and cancer expression data pointed to

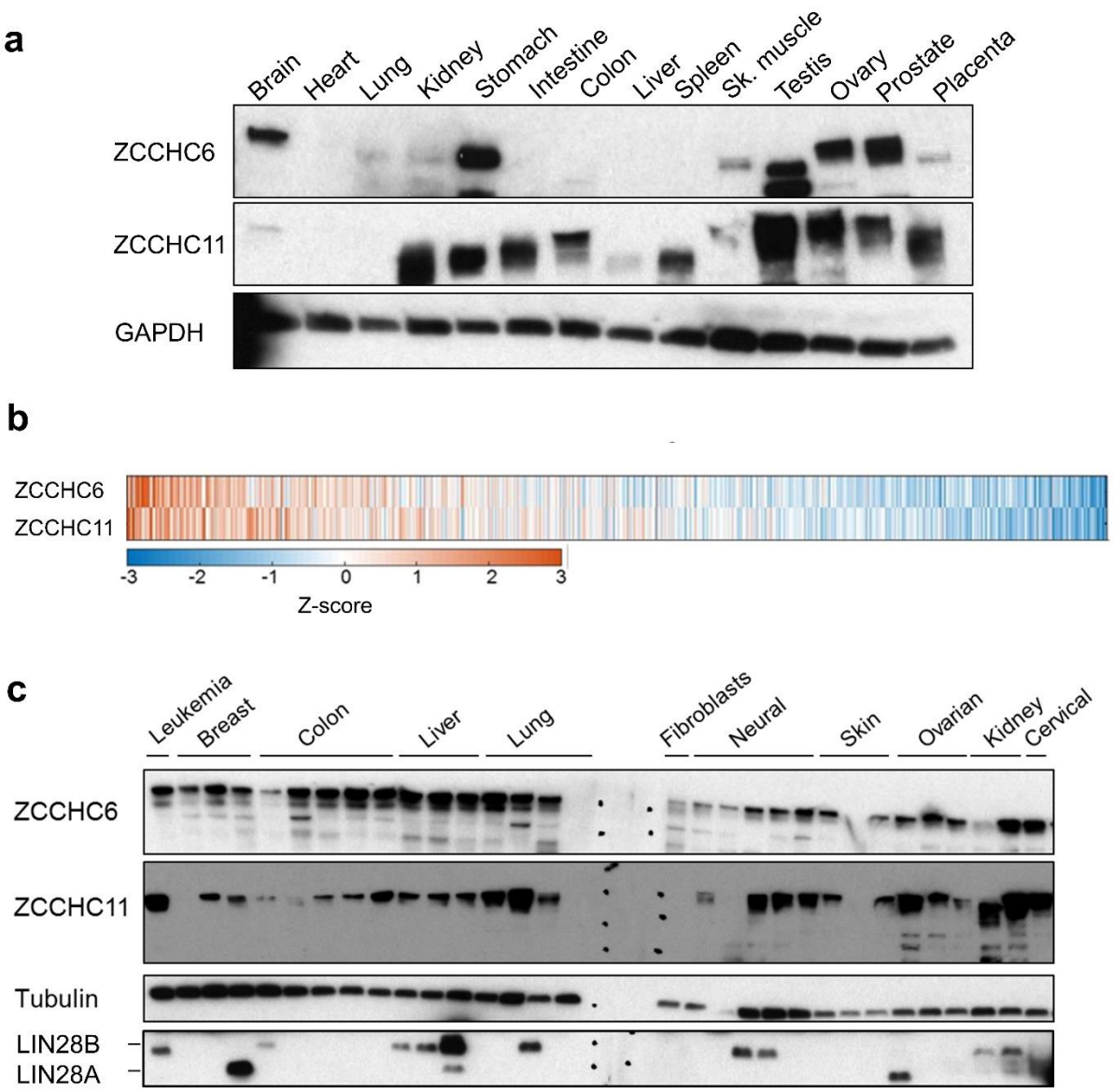

Figure 3.1. ZCCHC6/11 expression in normal and cancer tissues and cell lines. (a) Western blot analysis of ZCCHC6/11 in human tissues from healthy adults. (b) RNA-seq analysis of ZCCHC6/11 in human tumor samples from different types of cancer. Each bar represents an individual patient. Distribution by cancer type is shown in Supplementary Figure 3.1. Data were obtained from cBioPortal (www.cbioportal.org) [1]. (c) Western blot analysis of ZCCHC6/11 and LIN28A/B in human cancer cell lines representing different types of cancer. BJ1 fibroblasts are included as a reference for normal tissue. Cell line identity is provided in the Methods.

several tumor types that appear to highly express ZCCHC6/11 specifically in the cancer context (e.g. colon, lung and liver), suggesting that these TUTases may become upregulated during

tumorigenesis. Importantly, ZCCHC6/11 expression was much broader and did not correlate with LIN28A/B expression, pointing to LIN28-independent roles of these TUTases (Figure 3.1c).

ZCCHC6/11 contribute to oncogenic transformation

In light of these expression data, we then asked whether ZCCHC6/11 play a role in oncogenic transformation. To address this question, NIH3T3 fibroblast cell lines that are double-knockout (DKO) for both ZCCHC6 and ZCCHC11 were generated using CRISPR/Cas9 technology (Figure 3.2a); these cell lines were then transformed by expressing oncogenic $KRAS^{G12V}$ and subjected to a number of assays. First, we assessed their proliferative capacity, which was unchanged in the DKO versus control cells, indicating that ZCCHC6/11 do not affect proliferation in this context (Figure 3.2b). Second, we performed colony-forming assays in soft agar to assess anchorage-independent growth. Unlike the proliferation data, DKO cells showed a 60-70% reduction in colony numbers compared to control cells, suggesting that ZCCHC6/11 contribute to $KRAS^{G12V}$-induced transformation (Figure 3.2c). In support of this conclusion, allograft assays further demonstrated impaired tumorigenicity of the DKO cells *in vivo* (Figure 3.2d). Lastly, we performed migration assays, which revealed an approximately 70% reduced migratory capacity of the DKO cells relative to the controls (Figure 3.2e). Collectively, these data indicate that ZCCHC6/11 can affect multiple oncogenic properties and contribute to cellular transformation.

ZCCHC6/11 support the growth and tumorigenicity of cancer cell lines

Next, we wanted to determine if ZCCHC6/11 are required for the growth and tumorigenicity of established cancer cells. To this end, we performed CRISPR/Cas9-mediated population-based TUTase depletion in cell lines representing different types of cancer. Three cell lines – HCT116 (colon), MCF7 (breast) and H1299 (lung) – exhibited impaired proliferation upon TUTase depletion, while another one – U2OS (osteosarcoma) – did not (Figure 3.3a). Interestingly,

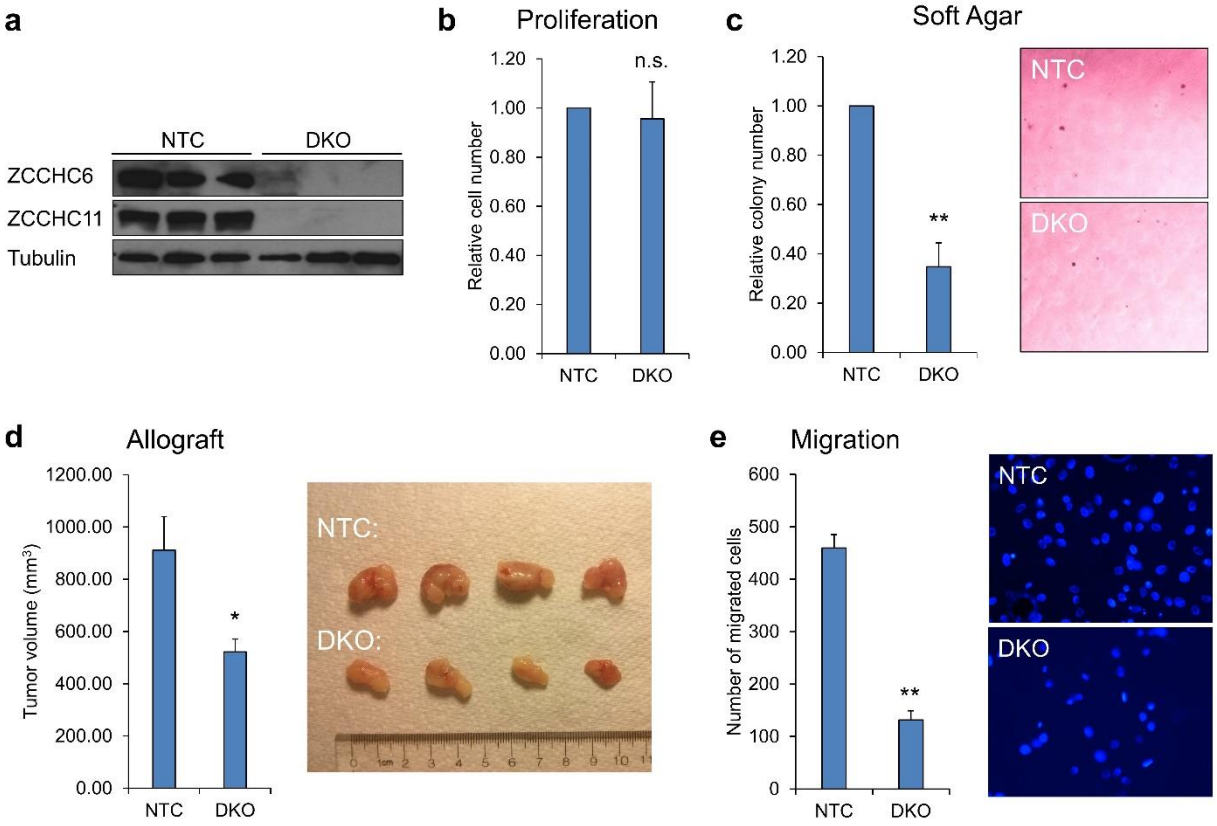

Figure 3.2. ZCCHC6/11 contribute to oncogenic transformation. (a) Western blot analysis of non-targeting control (NTC) or ZCCHC6/11 double-knockout (DKO) NIH3T3 cells. (b) Proliferation analysis of NTC and DKO NIH3T3-KrasG12V cells. Error bars indicate s.e.m. (n=3); n.s. = non-significant (P>0.05). (c) Colony formation in soft agar of NTC and DKO NIH3T3-KrasG12V cells. Quantification (left) and representative images (right) of colonies are shown. Error bars indicate s.e.m. (n=3); **P<0.01. Magnification: 4X. (d) Allograft analysis of NTC and DKO NIH3T3-KrasG12V cells. End-point tumor volume measurements (left) and representative tumor images (right) are shown. Error bars indicate s.e.m. (n=5); *P<0.05. Data are representative of two independent pairs of clones. (e) Transwell migration analysis of NTC and DKO NIH3T3-KrasG12V cells. Quantification (left) and representative images (right) of migrated cells are shown. Error bars indicate s.e.m. (n=3); **P<0.01. Magnification: 10X. Data are representative of two independent pairs of clones.

ZCCHC6 depletion alone was sufficient to cause impaired proliferation in HCT116 and MCF7 cells, while both ZCCHC6 and ZCCHC11 had to be depleted to impair proliferation in H1299 cells (Figure 3.3a and data not shown), suggesting that the reported functional redundancy of these TUTases [260] may be context-dependent. We then assessed the impact of TUTase depletion in tumorigenic assays. Using HCT116 cells as a model, we observed decreased colony-forming ability in soft agar and reduced tumorigenic growth in xenograft assays in the ZCCHC6-depleted

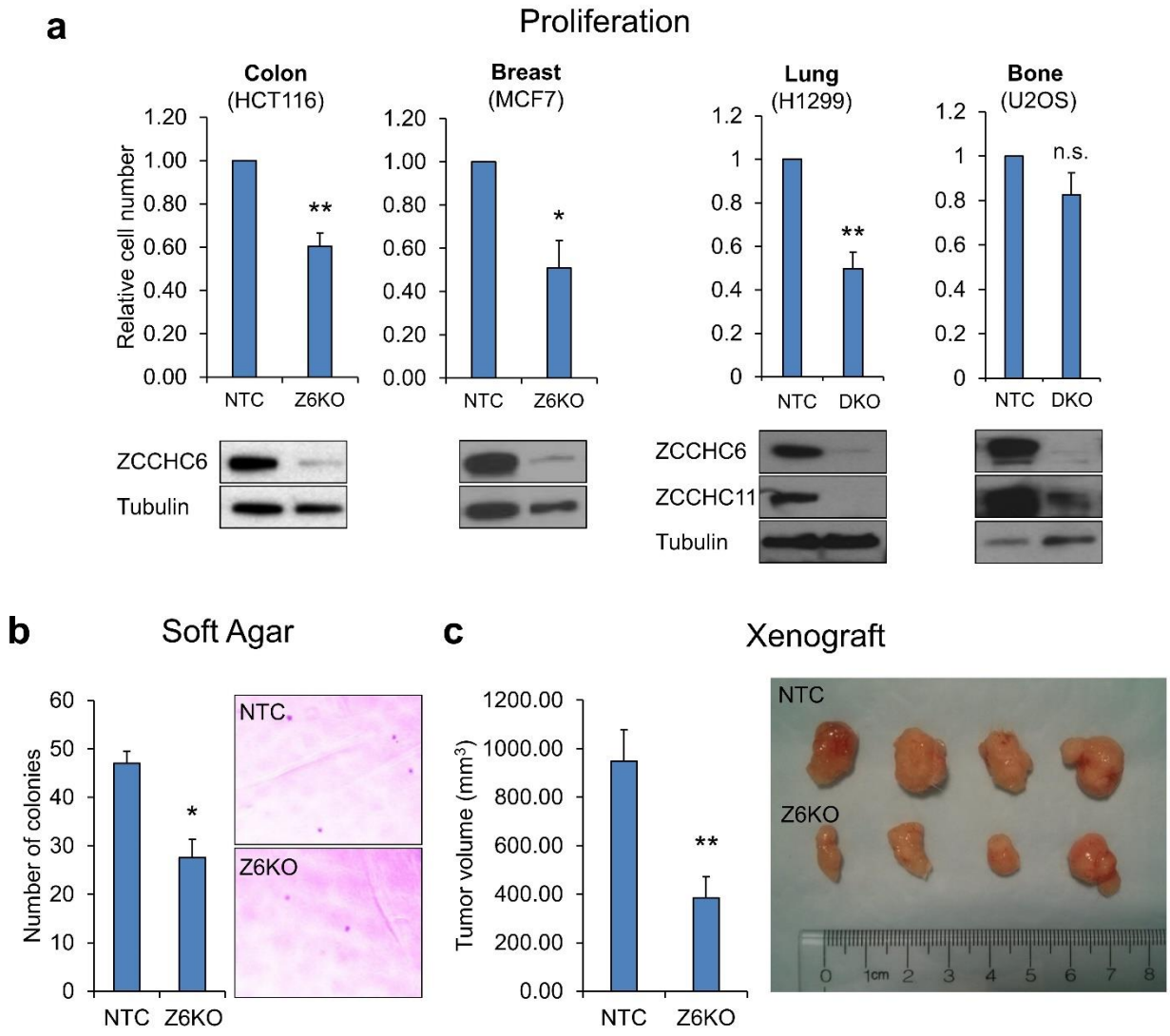

Figure 3.3. ZCCHC6/11 support the growth and tumorigenicity of cancer cell lines. (a) Proliferation analysis of representative TUTase-dependent cell lines after CRISPR/Cas9-mediated knockout using GFP-targeting control sgRNAs (NTC), ZCCHC6-targeting sgRNAs (Z6KO), or ZCCHC6/11-targeting sgRNAs (DKO). Error bars indicate s.e.m. (n=3); *P<0.05; **P<0.01. (c) Colony formation in soft agar of NTC and Z6KO HCT116 cells. Error bars indicate s.e.m. (n=3); *P<0.05. (d) Xenograft analysis of NTC and Z6KO HCT116 cells. End-point tumor volume measurements (left) and representative tumor images (right) are shown. Error bars indicate s.e.m. (n=7); **P<0.01.

cells compared to controls (Figure 3.3b,c). Importantly, HCT116 and MCF7 cells do not express LIN28A/B (Figure 3.1c), indicating that the observed effects cannot be attributed to ZCCHC6/11's roles in the LIN28 pathway. Taken together, these results demonstrate that ZCCHC6/11 support the proliferative and tumorigenic properties of established cancer cell lines, and can do so in a LIN28-independent manner.

ZCCHC6 promotes mRNA uridylation and turnover in cancer cells

We then proceeded to explore the molecular basis of the observed cancer cell line phenotypes. As ZCCHC6/11 have been shown to regulate both miRNAs and mRNAs [374], we first asked if the phenotypes are due to their miRNA-directed activity. To do so, we performed proliferation assays using an isogenic pair of HCT116 cell lines that either express wild-type *DICER1* ($DICER^{WT}$) or are homozygous for a hypomorphic *DICER1* allele ($DICER^{Ex5}$) and thus deficient in mature miRNAs [460]. Upon ZCCHC6 knockdown, we observed comparable reduction in proliferation between the two cell lines (versus control knockdowns), suggesting that the effects of ZCCHC6 are miRNA-independent and implicating its mRNA-specific activity (Figure 3.4a).

To assess this mRNA-based activity, we employed the recently developed TAIL-seq method for global investigation of the 3' mRNA terminome [372]. ZCCHC6 knockdown resulted in dramatically reduced mRNA uridylation on a transcriptome-wide scale (relative to the control knockdown), indicating that ZCCHC6 uridylates mRNAs in HCT116 cells (Figure 3.4b,c). To examine if the decreased uridylation impacts mRNA turnover, we then performed mRNA half-life measurements after ZCCHC6 or control knockdown using actinomycin D chase coupled with RNA-seq (Figure 3.4d). Our data revealed a global increase of mRNA half-life upon ZCCHC6 depletion, demonstrating that ZCCHC6 promotes mRNA turnover (Figure 3.4e). Half-life measurements of representative mRNA transcripts were further validated by qRT-PCR analysis (Supplementary Figure 3.3a). We also measured the half-lives of selected short non-coding RNAs under the same experimental conditions, which did not indicate a difference between ZCCHC6-depleted and control cells (Supplementary Figure 3.3b). Together with our $DICER^{Ex5}$ data (Figure 3.4a), these results further implicate mRNAs (or other polyadenylated RNAs) as functionally relevant TUTase targets, at least in this context.

Figure 3.4. ZCCHC6 promotes mRNA uridylation and turnover in cancer cells. (a) Proliferation analysis of $DICER^{WT}$and $DICER^{Ex5}$ HCT116 cells after knockdown with a control (siNC) or ZCCHC6 (siZ6) siRNA. Error bars indicate s.e.m. (n=3); **P<0.01 (siZ6 vs. siNC); n.s. = non-significant (P>0.05). Western blot validation of ZCCHC6 knockdown is shown on the bottom. (b-c) TAIL-seq analysis of mRNA uridylation in siNC and siZ6 HCT116 cells. Schematic (b) depicts experimental workflow and graphs (c) show uridylation frequency data from three independent experiments. Fraction of mRNA reads among the total poly(A)+ reads is shown for each poly(A) tail size range. Light blue refers to non-uridylated reads, while darker shades represent reads with different numbers of uridines added, as indicated. (d-e) Transcriptome-wide mRNA half-life analysis in siNC and siZ6 HCT116 cells. Schematic (d) depicts experimental workflow and graphs (e) show average mRNA half-life on a per gene basis (left) or aggregated (right). Data represent the average of three independent experiments. $P=2.2 \times 10^{-16}$.

Figure 3.4 (Continued)

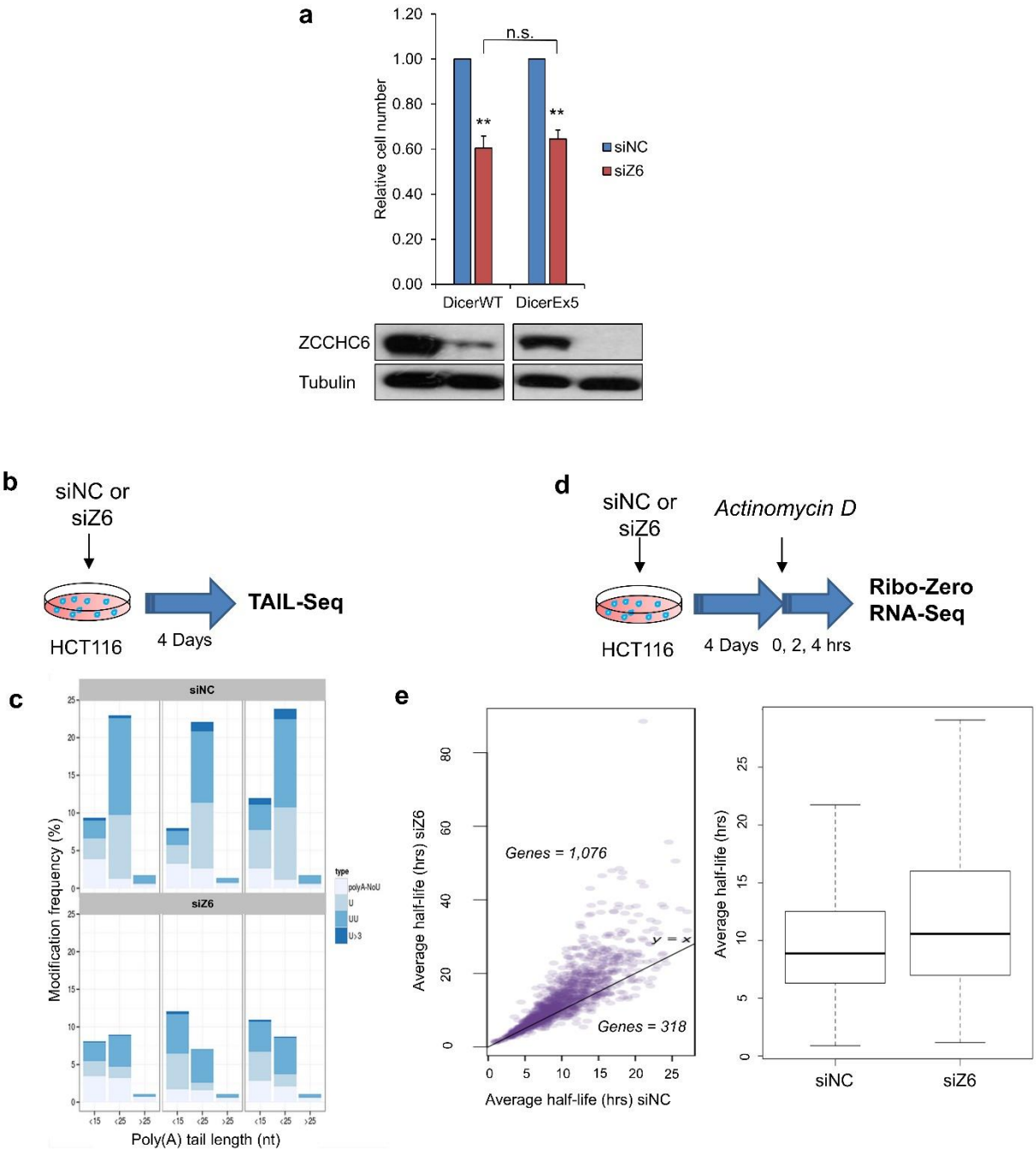

Lastly, we performed RNA-seq analysis of steady-state mRNA levels, which revealed little difference between ZCCHC6-depleted and control cells (Supplementary Figure 3.4). We employed two alternative library preparation strategies, poly(A) selection and rRNA depletion, to avoid potential bias against the preferentially uridylated short poly(A) tails [372]. The two strategies yielded comparable results, ruling out transcript bias as the reason for lack of considerable changes in mRNA levels (Supplementary Figure 3.4c). These data suggest that ZCCHC6 activity may be particularly relevant to maintaining mRNA flux rather than steady-state mRNA levels, which warrants further investigation. Collectively, our findings demonstrate that ZCCHC6 uridylates mRNAs and enhances their turnover in cancer cells.

ZCCHC6 regulates the cell cycle in cancer cells

How does the altered mRNA turnover cause impaired proliferation? To address this question, we performed gene ontology (GO) analysis of the transcripts with significantly increased mRNA half-lives. Interestingly, the top GO categories all involved aspects of the cell cycle, such as “regulation of cell cycle process,” “mitotic cell cycle” and “cell cycle phase transition,” and included histones and cell cycle regulatory genes such as *CDKN1A*, *CHEK2* and *BUB1* (Figure 3.5a,b). These data suggested that ZCCHC6 may regulate cell cycle progression, which we examined further. HCT116 cells were synchronized in S-phase by double-thymidine block and ZCCHC6 expression profiled every two hours after block release (we also profiled expression of key cyclins as markers for different cell cycle phases). ZCCHC6 showed a marked upregulation at the end of S-phase, suggesting that its function may be particularly relevant to the exit from S-phase (Figure 3.5c). To test this hypothesis, we then performed cell cycle profiling in HCT116 cells after ZCCHC6 or control knockdown. This analysis revealed an increased fraction of ZCCHC6-depleted cells in S-phase, consistent with a role for ZCCHC6 in promoting the S-to-G2 transition (Figure 3.5d). Together, these data indicate that ZCCHC6 regulates the cell cycle in cancer cells, which likely contributes to the observed proliferation phenotypes upon TUTase depletion.

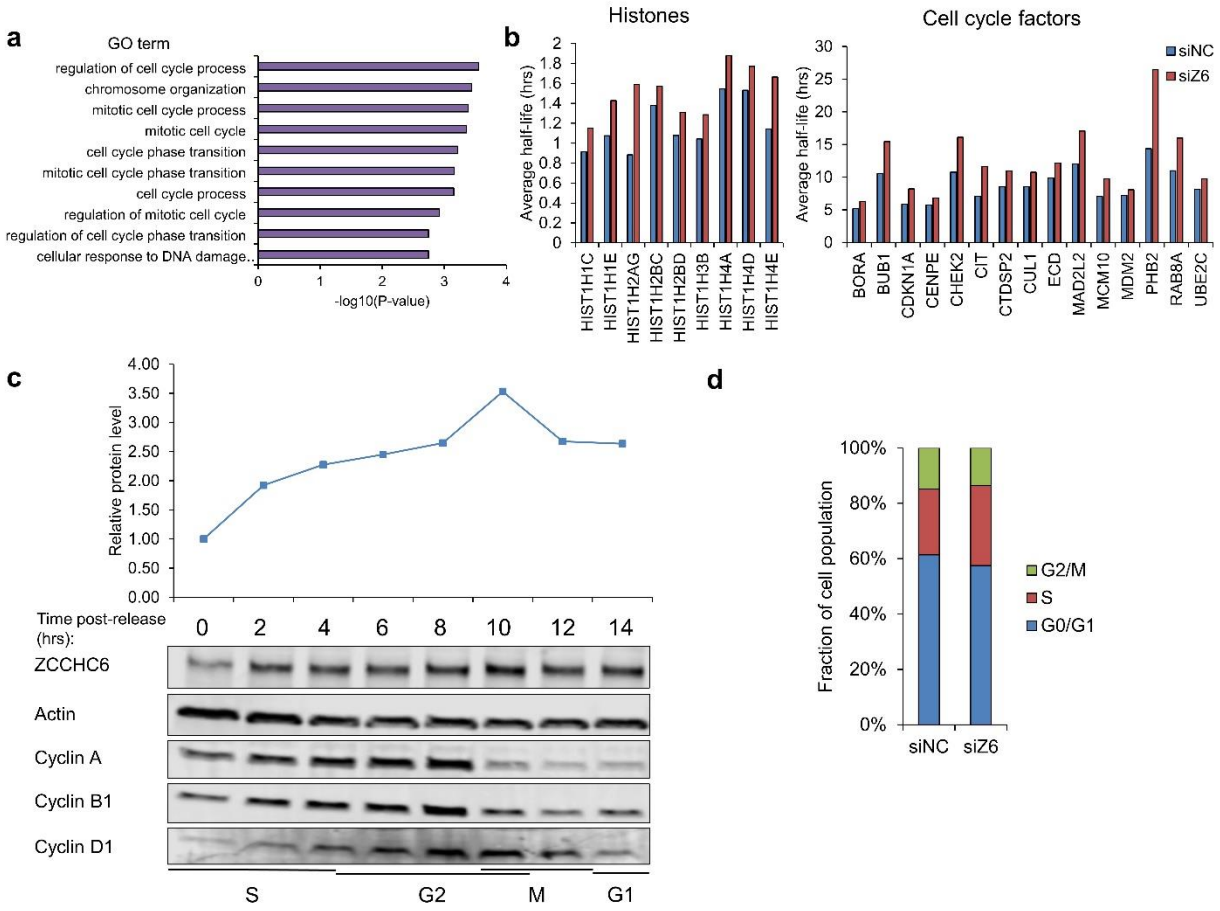

Figure 3.5. ZCCHC6 regulates the cell cycle in cancer cells. (a) Gene ontology (GO) analysis of mRNAs with statistically significant increase in half-lives (P<0.05) from Figure 3.4e. (b) mRNA half-life measurements for indicated histone and cell-cycle-regulatory genes analyzed in Figure 3.4e. (c) Western blot analysis of indicated proteins in HCT116 cells at the specified time-points after release from double-thymidine block. Quantification of Western blot data is shown on top. Estimated cell cycle phases are indicated on the bottom. (d) Cell cycle profile of HCT116 cells after knockdown with a control (siNC) or ZCCHC6 (siZ6) siRNA. Analysis was performed five days after transfection. Data are representative of two independent experiments.

ZCCHC6/11 promote a less differentiated state in mESCs and muscle progenitors

In light of their reported high expression in embryonic tissues [426] and the above data implicating ZCCCHC6/11 in the control of the oncogenic state, we also wondered if these TUTases play a broader role in regulating cell identity. To explore this question, we first analyzed mESCs upon exit from naïve pluripotency after 2i/LIF withdrawal. qRT-PCR analysis revealed that both TUTases are rapidly downregulated under these conditions (Supplementary Figure 3.5a),

suggesting that ZCCHC6/11 may support the pluripotent state. To examine this hypothesis, mESC lines that overexpress ZCCHC6 or ZCCHC11 in a doxycycline-inducible fashion were generated. We transferred these cells to serum/LIF culture conditions, which allow for the co-existence of naïve and more primed-like pluripotent states, induced ZCCHC6/11 overexpression, and stained the emerging colonies for the pluripotency marker alkaline phosphatase. Overexpression of either TUTase resulted in smaller, more compact and stronger-stained colonies relative to the uninduced controls, suggesting that ZCCHC6/11 stabilize the pluripotent state (Supplementary Figure 3.5b). We also generated ZCCHC6/11 double-knockout mESCs and performed the same analysis. Opposite to the gain-of-function effects, TUTase loss resulted in flatter colonies with weaker and more heterogeneous staining pattern, suggesting a propensity toward differentiation and corroborating the overexpression results (Supplementary Figure 3.5c).

We then asked if these observations reflect a more general role for ZCCHC6/11 in promoting a less differentiated state beyond pluripotency. To this end, we turned to the C2C12 muscle progenitor system, whereby myoblasts can be differentiated into mature myotubes upon serum reduction, recapitulating defined stages of myogenesis [461]. Similarly to our mESC observations, one of the TUTases, ZCCHC11, was rapidly downregulated upon myoblast differentiation (Supplementary Figure 3.5d). Further, TUTase overexpression suppressed while TUTase depletion promoted differentiation, which was evident in the lower and higher degree of myotube formation, respectively (Supplementary Figure 3.5e,f). Together with the mESC data, these results indicate that ZCCHC6/11 may promote “stemness” properties across cells of distinct lineages and developmental potencies, and suggest a broader role for these TUTases in cell fate control in normal and oncogenic settings.

3.3. Discussion.

Our results reveal novel functions of the TUTases ZCCHC6/11 in oncogenesis, and in shaping cell identity more broadly, which could be attributed at least in part to uridylation-mediated

regulation of mRNA turnover. As such, these findings have important implications for cancer and stem cell biology, and raise a number of pertinent questions.

First, our findings extend the scope of ZCCHC6/11 involvement in oncogenesis beyond their reported functions in the LIN28 pathway [255, 439]. It would be interesting to explore if these TUTases contribute to different transforming events (besides mutant KRAS) and to define what determines dependence on TUTase activity in established cancer cell lines. As we focused on proliferation and tumorigenicity, it would also be informative to assess if ZCCHC6/11 influence other cancer cell properties, such as invasiveness, metastatic ability or stress response. All of these questions should ultimately be addressed in transgenic or knockout mouse models to determine their relevance during tumor development in a complex *in vivo* environment.

Next, we mechanistically implicate cell cycle changes due to altered uridylation-mediated mRNA turnover. This model is consistent with the reported roles of TUTases in replication-dependent histone mRNA decay and cell cycle regulation across evolution [389, 391, 393, 395, 396, 433, 434], and suggests that dysregulated mRNA turnover may be a hallmark of cancer. However, our model warrants further investigation. Additional support for this mechanism would be provided by analysis of catalytically inactive ZCCHC6/11, as one study has reported a non-catalytic function of ZCCHC11 [434], as well as by genetic rescue experiments with relevant downstream mRNA targets.

Finally, our stem and progenitor cell data demonstrate a broader role for ZCCHC6/11 in the control of cell identity. It is necessary to explore these phenotypes mechanistically through in-depth analysis of differentiation markers and interrogation of RNA uridylation, RNA turnover and cell cycle regulation. It would also be interesting to examine whether these TUTases are involved in the dedifferentiation that occurs during somatic cell reprogramming or in certain tumors (especially given their role in cancer). The possibility of a more general role for mRNA uridylation and turnover in regulating differentiation state is intriguing and may add to the emerging roles of mRNA methylation-mediated turnover in stem cell and cancer biology [166].

3.4. Methods.

Plasmids

For clonal-based CRISPR/Cas9 knockout (in NIH3T3 and mESCs), sgRNAs against mouse Zcchc6 or Zcchc11, or non-targeting control ("NTC") sgRNAs were subcloned into the pSpCas9(BB)-2A-GFP or pSpCas9(BB)-2A-mCherry vector. For population-based CRISPR/Cas9 knockout (in cancer cell lines), sgRNAs against GFP (labeled "NTC") or human ZCCHC6 (labeled "Z6KO") were subcloned into the pLentiCRISPRv2-Puro vector. For generation of double-knockouts (labeled "DKO"), a sgRNA against human ZCCHC11 was further cloned into pLentiGuide-Puro. A list of the utilized sgRNAs is provided below; sgRNA sequences were either obtained from published studies or designed *de novo* using the CRISPR Design Tool (http://crispr.mit.edu/), as indicated. To produce lentivirus, the pMD2.G and psPAX2 packaging plasmids were used, as described later. To transform NIH3T3 cells, the pBabe-Puro-KrasG12V plasmid was used and retrovirus was produced using gag/pol and VSV.G packaging plasmids, as described later. For generation of doxycycline-inducible transgenic mESCs, FLAG-tagged human ZCCHC6 or ZCCHC11 ORFs were subcloned into the pBS31 vector (Open Biosystems #MES4486), and used in conjunction with the pCAGGS-FLPe plasmid (Open Biosystems #MES4488) [462]. For stable overexpression, the pLentiCas9-Blast plasmid was digested at *NheI* and *BamHI*, and a FLAG-tagged mouse Zcchc6 ORF was introduced at these sites or the vector was blunted and re-ligated to generate an empty vector control. pLentiCas9-Blast (Addgene plasmid #52962), pLentiCRISPRv2-Puro (Addgene plasmid #52963), pLentiGuide-Puro (Addgene plasmid #52963), and pSpCas9(BB)-2A-GFP (Addgene plasmid #48138) were gifts from F. Zhang (MIT, USA) [463, 464]. pSpCas9(BB)-2A-mCherry was a gift from M. Stitzel (The Jackson Laboratory, USA). pMD2.G (Addgene plasmid #12259) and psPAX2 (Addgene plasmid #12260) were gifts from D. Trono (EPFL, Switzerland). pBabe-Puro-KrasG12V (Addgene plasmid #9052) was a gift from W. Hahn (DFCI, USA). gag/pol (Addgene plasmid #14887) and VSV.G

(Addgene plasmid #14888) were gifts from T. Reya (UCSD, USA) [465]. The following sgRNAs were used in this study:

sgRNA name	sgRNA sequence	Reference	Used in: (cell lines)
NTC-1	GTAGGCGCGCCGCTCTCTAC	[464]	NIH3T3; mESC
NTC-2	GGGCCCGCATAGGATATCGC	[464]	
mZcchc6	GTGCTTATGAGCAAACGGAA	CRISPR Design Tool	
mZcchc11	AATCCGCCAGGACATTGTGG	CRISPR Design Tool	
GFP-1	GGGCGAGGAGCTGTTCACCG	[466]	HCT116; MCF7; H1299; U2OS
GFP-2	GAGCTGGACGGCGACGTAAA	[466]	
hZCCHC6	GTGGCTGTCATTCATCCAAG	CRISPR Design Tool	
hZCCHC11	TGTCCCAAGGATACCCGATT	CRISPR Design Tool	

Cell Culture

HCT116 DICER^{WT} and DICER^{Ex5} (Horizon Discovery #HD R02-019) [460], MCF7 (ATCC #HTB-22), U2OS (ATCC #HTB-96), 293T (ATCC #CCL-3216) and C2C12 (ATCC #CRL-1772) cells were maintained in DMEM/10% FBS. H1299 (ATCC #CRL-5803) cells were maintained in RPMI/10% FBS. NIH3T3 cells (ATCC #CRL-1658) were maintained in DMEM/10% calf bovine serum (CBS) (ATCC #30-2031). The identity and culture conditions of the cancer cell lines profiled in Figure 3.1d are shown below. v6.5 [450], KH2 [462], doxycycline-inducible FLAG-ZCCHC6 (iZ6) and FLAG-ZCCHC11 (iZ11), non-targeting control (NTC) and Zcchc6/11 double-knockout (DKO) mESCs were maintained on laminin (Sigma) in 2i/LIF medium [15] or on irradiated CF1 MEFs (GlobalStem) in mESC medium (DMEM, 15% FBS, 1 U/ml Penicillin, 1 µg/ml Streptomycin, 2 mM L-glutamine, 0.1 mM NEAA, 0.1 mM BME, 1,000 U/ml LIF). iZ6 and iZ11 cells were generated using KH2 cells as described previously [462], and transgene expression was induced by treatment with 2 ug/ml doxycycline (Sigma). NTC and DKO cells were generated from v6.5 mESCs using the pSpCas9(BB)-2A-GFP and pSpCas9(BB)-2A-mCherry plasmids. In 2i/LIF withdrawal experiments, 2i and LIF were omitted from the medium. For alkaline phosphatase staining, mESCs were plated on MEFs in mESC medium, grown for five days, and stained using the Leukocyte Alkaline Phosphatase kit (Sigma), as per the manufacturer's protocol. For C2C12 differentiation, DMEM/10% FBS medium was replaced with DMEM/2% horse serum (Thermo

Scientific #26050088). The following cancer cell lines were profiled in Figure 3.1d (as shown on gel, left to right):

Cancer type	Cell line	Culture medium
Leukemia	K562	DMEM/10%FBS
Breast	MCF7	DMEM/10%FBS
	MDA-MB-231	DMEM/10%FBS
	T47D	RPMI/10%FBS
Colon	Caco-2	DMEM/10%FBS
	HCT116	DMEM/10%FBS
	LS174T	DMEM/10%FBS
	RKO	RPMI/10%FBS
	SW620	DMEM/10%FBS
Liver	HepG2	DMEM/10%FBS
	Huh6	DMEM/10%FBS
	Huh7	DMEM/10%FBS
Lung	A549	DMEM/10%FBS
	H1155	DMEM/10%FBS
	H1299	DMEM/10%FBS
	H460	RPMI/10%FBS
Fibroblasts	BJ1	DMEM/10%FBS
Neural	D283	EMEM/10%FBS
	Daoy	EMEM/10%FBS
	BE2C	DMEM/10%FBS
	NBLS	DMEM/10%FBS
	SK-N-FI	DMEM/10%FBS
Skin	M14	EMEM/10%FBS
	SKMEL2	EMEM/10%FBS
	SKMEL28	EMEM/10%FBS
Ovarian	A2780	DMEM/10%FBS
	OVCAR3	DMEM/10%FBS
	SKOV3	DMEM/10%FBS
Kidney	CCG	DMEM/10%FBS
	293T	DMEM/10%FBS
Cervical	HeLa	DMEM/10%FBS

Human Colorectal Cancer Samples

Samples from colorectal cancer patients analyzed in Supplementary Figure 3.1b were collected as described before [326]. Written informed consent was obtained from all study subjects. The study was approved by the human subject committees at the Harvard T.H. Chan School of Public Health and Brigham and Women's Hospital.

siRNA Transfections

For siRNA transfections, 1.5 x 10^5 HCT116 or C2C12 cells were reverse transfected with 40 pmol of each siRNA using Lipofectamine RNAiMAX following the manufacturer's protocol (Invitrogen). For siZ6+11 double-knockdowns, the control siRNA amount was doubled to match the total siRNA load in the knockdown condition. The following siRNAs were used: siNC (Ambion #4390843); siZcchc6 (mouse) (Ambion #4390815-s103051); siZcchc11 (mouse) (Ambion #4390815-s106497); siZCCHC6 (human) (Ambion #4392421-s36058).

Viral Production and Stable Cell Line Generation

To produce retrovirus, published protocols were followed [254]. To produce lentivirus, 2.5 x 10^6 293T cells were seeded in a 10-cm plate and transfected 16-24 h later using Lipofectamine 2000 and OptiMEM (Life Technologies). The following amounts were used per plate: 6.6 ug transfer plasmid, 3.3 ug pMD2.G, 4.8 ug psPAX2, 36 ul Lipofectamine 2000, and 600 ul OptiMEM. After 12-16 h, medium was changed to DMEM/20% FBS and supernatant was harvested 24 and 48 h later, with medium replacement at 24 h. The supernatant was centrifuged at 1,200 RPM for 5 min to pellet cell debris and used immediately or stored at 4°C for later use. Stable cell lines were generated by transduction with unconcentrated viral supernatant and selection with 5 ug/ml Blasticidin or 1 ug/ml Puromycin, depending on the plasmid.

CRISPR/Cas9-based Knockout Cell Line Generation

To generate clonal-based CRISPR/Cas9 knockout, NIH3T3 or v6.5 mESCs were transfected with sgRNA-containing pSpCas9(BB)-2A-GFP and pSpCas9(BB)-2A-mCherry plasmids and clones were isolated via single-cell fluorescence-activated cell sorting. To generate population-based CRISPR/Cas9 knockouts, lentivirus was produced as described above. Cells were transduced with unconcentrated viral supernatant produced using a respective pLentiCRISPRv2-Puro

transfer plasmid and selected with 1 ug/ml Puromycin. For double-knockouts, H1299 cells were further transduced with viral supernatant produced using a pLentiGuide-Puro transfer plasmid.

Proliferation Assays

Cell proliferation was assessed using manual counting. Cells were seeded at 2.5 x 10^5 (NIH3T3) or 7.5 x 10^5 (HCT116, MCF7, H1299, U2OS) cells/well of a 12-well plate, counted 24 h later to establish starting numbers, and re-counted 96 h later to determine final numbers. Cells were split once as needed to prevent them from getting confluent. Final numbers were normalized to starting numbers and respective controls, with split ratios taken into account, as indicated in the figures.

Soft Agar Assays

Soft agar assays were performed as describes previously [467], with the following modifications. NIH3T3-KrasG12V and HCT116 cells were seeded at 2 x 10^3 or 0.5 x 10^3 cells per well of a 12-well plate, respectively. SeaKem LE agarose (Lonza) was melted in the respective cell culture medium to generate bottom (0.5%) and top (0.37%) agar layers. Colonies were grown for 3-4 weeks, with periodic media change, and manually counted under a microscope at the end of the assay. HCT116 cells were stained with 0.05% crystal violet to facilitate counting.

Allograft and Xenograft Assays

Allograft and xenograft assays were performed as described previously [467], with the following modifications. NIH3T3-KrasG12V and HCT116 cells were injected subcutaneously into the flanks of $Rag2^{-/-}\gamma c^{-/-}$ mice (JAX #014593) at 0.5 x 10^6 or 1 x 10^6 cells per site, respectively. Animals were sacrificed and tumors harvested after 15-17 or 41-43 days for NIH3T3-KrasG12V and HCT116 cells, respectively. End-point tumors were caliper-measured and photographed. All animal procedures were performed according to animal care guidelines approved by the Boston Children's Hospital Institutional Animal Care and Use Committee.

Migration Assays

Migration assays were performed as describes previously [467], with the following modifications. NIH3T3-KrasG12V cells were seeded at 1 x 10^3 cells per membrane in DMEM/1% CBS on Transwell permeable support membranes (Corning #3422) and the membranes were placed in DMEM/10% CBS. After 24 h, cells were wiped from the seeding side, membranes were fixed in 4% PFA (Electron Microscopy Sciences), washed twice in PBS (Life Technologies), and mounted on slides in VectaShield mounting medium with DAPI (Vector Labs). The number of migrated cells was determined by manual counting of DAPI-stained nuclei, visualized on an epifluorescent Nikon microscope.

Cell Cycle Analysis

For double-thymidine block, 20-30% confluent HCT116 cells were treated with 2 mM thymidine (Sigma) for 18 h (first block) and then released by washing with PBS and re-feeding with fresh complete medium. After an 8-hour recovery, cells were re-treated with 2 mM thymidine for another 16 h (second block) and released as before. For cell cycle profiling, the PI/RNase Staining Buffer (BD Pharmingen) was used, as per manufacturer's protocol. PI-stained cells were analyzed on a MACSQuant VYB instrument (Miltenyi Biotec) and cell cycle profile was generated using the ModFit LT software (Verity).

Western Blot

Normal human tissue lysates were purchased from Zyagen (San Diego, CA), while colorectal tumor samples were obtained as described above. All analyzed samples (tissues and cells) were lysed in RIPA buffer containing protease inhibitors (Pierce). Proteins were separated on a 4-20% polyacrylamide gel (Bio-Rad) and transferred to a methanol-activated PVDF membrane (Millipore). The membrane was blocked for 30-60 minutes in 3%BSA/PBST (chemiluminescent

blots) or 3%BSA/PBS (fluorescent blots), and probed with primary antibodies at 4°C overnight. Secondary antibody incubation was performed at room temperature for 1-4 hours or at 4°C overnight. Protein levels were detected using the SuperSignal West Pico and Femto Luminol reagents (Thermo Scientific) or the Odyssey CLx near-infrared fluorescence imaging system (LI-COR). Primary antibodies used were: anti-ZCCHC6 (Proteintech #25196-1-AP; 1:1,000), anti-ZCCHC11 (Proteintech #18980-1-AP; 1:500), anti-LIN28A (Cell Signaling #3978; 1:1,000), anti-LIN28B (Cell Signaling #4196; 1:1,000), anti-α/β-tubulin (Cell Signaling #2148; 1:1,000), anti-GAPDH (Santa Cruz sc-25778; 1:10,000), anti-Actin (Santa Cruz sc-1616; 1:2,000), anti-cyclin A (Santa Cruz sc-239; 1:500), anti-cyclin B1 (Santa Cruz sc-245; 1:500), and anti-cyclin D1 (Santa Cruz sc-753; 1:500). Secondary antibodies used were: for chemiluminescence, HRP-conjugated anti-rabbit IgG (GE Healthcare NA934, 1:2,000), anti-mouse IgG (GE Healthcare NA931; 1:2,000), and anti-goat IgG (Santa Cruz sc-2020; 1:2,000); for fluorescence, IRDye 680RD anti-rabbit IgG (LI-COR #925-68071; 1:20,000), IRDye 800CW anti-mouse IgG (LI-COR #925-32210; 1:20,000), and IRDye 680RD anti-goat IgG (LI-COR #925-68074; 1:20,000). Quantifications were performed using Image Studio for Odyssey CLx (fluorescent blots) (LI-COR).

Quantitative RT-PCR

Total RNA was isolated using Trizol (Invitrogen) combined with miRNeasy columns (Qiagen). 100-250 ng RNA were reverse-transcribed using the miScript II RT kit (Qiagen) and subjected to standard primer assays (mRNAs) or miScript miRNA assays (miRNAs) (Qiagen). RNA expression was measured by SYBR Green quantitative PCR using the ΔΔCt method. Gapdh (or Actb for mESCs) were used for normalization. The following primers were used:

Name	Sequence or Cat. No.
mZcchc6-F	CAGTCAGGTAGCCTTTCCAGTA
mZcchc6-R	GCAGTTCCTTCCCTCATGATTC
mZcchc11-F	TCTATGCTCAAGCAGACAGATG
mZcchc11-R	ACTGACACTGAGGTACGGATA
mGapdh-F	CATGGCCTTCCGTGTTCCT
mGapdh-R	GCGGCACGTCAGATCCA

mActb-F	CAGAAGGAGATTACTGCTCTGGCT
mActb-R	TACTCCTGCTTGCTGATCCACATC
hHMGA2-F	GACCTAGGAAATGGCCACAA
hHMGA2-R	ACTGCTGCTGAGGTAGAAATC
hMTF2-F	CTAGATGGTCAGATGGCTTGTT
hMTF2-R	AGTGGCTCCTGTTTGAATGT
hENTPD7-F	GCATTCCTGGGACTCTTCTT
hENTPD7-R	CGAGCCAAATACCTTTCGTATTG
hTLDC1-F	AGCTGCAAGATGGCAAGA
hTLDC1-R	ACGAGCACAGGATGAGAAAG
hGAPDH-F	ACCCAGAAGACTGTGGATGG
hGAPDH-R	TTCAGCTCAGGGATGACCTT
miR-154	Qiagen #MS00003598
miR-211	Qiagen #MS00003808
miR-382	Qiagen #MS00031836
U6	Qiagen #MS00033740

RNA Sequencing

Total RNA >200 nt was isolated using Trizol (Invitrogen) combined with RNeasy columns (Qiagen). 50 ng purified RNA was subjected to rRNA depletion using the Ribo-Zero rRNA Removal Kit (Illumina) or to poly(A) selection using the NEBNext Poly(A) mRNA Magnetic Isolation Module (NEB), as indicated in the text. Purified RNA was subsequently used for library preparation with the NEBNext Ultra RNA Library Prep Kit (NEB). Libraries were analyzed on a Bioanalyzer (Agilent) for quality control, quantified using the Qubit dsDNA HS Assay (Invitrogen) and qRT-PCR (Kapa Biosystems), and equimolar pools were sequenced on HiSeq 2500 or NextSeq 500 instruments (Illumina) using 50-bp or 76-bp single-end protocols, respectively. Expression values (RPKM) were estimated using the TopHat [454] and HTSeq-count tools [455]. RNA half-life analysis was performed following published procedures [401]. TAIL-seq was performed and data analyzed as described before [372, 401], except that a standard base-calling algorithm was used instead of raw fluorescence signal to crudely estimate poly(A) tail length. Gene ontology analysis was performed using the DAVID 6.8 Functional Annotation Tool [468, 469].

Statistics and Reproducibility

Data are presented as mean ± s.e.m. (unless noted otherwise). Statistical significance is displayed as $P<0.05$ (one asterisk) or $P<0.01$ (two asterisks). Differences between groups were assessed using a two-tailed Student's *t*-test in Microsoft Excel, with data assumed to fulfill *t*-test requirements. For RNA half-life measurements, differences were assessed described previously [401]. Sample sizes and reproducibility are described in the respective figure legends.

Data Availability

RNA-sequencing data that support the findings of this study are pending deposition in the Gene Expression Omnibus (GEO). All data supporting the findings of this study are available upon reasonable request.

AUTHOR CONTRIBUTIONS

This chapter represents a manuscript in preparation. K.M. Tsanov conceived the study and wrote the manuscript in close collaboration with D.S. Pearson. K.M.T. and D.S.P. designed and performed most of the experiments, as follows. K.M.T. generated Figures 3.1a, c; 3.2c, d, e; 3.3a (part), b, c; 3.4a (part), b (cell culture), d (cell culture); 3.5; Supplementary Figures 3.1a; 3.5a, b, c (part), d, e (part), f (part). D.S.P. performed most of the cloning and generated Figures 3.2a, b; 3.3a (part), 3.4a (part), c (TAIL-seq), e (RNA-seq); Supplementary Figures 3.1b; 3.3; 3.5c (part), e (part), f (part). Y.C. Huang, G.S. LaPier and J. Barragan helped with cloning, cell culture and Western blot analysis. A. Han, L. Pantano, J. Han and A. Bohmer performed bioinformatics analysis. H.C. Tu, Z. Qian, S. Ogino and C.S. Fuchs provided colorectal cancer patient samples. J.K. Osborne and J.T. Powers provided cancer cell line samples (for Figure 3.1c) and helped with experimental design. O. Hofmann supervised TAIL-seq bioinformatics analysis. G.Q. Daley supervised the study and edited the manuscript.

ACKNOWLEDGMENTS

We thank P. Sharp, G. Ruvkun, L. Cantley, R. Horvitz, J. Rinn, S. Buratowski, and members of the Daley lab for invaluable discussions, X. Wu/Yi Zhang's lab and R. Rubio/DFCI CCCB for assistance with RNA-seq, R. Mathieu and M. Paktinat for assistance with flow cytometry. Bioanalyzer analysis was performed in the BCH IDDRC Molecular Genetics Core, which is supported by NIH (NIH-P30-HD 18655). Sequencing analysis was conducted on the Orchestra High Performance Computing Cluster at Harvard Medical School. K.M.T. was an HHMI International Student Research Fellow and a Herchel Smith Graduate Fellow. D.S.P. was supported by a grant from NIGMS (T32GM007753). G.Q.D. was an investigator of the Howard Hughes Medical Institute and the Manton Center for Orphan Disease Research, and was supported by a grant from NIGMS (R01GM107536).

CHAPTER 4

Discussion and Perspective

4.1. RBPs as Links between Signaling and Cell Fate Regulation.

Signal-transduction pathways are master choreographers of cell identity, as they ensure execution of appropriate gene expression programs in accordance with key environmental cues, thereby providing critical spatial and temporal control of cell fate [470]. Given their roles in shaping cell identity, RBPs and their associated post-transcriptional regulatory mechanisms are well-positioned to be under the control of signaling pathways; yet, we have a rudimentary understanding of the integration between these two regulatory layers.

Our LIN28 phosphorylation findings (Chapter 2) provide an example of what is likely a widespread regulatory mechanism, whereby signaling pathways modulate RBPs and their mRNA networks to influence cell identity. Such an integration offers a number of unique opportunities for robust cell fate control. First, post-transcriptional regulation can act faster than transcriptional control, a feature that is well-aligned with the rapid-response nature of signal transduction and the critical role of timing in developmental processes. Second, since signaling is driven by environmental cues, coupling it to RBP activity enables direct influence of the niche on the existing cellular transcriptome, communication that is essential to cell fate specification. Third, this type of regulation allows for multi-faceted control of RNA molecules by affecting properties other than their expression levels alone, thus providing additional mechanisms for signaling pathways to impact cell identity.

Direct signaling input into an RBP – such as LIN28 phosphorylation – can affect various RBP properties (Figure 4.1). In the case of LIN28, we uncovered an effect on its stability, which fundamentally alters the stoichiometry of the RBP relative to its targets. However, an RBP's subcellular localization or association with critical protein co-factors and RNA targets may also be influenced through changes in the RBP's binding affinity or availability of relevant domains. And, for RBPs that enzymatically alter RNAs, their catalytic activity might be modulated too. At the same time, as already noted, an RBP can regulate various aspects of RNA metabolism, including processing, localization, translation, and degradation. Altogether, the combination of possible

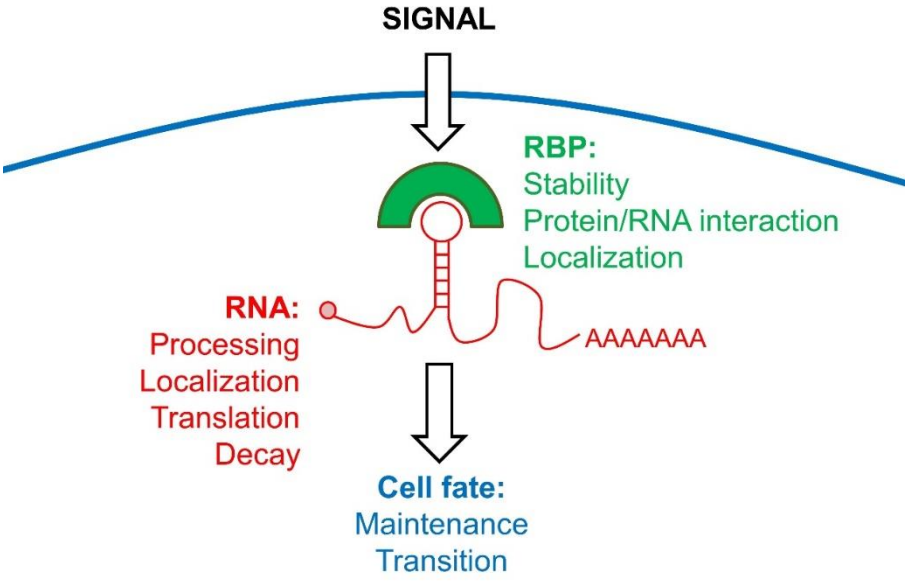

Figure 4.1. RBPs as links between signaling, post-transcriptional regulation, and cell fate. Listed are the range of effects of signaling pathways on a given RBP (green), its RNA targets (red), and cell fate (blue). An individual RBP binding an mRNA stem-loop structure is shown as an example. Note that RBPs are typically found complexed with multiple other proteins and can bind various structure- or sequence-based motifs in diverse RNA species. See text for details.

effects on RBP properties and downstream impact on its cognate RNA targets generates a diverse array of outputs that can be controlled by signaling pathways, as evident from various studies of individual RBPs (see Chapter 1.2).

Building a more complete picture of these regulatory relationships will require a systematic interrogation of the RNA-binding proteome [80]. While LIN28 provides a valuable lens into this biology, there are over 500 RBPs associated with pluripotency alone, the vast majority of which have not been functionally characterized [448]. Hence, a first step would be to define their functions through a combination of genetic and biochemical approaches. PSCs provide a good starting platform, which could be expanded to differentiated cell types, since RBP function is highly context-dependent (as it is restricted by the available transcriptome). It would also be informative to analyze transitions between cell fates, as RBPs may be particularly relevant in these settings (by enforcing transcriptome switches). And, while rare, systems that rely entirely on post-transcriptional control, such as the earliest stages of embryogenesis or reticulocyte

maturation, could provide powerful insights into core regulatory principles. Once a functional understanding is gained, the connection to signaling pathways can be explored. This can be done in a signaling-centric manner, by analyzing changes in an RBP and its targets upon pathway perturbation, or in an RBP-centric manner, such as the phosphoproteomic analysis performed for LIN28. The accumulating public data from global transcriptomic and proteomic studies may offer a useful resource in that respect. Ultimately, such an approach can bring us closer to charting RBP-based post-transcriptional regulatory networks and yield a more comprehensive understanding of the molecular foundations of cell identity.

4.2. Enhanced mRNA Turnover as a Potential Cancer Hallmark and Cell Fate Determinant.

All of the major cancer-related pathways, such as c-MYC, p53, KRAS and PI3K/mTOR, profoundly impact mRNA synthesis and translation [101, 457] (see Chapter 1.2). Consequently, their activity puts high pressure on mRNA and protein turnover mechanisms. While the role of protein turnover in cancer has been appreciated for over two decades [471], the involvement of mRNA turnover pathways has not been extensively explored (Figure 4.2).

Our ZCCHC6/11 findings (Chapter 3) suggest an important role for mRNA turnover mechanisms in cancer. Although we implicate cell cycle factors as key TUTase targets, it is possible that the global effect on mRNA half-lives is also relevant to oncogenic phenotypes. Indeed, a recent meta-analysis of 80 yeast experiments showed that cellular growth is coupled with global mRNA turnover rates [472], which could be an evolutionarily conserved phenomenon. But how would global dysregulation of mRNA turnover influence the cancer state? At the target level, TUTase depletion may increase the half-lives of both oncogene and tumor-suppressor transcripts, creating a “tug-of-war” situation. Indeed, it is possible that TUTase effects are context-

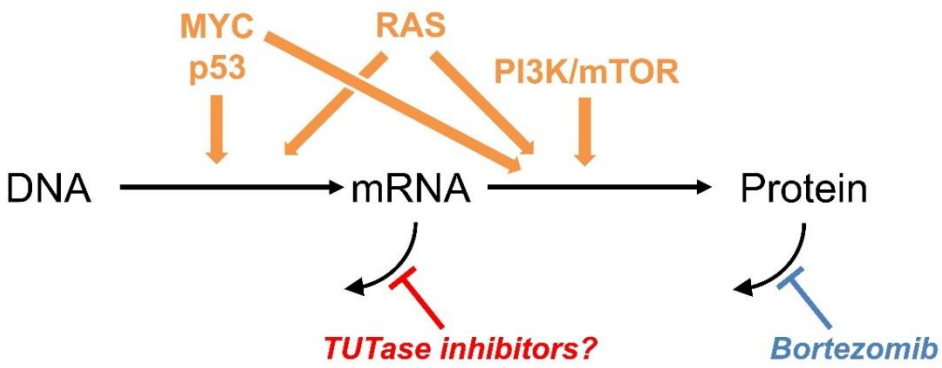

Figure 4.2. Targeting turnover pathways in cancer. Shown is the flow of genetic information (black), pathways commonly dysregulated in cancer and their impact on this flow (orange), and established (blue) and putative (red) therapeutic agents.

dependent so that settings where oncogenes "win" this competition could actually benefit from low TUTase levels. Yet, another way to look at the issue is that rapid mRNA turnover provides additional flexibility in gene regulation that increases the cancer cell's fitness in the face of changing conditions. This adaptability may be especially relevant in transition states that involve transcriptome shifts. Our analysis focused on cell cycle transitions, yet this concept can be extended to transitions in other conditions, such as tumor progression or response to stressors, which warrant further study. Finally, from a metabolic perspective, mRNA turnover may affect the cellular nucleotide pool, which is increasingly appreciated as an important player in oncogenesis [473]. Conceptually, it could be beneficial for the cell to rely on mRNAs as a source of nucleotides, since the most abundant RNA species, ribosomal RNAs (rRNAs), are complexed in ribosomes and thereby not readily accessible. Indeed, in mammalian cells, the median half-life is 9 h for mRNAs [92] versus several days for rRNAs [474].

Our study focused on mRNAs as relevant ZCCHC6/11 targets for three main reasons: (i) prior work has linked ZCCHC6/11 to global mRNA decay [401]; (ii) the time-frames for our proliferation studies are most compatible with effects on the shorter-lived mRNAs rather than other long-lived RNAs; (iii) mRNA targets were enriched for cell cycle regulators, in agreement with the observed phenotypes. However, it should be noted that other RNA species, including long noncoding RNAs, transfer RNAs (tRNAs) and even rRNAs, may also play a role downstream of ZCCHC6/11.

Indeed, uridylation of these RNAs has recently been reported, although its molecular and cellular consequences are unclear [436, 437]. One might imagine that rRNA or tRNA changes could globally influence translation, with a significant impact on the cell. In line with these ideas is an intriguing yet unexplained observation dating back to the 1970s: cancer patients excrete high levels of ribonucleosides in their urine [475, 476]. Although the reported nucleosides were associated with tRNAs, modern technology allows for re-evaluation of the identity of excreted nucleosides, potentially tracing them back to dysregulated turnover mechanisms in tumor cells.

In any case, our findings suggest that at least some cancer cells rely on ZCCHC6/11 activity, raising the possibility that enhanced RNA turnover may be an unappreciated hallmark of cancer and a vulnerability that could be exploited therapeutically (Figure 4.2). This could be achieved through distinct mechanisms in different cancer cells, which warrants a systematic interrogation of the RNA decay pathways in cancer and could extend this concept to a broad range of tumors. Importantly, the clinical success of Bortezomib, a drug targeting the protein-degradation machinery [477], provides a proof-of-concept for the effectiveness of targeting turnover mechanisms in certain cancers. It is appealing to speculate that inhibitors of TUTases – or other RNA decay factors – could prove similarly useful in the treatment of cancer (Figure 4.2). In support of this proposition, 5-fluorouracil, a common chemotherapeutic agent, has been reported to act through effects on RNA metabolism [478] and to specifically target the RNA exosome component RRP6 [479, 480]. It would be interesting to determine if ZCCHC6/11 inhibition sensitizes cancer cells to 5-FU treatment, and to explore the contribution of TUTases and RNA turnover mechanisms to the effects of other chemotherapeutic agents, which could inform potential combination therapies. Of note, it is encouraging that not all cells respond to ZCCHC6/11 depletion, as this suggests the existence of a therapeutic window for TUTase inhibitors. With regard to that, it would also be critical to examine what determines responsiveness to TUTase perturbation and to assess the long-term effects of TUTase loss, especially since dysregulation of histone turnover can promote genome instability [481, 482].

Finally, our stem/progenitor findings suggest that uridylation-mediated RNA turnover may also have a broader role in cell fate control. As pointed out earlier, without mechanistic interrogation of the observed phenotypes, this model remains a speculation. Nonetheless, it is an intriguing possibility, especially given recent studies implicating mRNA methylation, a mark that also regulates mRNA stability, in the control of pluripotency [483-485]. Interestingly, while our data would associate mRNA destabilization with the pluripotent state, these methylation studies suggested the opposite model [483, 484]. However, as shown in one of these papers [484], the outcomes are context-dependent and may thus reflect specificity of modification pathways toward their mRNA targets.

4.3. Expanding Roles for TUTases.

TUTases are found in all domains of life, suggesting that they play fundamental regulatory roles, yet we are only beginning to understand their functions [374] (see Chapter 1.4). Our findings reveal novel contributions of ZCCHC6/11 to oncogenesis and, more broadly, to cell fate control. As noted before, it will be important to determine whether any of their functions are due to non-catalytic activity, which has been reported in one study of ZCCHC11 [434]. While we implicated their enzymatic functions, a non-enzymatic activity remains possible given that ZCCHC6/11 are large proteins that contain multiple RNA-binding domains in addition to their catalytic region.

As far as catalytic activity is concerned, our data point to many future directions for terminal RNA uridylation in cancer. First, it is currently unknown if uridylation is reversible. It can be countered by adenylation on miRNAs [486] or possibly guanylation on mRNAs [372], and exonucleases like DIS3L2 recognize and remove U-tails [402]. It would be interesting to explore whether “deuridylases” exist and what their functions in cancer might be. Likewise, the identity and roles of guanylyltransferases, as well as the contribution of DIS3L2 and other decay factors to oncogenesis need to be addressed. At least for DIS3L2, there is genetic evidence suggesting it can function as a tumor suppressor [224, 435], which warrants further investigation. Second, it

would be interesting to explore the relative contribution of uridylation to homeostatic mRNA turnover versus mRNA quality control, as both have been linked to uridylation [401, 436, 437]. It is likely that certain cancer-related conditions, such as genotoxic stress, can cause mRNA damage [487] and that the clearance of damaged transcripts may involve TUTase-mediated uridylation. Third, it would be prudent to explore the impact of mRNA uridylation on translation, given that translation and decay are intimately linked (see Chapter 1.2) and a few studies have suggested TUTase contributions to translational control [397, 408, 409]. Finally, it remains to be elucidated what determines the target specificity of uridylation. While poly(A) tails and specific motifs have been implicated as recognition sites on mRNAs and miRNAs, respectively [Thornton 2014; Lim 2014], and two protein factors, LIN28 and TRIM25, have been reported to activate ZCCHC11 in pre-*let-7* uridylation [257, 259, 275, 488], our knowledge of such regulatory determinants is limited.

4.4. Extrinsic and Intrinsic Signals in the Post-transcriptional Control of Cell Identity.

As described at the onset of this dissertation, the mRNA life cycle is complex and subject to elaborate post-transcriptional regulatory mechanisms. To adequately choreograph these processes, the cell has to respond to cues from its environment and to employ an internal system for control of its intracellular mRNA dynamics. However, it is poorly understood how extrinsic and intrinsic signals control mRNA fate to influence cell identity. The work presented herein offers new insights into this problem by showing that mRNA fate (and, in turn, cell fate) is controlled by: (i) extrinsic signals provided by growth factors that induce MAPK/ERK-dependent LIN28 phosphorylation to affect mRNA translation, and (ii) intrinsic signals provided by TUTase-mediated terminal mRNA uridylation that affect mRNA decay. Taken together, these findings advance our understanding of the post-transcriptional control of cell identity, with important implications for stem cell and cancer biology.

AUTHOR CONTRIBUTIONS

Section 4.1 was partially adapted from [441]. The rest of the chapter has not been published. K.M. Tsanov wrote the text and generated the figures, with edits from T.E. North and G.Q. Daley.

APPENDIX

Supplementary Material

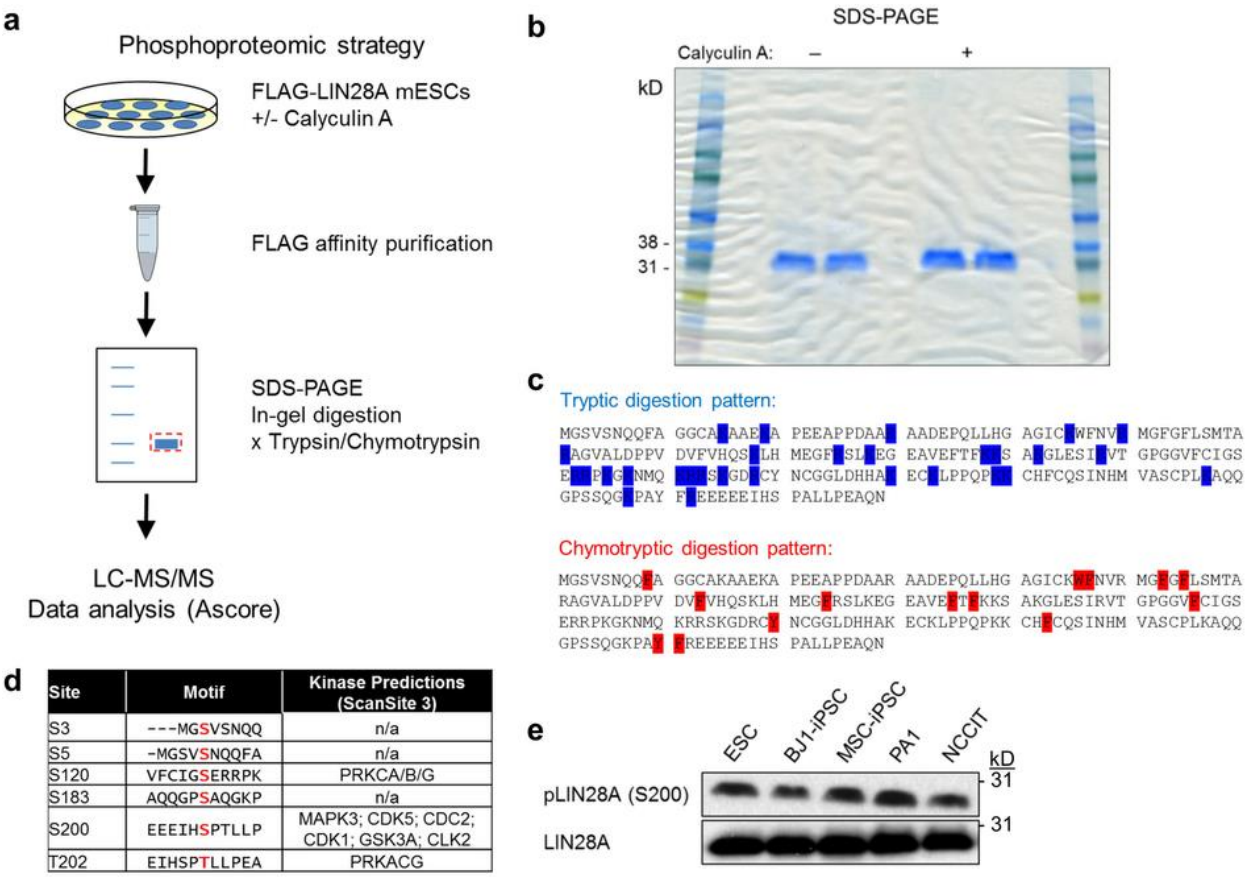

Site	Motif	Kinase Predictions (ScanSite 3)
S3	---MGSVSNQQ	n/a
S5	-MGSVSNQQFA	n/a
S120	VFCIGSERRPK	PRKCA/B/G
S183	AQQGPSAQGKP	n/a
S200	EEEIHSPTLLP	MAPK3; CDK5; CDC2; CDK1; GSK3A; CLK2
T202	EIHSPTLLPEA	PRKACG

Supplementary Figure 2.1. Phosphoproteomic analysis of LIN28A. (a) Schematic of the phosphoproteomic strategy. (b) Coomassie-stained SDS-PAGE gel showing FLAG-LIN28A purified from mESCs, without or with Calyculin A (100 nM) treatment. (c) Digestion patterns of proteases used for generation of LIN28A peptides. The amino acid sequence of mouse LIN28A is shown. Trypsin and chymotrypsin sites are highlighted in blue and red, respectively. (d) LIN28A phosphosites and kinases predicted to phosphorylate them, as determined by ScanSite 3 (http://scansite3.mit.edu/). Site numbers refer to human LIN28A. (e) Western blot analysis of LIN28A (S200) phosphorylation in a panel of human PSCs. A representative image of two independent experiments is shown.

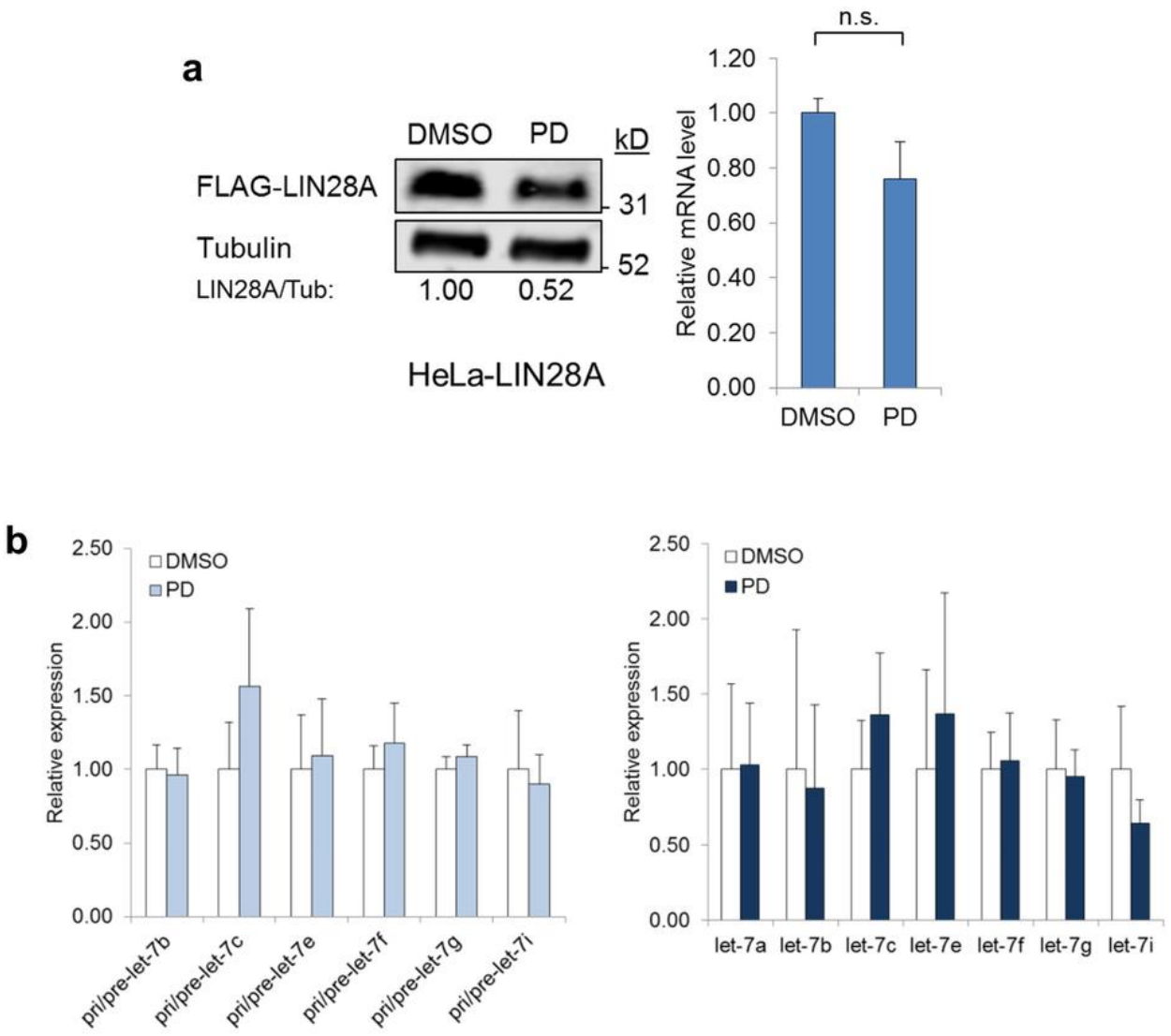

Supplementary Figure 2.2. LIN28A and *let-7* levels after MEK/ERK inhibitor treatment. (a) Western blot (left) and qRT-PCR (right) analysis of transgenic FLAG-LIN28A in HeLa-LIN28A cells after 48-hour treatment with DMSO or PD0325901 (1 μM). n=3 independent experiments. Error bars represent s.e.m. n.s. = non-significant; P=0.19 (two-tailed Student's *t*-test). (b) qRT-PCR analysis of pri/pre- (left) and mature (right) *let-7*s in PA1 cells treated with DMSO or PD0325901 (1 μM) for 48 h. n=3 independent experiments. Error bars represent s.e.m. P>0.05 (two-tailed Student's *t*-test, PD vs. DMSO).

Supplementary Figure 2.3. Effects of mild LIN28A depletion on *let-7* and LIN28's direct mRNA targets. qRT-PCR analysis of mature *let-7*s (a) and LIN28A's mRNA targets (b), and Western blot analysis of LIN28A's mRNA targets (c) in PA1 cells after mild LIN28A knockdown. siNC = negative control siRNA. n=3 independent experiments. Error bars represent s.e.m. P>0.05 (two-tailed Student's *t*-test, siLIN28A vs. siNC).

Supplementary Figure 2.3 (Continued)

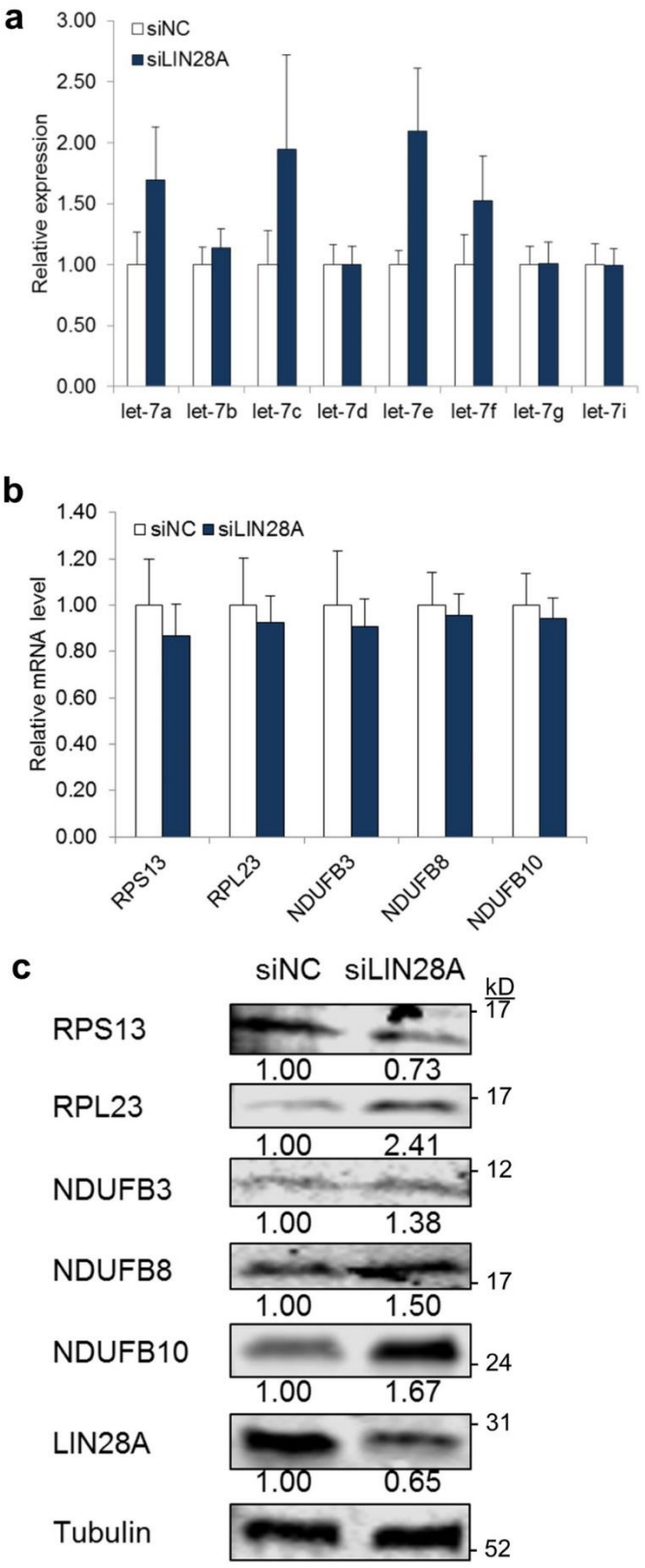

Supplementary Figure 2.4. Effects of LIN28A level and S200 phosphorylation on *let-7* and LIN28A's direct mRNA targets. (a) Corresponding levels of mature *let-7*s (top) and transgenic FLAG-LIN28A protein (middle and bottom) in a clonal series of HeLa-LIN28A cells. PA1 cells are included as a reference for native levels of LIN28A in hPSCs. Data are representative of two independent experiments. (b) Western blot analysis of transgenic FLAG-LIN28A in HeLa Flp-In cells stably expressing Dox-inducible wild-type (WT) or phospho-null (S200A) FLAG-LIN28A, without or with treatment with Dox. Dox = doxycycline (100 ng/ml). A representative image of three independent experiments is shown. (c) qRT-PCR analysis of mature *let-7* species in HeLa Flp-In cells stably expressing Dox-inducible wild-type (WT) or phospho-null (S200A) LIN28A, without or with treatment with Dox. Dox = doxycycline (100 ng/ml). n=3 independent experiments. Error bars represent s.e.m. P>0.05 (two-tailed Student's *t*-test). (d) Quantification of immunoprecipitated RNA (>200 nt) from HeLa Flp-In cells stably expressing wild-type (WT) or phospho-null (S200A) LIN28A. Western blot validation of the immunoprecipitation is shown on the bottom. n=3 independent experiments. Error bars represent s.e.m. *P<0.05 (two-tailed Student's *t*-test). (e) RNA-seq analysis of mRNAs immunoprecipitated by wild-type (WT) or phospho-null (S200A) FLAG-LIN28A in HeLa Flp-In cells. Each dot represents an average enrichment value for transcripts from a given gene. n=3 independent experiments. Data were normalized to the amount of immunoprecipitated LIN28A prior to sequencing. Detailed description of the analysis is provided in the Methods section. (f) Western blot analysis of RNA immunoprecipitation in HeLa Flp-In cells overexpressing wild-type (WT) or phospho-mimetic (S200E) FLAG-LIN28A. Cells were treated with doxycycline (100 ng/ml) to induce FLAG-LIN28A 48h prior to analysis. A representative image of three independent experiments is shown. (g) qRT-PCR analysis of representative mRNA targets immunoprecipitated by wild-type (WT) or phospho-mimetic (S200E) FLAG-LIN28A in HeLa Flp-In cells. n=3 independent experiments. Data were normalized to cell number prior to RT. Error bars represent s.e.m. *P<0.05; **P<0.01 (two-tailed Student's *t*-test, S200E vs. WT).

Supplementary Figure 2.4 (Continued)

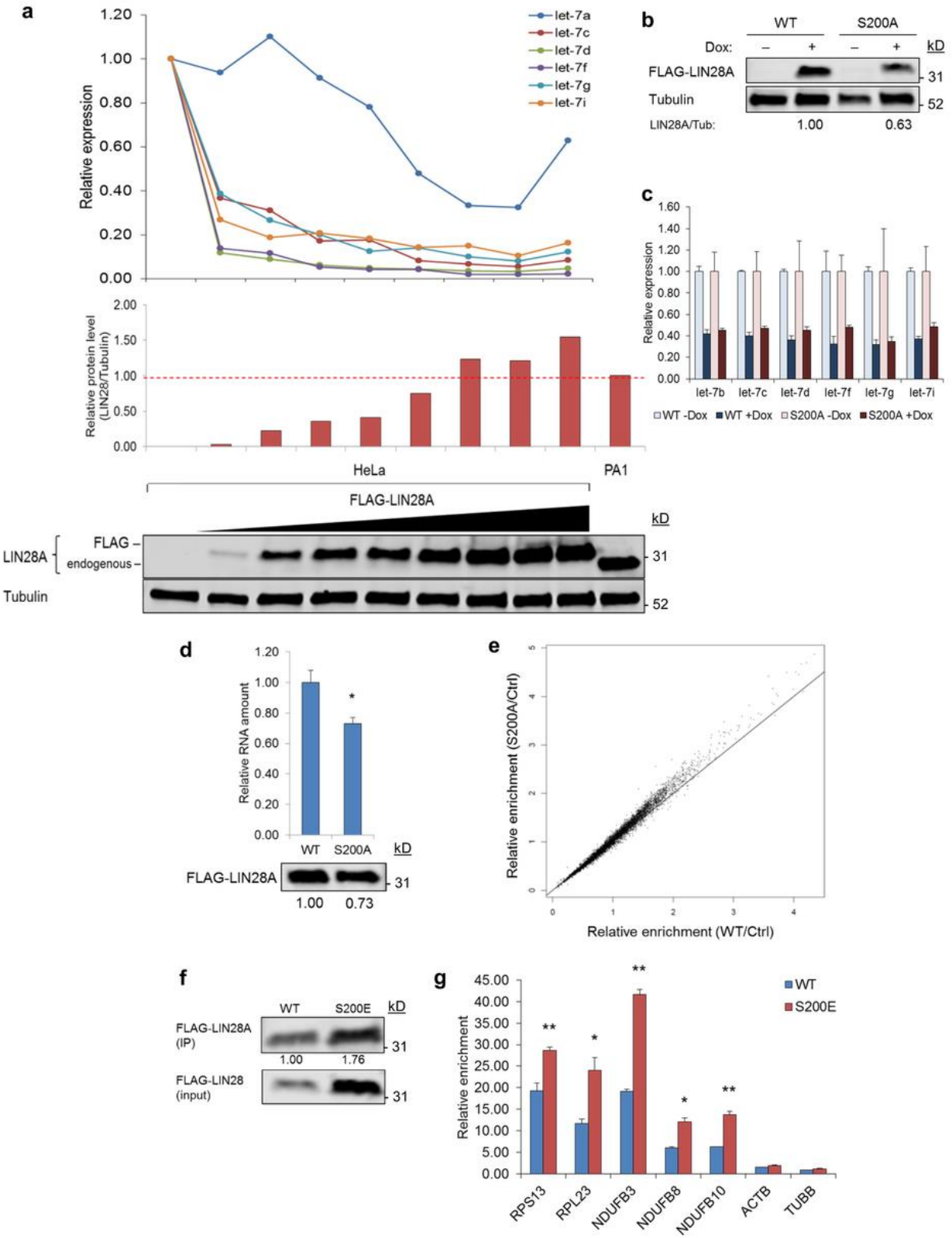

Supplementary Table 2.1. LIN28A phosphosites mapped in this study. Shown are the protein coverage, fraction of phosphopeptides (vs. total), and the highest phosphopeptide localization score (Ascore) corresponding to each site. Phosphosites localized with high confidence (Ascore > 13.0) are highlighted in bold. Data analysis was performed as described in the Methods section.

	-Calyculin A				+Calyculin A			
	Trypsin		Chymotrypsin		Trypsin		Chymotrypsin	
	Coverage: 99.1 %		Coverage: 90.1 %		Coverage: 97.8%		Coverage: 91.5%	
Site	No. peptides (phospho/total)	Ascore	No. peptides (phospho/total)	Ascore	No. peptides (phospho/total)	Ascore	No. peptides (phospho/total)	Ascore
S3	1/61	6.1	0/93	n/a	2/48	10.4	3/163	8.5
S5	1/61	10.4	0/93	n/a	0/48	n/a	1/163	7.5
S184	1/7	**16.2**	1/37	**26.4**	1/8	0	1/37	**16.2**
S200	1/6	8.7	2/22	**1000**	0/7	n/a	2/27	**1000**

Supplementary Figure 3.1. ZCCHC6/11 expression in human tumors. (a) RNA-seq analysis of ZCCHC6/11 in diverse human tumors grouped by cancer type. Each bar represents an individual patient. Data were obtained from cBioPortal (www.cbioportal.org) [1]. (b) Western blot analysis of ZCCHC6/11 in normal mucosa (N) and tumor (T) tissue from human colorectal cancer patients. Samples were either unmatched (left) or matched (right) per patient. Each lane represents an independent tumor, with matched samples being grouped by a bracket.

Supplementary Figure 3.1 (Continued)

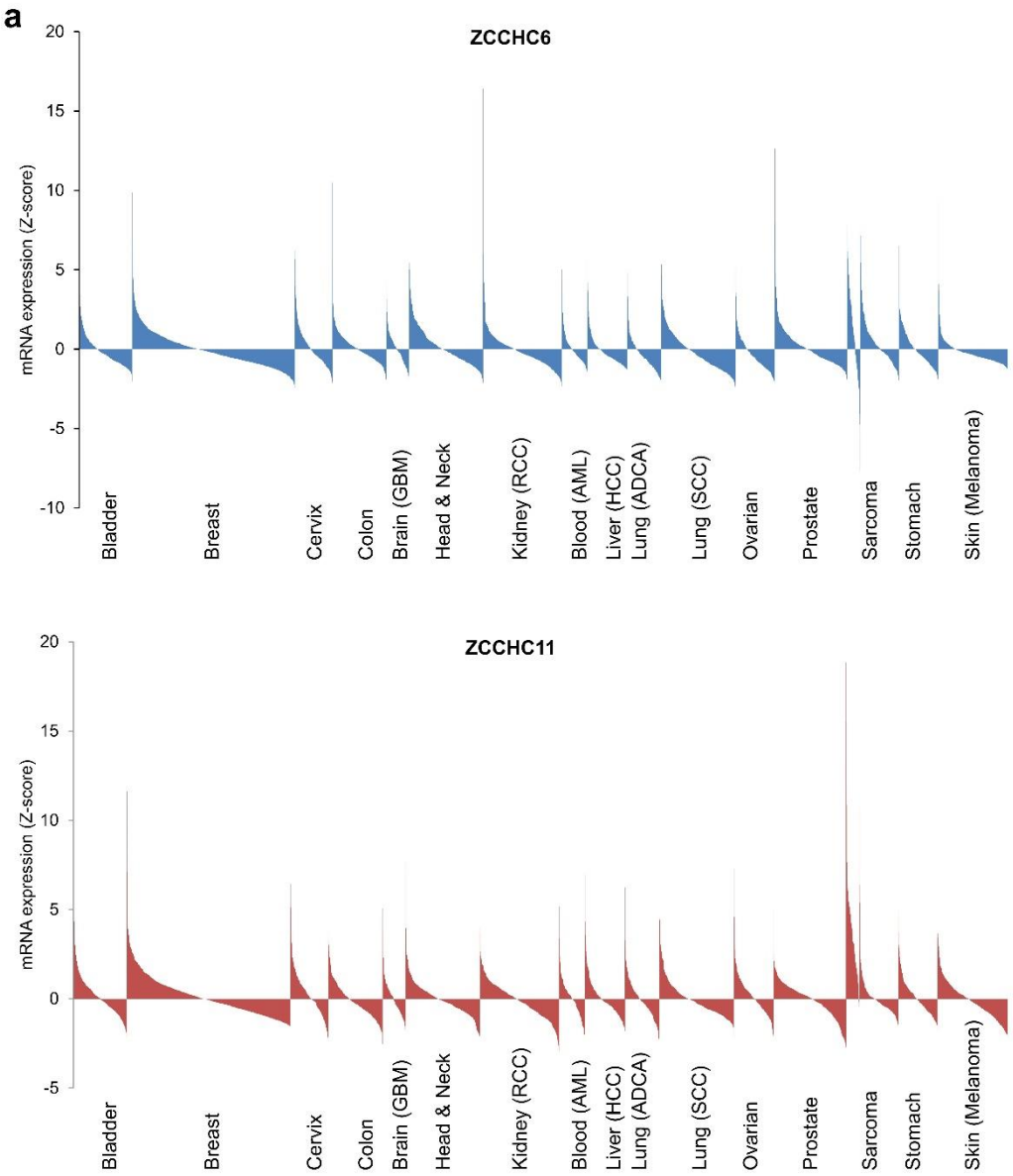

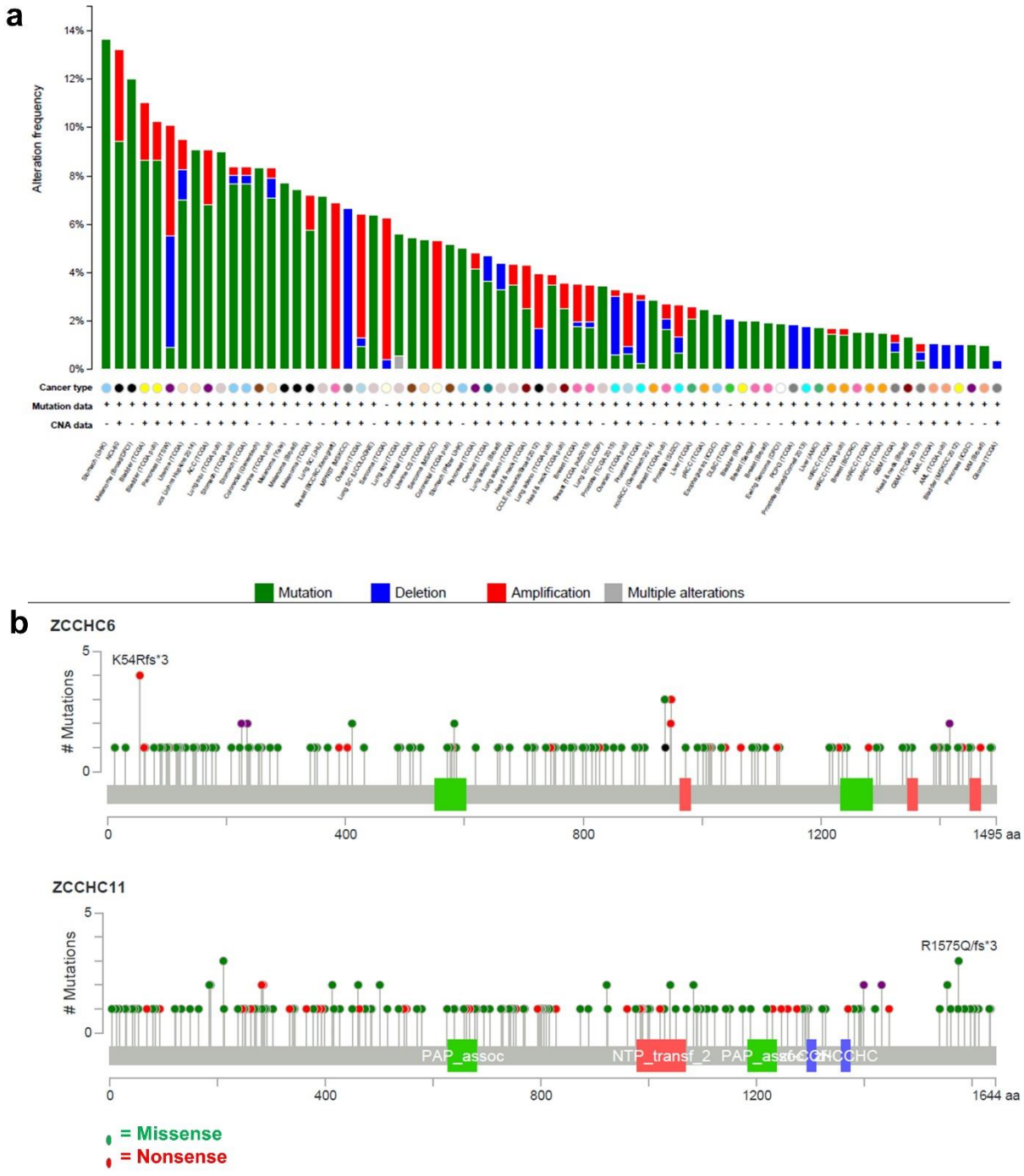

Supplementary Figure 3.2. ZCCHC6/11 amplifications, deletions and point mutations in human tumors. (a) Frequency of ZCCHC6/11 mutations, deletions and amplifications in human tumor samples from different types of cancer. Each bar represents a distinct cancer type. (b) Map of specific ZCCHC6/11 point mutations in human tumor samples from different types of cancer. The ZCCHC6/11 domain structure is shown on the x-axis while the frequency of mutations is indicated on the y-axis. All data were obtained from cBioPortal (www.cbioportal.org) [1].

Supplementary Figure 3.3. qRT-PCR validation of RNA-seq half-life analysis in HCT116 cells. (a) Half-life analysis of mRNAs corresponding to four representative genes from Figure 3.4e. (b) Half-life analysis of short non-coding RNAs. Experiments were performed essentially as shown in Figure 3.4d, with the addition of a 12 h time-point for the non-coding RNAs. Error bars indicate s.e.m. (n=3).

Supplementary Figure 3.3 (Continued)

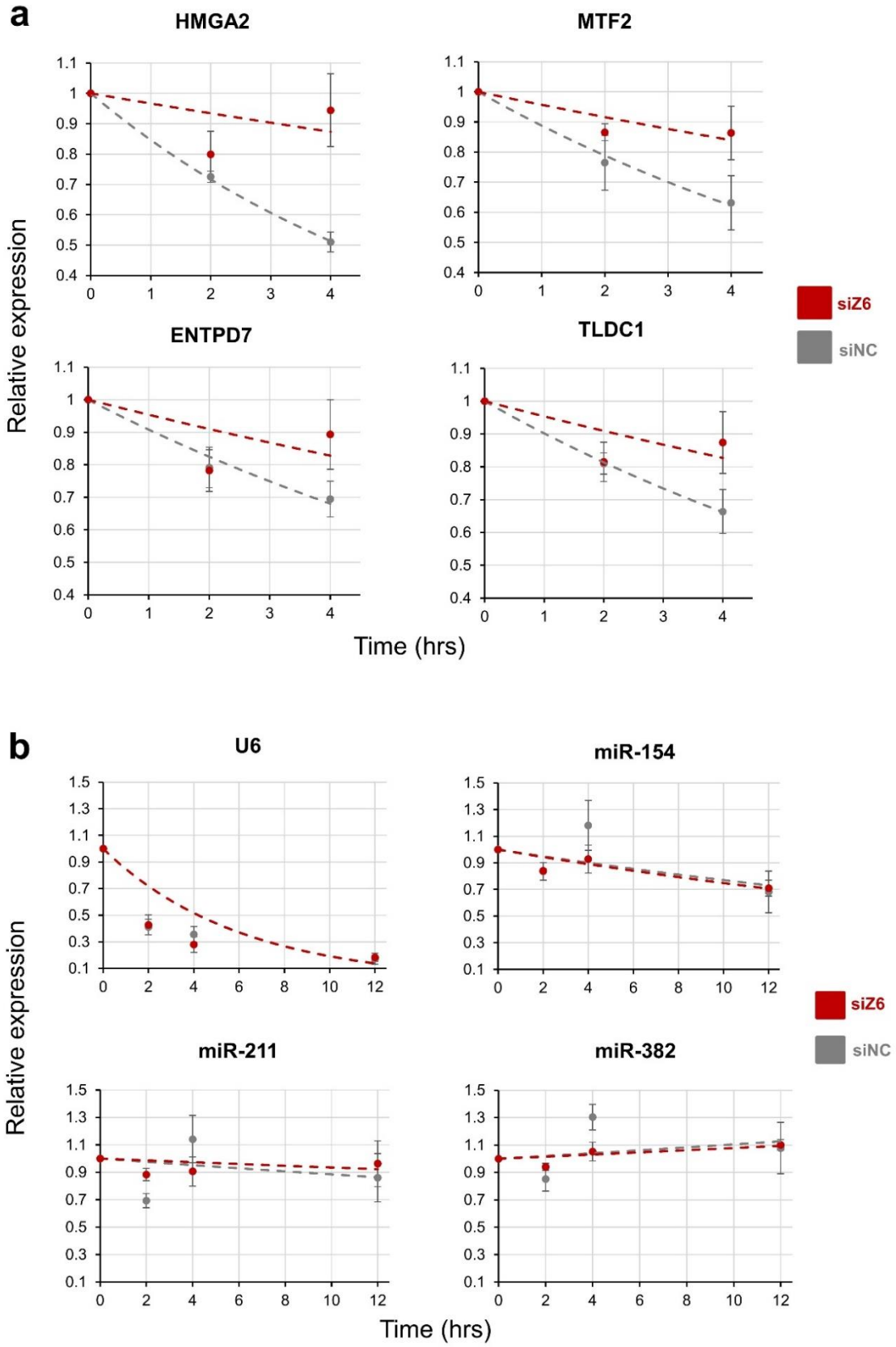

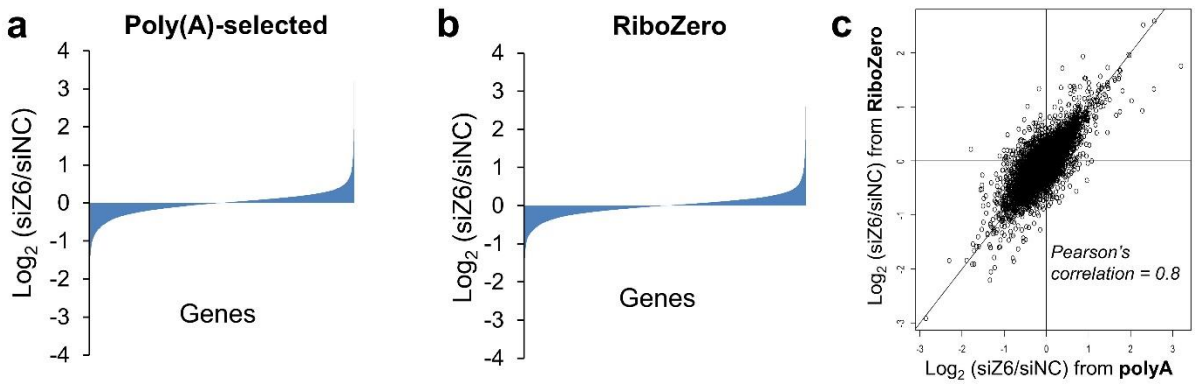

Supplementary Figure 3.4. RNA-seq analysis of steady-state mRNA levels after ZCCHC6 depletion in HCT116 cells. Distribution of mRNA expression changes in siZ6 vs. siNC HCT116 cells. The x-axis depicts individual genes and the y-axis indicates corresponding Log2 fold-changes in their mRNA levels. Libraries were prepared using poly(A) selection (a) or RiboZero rRNA depletion (b), as described in the Methods. (c) Correlation between data obtained from the two protocols.

Supplementary Figure 3.5. ZCCHC6/11 promote a less differentiated state in mouse ESCs and muscle progenitors. (a) qRT-PCR analysis of ZCCHC6/11 (Z6/11) in v6.5 mESCs after 2i/LIF withdrawal for the indicated amounts of time (0-72h). (b) Alkaline phosphatase staining of doxycycline-inducible ZCCHC6 (iZ6) and ZCCHC11 (iZ11) transgenic mESC lines. Cells were untreated (-Dox) or treated with doxycycline (+Dox) for 5 days. Images are representative of three independent experiments. Magnification: 4X. Western blot validation of ZCCHC6/11 overexpression is shown on the bottom. (c) Alkaline phosphatase staining of non-targeting control (NTC) and ZCCHC6/11 double-knockout (DKO) mESC lines. Two independent clones were analyzed. Images are representative of three independent experiments. Magnification: 4X. Western blot validation of ZCCHC6/11 knockout is shown on the bottom. (d) Western blot analysis of ZCCHC6/11 at different time-points during C2C12 cell differentiation. Day 0 indicates the onset of differentiation. Data are representative of two independent experiments. (e) Bright-field images of empty-vector control (EV) and ZCCHC6 overexpression (Z6OE) C2C12 cells at the onset (D0) and after three days (D3) of differentiation. Western blot validation of ZCCHC6 overexpression is shown on the right. Data are representative of three independent experiments. (f) Bright-field images of control (siNC) or ZCCHC6/11 double-knockdown (siZ6+11) C2C12 cells at the onset (D0) and after three days (D3) of differentiation. Differentiation was initiated 48 h after siRNA transfection. Western blot validation of ZCCHC6/11 knockdown is shown on the right. Data are representative of four independent experiments.

Supplementary Figure 3.5 (Continued)

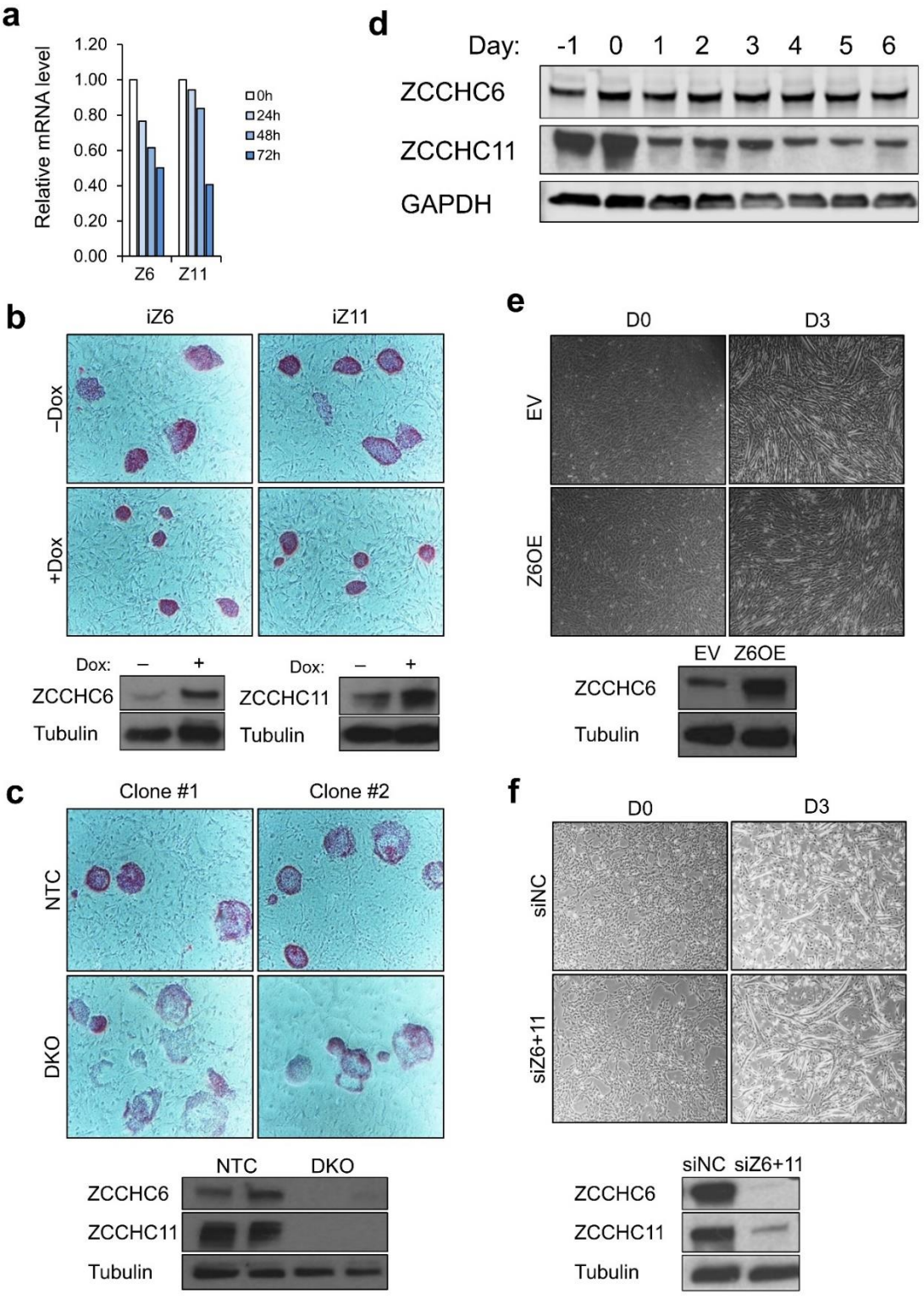

BIBLIOGRAPHY

1. Cerami, E., et al., *The cBio cancer genomics portal: an open platform for exploring multidimensional cancer genomics data.* Cancer Discov, 2012. **2**(5): p. 401-4.

2. Hooke, R. and Lessing J. Rosenwald Collection (Library of Congress), *Micrographia: or, Some physiological descriptions of minute bodies made by magnifying glasses. With observations and inquiries thereupon*. 1665, London,: Printed by J. Martyn and J. Allestry. 18 p. l., 246, 10 p.

3. Trapnell, C., *Defining cell types and states with single-cell genomics.* Genome Res, 2015. **25**(10): p. 1491-8.

4. McCulloch, E.A. and J.E. Till, *The radiation sensitivity of normal mouse bone marrow cells, determined by quantitative marrow transplantation into irradiated mice.* Radiat Res, 1960. **13**: p. 115-25.

5. Till, J.E. and C.E. Mc, *A direct measurement of the radiation sensitivity of normal mouse bone marrow cells.* Radiat Res, 1961. **14**: p. 213-22.

6. Martello, G. and A. Smith, *The nature of embryonic stem cells.* Annu Rev Cell Dev Biol, 2014. **30**: p. 647-75.

7. Nichols, J. and A. Smith, *Naive and primed pluripotent states.* Cell Stem Cell, 2009. **4**(6): p. 487-92.

8. Evans, M.J. and M.H. Kaufman, *Establishment in culture of pluripotential cells from mouse embryos.* Nature, 1981. **292**(5819): p. 154-6.

9. Martin, G.R., *Isolation of a pluripotent cell line from early mouse embryos cultured in medium conditioned by teratocarcinoma stem cells.* Proc Natl Acad Sci U S A, 1981. **78**(12): p. 7634-8.

10. Smith, A.G., et al., *Inhibition of pluripotential embryonic stem cell differentiation by purified polypeptides.* Nature, 1988. **336**(6200): p. 688-90.

11. Williams, R.L., et al., *Myeloid leukaemia inhibitory factor maintains the developmental potential of embryonic stem cells.* Nature, 1988. **336**(6200): p. 684-7.

12. Lanner, F. and J. Rossant, *The role of FGF/Erk signaling in pluripotent cells.* Development, 2010. **137**(20): p. 3351-60.

13. Doble, B.W., et al., *Functional redundancy of GSK-3alpha and GSK-3beta in Wnt/beta-catenin signaling shown by using an allelic series of embryonic stem cell lines.* Dev Cell, 2007. **12**(6): p. 957-71.

14. Sato, N., et al., *Maintenance of pluripotency in human and mouse embryonic stem cells through activation of Wnt signaling by a pharmacological GSK-3-specific inhibitor.* Nat Med, 2004. **10**(1): p. 55-63.

15. Ying, Q.L., et al., *The ground state of embryonic stem cell self-renewal.* Nature, 2008. **453**(7194): p. 519-23.

16. De Los Angeles, A., et al., *Hallmarks of pluripotency.* Nature, 2015. **525**(7570): p. 469-78.

17. Hackett, J.A. and M.A. Surani, *Regulatory principles of pluripotency: from the ground state up.* Cell Stem Cell, 2014. **15**(4): p. 416-30.

18. Kalkan, T. and A. Smith, *Mapping the route from naive pluripotency to lineage specification.* Philos Trans R Soc Lond B Biol Sci, 2014. **369**(1657).

19. Briggs, R. and T.J. King, *Transplantation of Living Nuclei From Blastula Cells into Enucleated Frogs' Eggs.* Proc Natl Acad Sci U S A, 1952. **38**(5): p. 455-63.

20. Gurdon, J.B., *The developmental capacity of nuclei taken from intestinal epithelium cells of feeding tadpoles.* J Embryol Exp Morphol, 1962. **10**: p. 622-40.

21. Spemann, H., *Die Entwicklung seitlicher und dorso-ventraler Keimhälften bei verzögerter Kernversorgung. .* Ztschr. f. Wiss. Zool., 1928. **132**: p. 105–134.

22. Takahashi, K. and S. Yamanaka, *Induction of pluripotent stem cells from mouse embryonic and adult fibroblast cultures by defined factors.* Cell, 2006. **126**(4): p. 663-76.

23. Park, I.H., et al., *Reprogramming of human somatic cells to pluripotency with defined factors.* Nature, 2008. **451**(7175): p. 141-6.

24. Takahashi, K., et al., *Induction of pluripotent stem cells from adult human fibroblasts by defined factors.* Cell, 2007. **131**(5): p. 861-72.

25. Yu, J., et al., *Induced pluripotent stem cell lines derived from human somatic cells.* Science, 2007. **318**(5858): p. 1917-20.

26. Friedmann-Morvinski, D. and I.M. Verma, *Dedifferentiation and reprogramming: origins of cancer stem cells.* EMBO Rep, 2014. **15**(3): p. 244-53.

27. Daley, G.Q., *Common themes of dedifferentiation in somatic cell reprogramming and cancer.* Cold Spring Harb Symp Quant Biol, 2008. **73**: p. 171-4.

28. Lensch, M.W. and C.L. Mummery, *From stealing fire to cellular reprogramming: a scientific history leading to the 2012 Nobel Prize.* Stem Cell Reports, 2013. **1**(1): p. 5-17.

29. Birch, S.T., E., *An extract of two letters from Mr. Sampson Birch, an Alderman and Apothecary at Stafford, concerning an extraordinary birth in Staffordshire, with reflections thereon by Edw. Tyson M.D. Fellow of the Coll. of Physitians, and of the R. Society.* Philos. Trans. R. Soc. London. , 1683. **13**: p. 281-284.

30. Scultetus, J., *Trichiasis Admiranda Sive Morbus Pilaris Mirabilis Observatus*, ed. M. Enderi. 1658, Norimbergae.

31. Yonge, J., *An Account of Balls of Hair Taken from the Uterus and Ovaria of Several Women; By Mr. James Yonge, F.R.S. Communicated to Dr. Hans Sloane, R.S. Secr.* Philos. Trans. R. Soc. London., 1706. **25**: p. 2387–2392.

32. Virchow, R., *Die Krankhaften Geschwülste*. 1863, Berlin: Hirschwald.

33. Durante, F., *Nesso fisio-pathologico tra la struttura dei nei materni e la genesi di alcuni tumori maligni.* Arch. Memor. Observ. Chir. Pract., 1874. **11**: p. 217-226.

34. Cohnheim, J., *Congenitales, quergestreiftes Muskelsarkom der Nieren.* Virchows Arch., 1875. **65**: p. 64-69.

35. Sell, S., *On the stem cell origin of cancer.* Am J Pathol, 2010. **176**(6): p. 2584-494.

36. Ribbert, H., *Das Karzinom des Menschen, sein Bau, sein Wachstum, seine Entstehung*. 1911, Bonn,: F. Cohen. vii, 526 p.

37. von Hansemann, D., *Ueber asymmetrische Zelltheilung in epithel Krebsen und deren biologische Bedeutung.* Virchow's Arch. Path. Anat., 1890. **119**: p. 299-326.

38. von Hansemann, D., *Studien über die Specificität, den Altruismus und die Anaplasie der Zellen.* 1893, Berlin: Hirschwald.

39. Kahan, B.W. and B. Ephrussi, *Developmental potentialities of clonal in vitro cultures of mouse testicular teratoma.* J Natl Cancer Inst, 1970. **44**(5): p. 1015-36.

40. Kleinsmith, L.J. and G.B. Pierce, Jr., *Multipotentiality of Single Embryonal Carcinoma Cells.* Cancer Res, 1964. **24**: p. 1544-51.

41. Martin, G.R. and M.J. Evans, *Differentiation of clonal lines of teratocarcinoma cells: formation of embryoid bodies in vitro.* Proc Natl Acad Sci U S A, 1975. **72**(4): p. 1441-5.

42. Stevens, L.C. and C.C. Little, *Spontaneous Testicular Teratomas in an Inbred Strain of Mice.* Proc Natl Acad Sci U S A, 1954. **40**(11): p. 1080-7.

43. Pierce, G.B. and F.J. Dixon, Jr., *Testicular teratomas. I. Demonstration of teratogenesis by metamorphosis of multipotential cells.* Cancer, 1959. **12**(3): p. 573-83.

44. Pierce, G.B., Jr., F.J. Dixon, Jr., and E.L. Verney, *Teratocarcinogenic and tissue-forming potentials of the cell types comprising neoplastic embryoid bodies.* Lab Invest, 1960. **9**: p. 583-602.

45. Potter, V.R., *Phenotypic diversity in experimental hepatomas: the concept of partially blocked ontogeny. The 10th Walter Hubert Lecture.* Br J Cancer, 1978. **38**(1): p. 1-23.

46. Sell, S., *Stem cell origin of cancer and differentiation therapy.* Crit Rev Oncol Hematol, 2004. **51**(1): p. 1-28.

47. Bonnet, D. and J.E. Dick, *Human acute myeloid leukemia is organized as a hierarchy that originates from a primitive hematopoietic cell.* Nat Med, 1997. **3**(7): p. 730-7.

48. Lapidot, T., et al., *A cell initiating human acute myeloid leukaemia after transplantation into SCID mice.* Nature, 1994. **367**(6464): p. 645-8.

49. Metcalf, D., *Potentiation of bone marrow colony growth in vitro by the addition of lymphoid or bone marrow cells.* J Cell Physiol, 1968. **72**(1): p. 9-19.

50. Moore, M.A., N. Williams, and D. Metcalf, *In vitro colony formation by normal and leukemic human hematopoietic cells: characterization of the colony-forming cells.* J Natl Cancer Inst, 1973. **50**(3): p. 603-23.

51. Robinson, W.A., J.E. Kurnick, and B.L. Pike, *Colony growth of human leukemic peripheral blood cells in vitro.* Blood, 1971. **38**(4): p. 500-8.

52. Siminovitch, L., E.A. McCulloch, and J.E. Till, *The Distribution of Colony-Forming Cells among Spleen Colonies.* J Cell Comp Physiol, 1963. **62**: p. 327-36.

53. Furth, J.K. and M.C. Kahn, *The transmission of leukemia of mice with a single cell.* Am J. Cancer, 1937. **31**: p. 276-282.

54. Kreso, A. and J.E. Dick, *Evolution of the cancer stem cell model.* Cell Stem Cell, 2014. **14**(3): p. 275-91.

55. Magee, J.A., E. Piskounova, and S.J. Morrison, *Cancer stem cells: impact, heterogeneity, and uncertainty.* Cancer Cell, 2012. **21**(3): p. 283-96.

56. Hanahan, D. and R.A. Weinberg, *The hallmarks of cancer.* Cell, 2000. **100**(1): p. 57-70.

57. Hanahan, D. and R.A. Weinberg, *Hallmarks of cancer: the next generation.* Cell, 2011. **144**(5): p. 646-74.

58. Knudson, A.G., Jr., *Mutation and cancer: statistical study of retinoblastoma.* Proc Natl Acad Sci U S A, 1971. **68**(4): p. 820-3.

59. Nowell, P.C., *Genetic changes in cancer: cause or effect?* Hum Pathol, 1971. **2**(3): p. 347-8.

60. Fearon, E.R. and B. Vogelstein, *A genetic model for colorectal tumorigenesis.* Cell, 1990. **61**(5): p. 759-67.

61. Garraway, L.A. and E.S. Lander, *Lessons from the cancer genome.* Cell, 2013. **153**(1): p. 17-37.

62. Greaves, M. and C.C. Maley, *Clonal evolution in cancer.* Nature, 2012. **481**(7381): p. 306-13.

63. Marusyk, A., V. Almendro, and K. Polyak, *Intra-tumour heterogeneity: a looking glass for cancer?* Nat Rev Cancer, 2012. **12**(5): p. 323-34.

64. Shackleton, M., et al., *Heterogeneity in cancer: cancer stem cells versus clonal evolution.* Cell, 2009. **138**(5): p. 822-9.

65. Reya, T., et al., *Stem cells, cancer, and cancer stem cells.* Nature, 2001. **414**(6859): p. 105-11.

66. Dang, C.V., *MYC on the path to cancer.* Cell, 2012. **149**(1): p. 22-35.

67. Farrugia, M.K., et al., *Kruppel-like Pluripotency Factors as Modulators of Cancer Cell Therapeutic Responses.* Cancer Res, 2016. **76**(7): p. 1677-82.

68. Jeter, C.R., et al., *Concise Review: NANOG in Cancer Stem Cells and Tumor Development: An Update and Outstanding Questions.* Stem Cells, 2015. **33**(8): p. 2381-90.

69. Sarkar, A. and K. Hochedlinger, *The sox family of transcription factors: versatile regulators of stem and progenitor cell fate.* Cell Stem Cell, 2013. **12**(1): p. 15-30.

70. Shyh-Chang, N. and G.Q. Daley, *Lin28: primal regulator of growth and metabolism in stem cells.* Cell Stem Cell, 2013. **12**(4): p. 395-406.

71. Wang, Y.J. and M. Herlyn, *The emerging roles of Oct4 in tumor-initiating cells.* Am J Physiol Cell Physiol, 2015. **309**(11): p. C709-18.

72. Dreesen, O. and A.H. Brivanlou, *Signaling pathways in cancer and embryonic stem cells.* Stem Cell Rev, 2007. **3**(1): p. 7-17.

73. Jiang, J. and C.C. Hui, *Hedgehog signaling in development and cancer.* Dev Cell, 2008. **15**(6): p. 801-12.

74. Reya, T. and H. Clevers, *Wnt signalling in stem cells and cancer.* Nature, 2005. **434**(7035): p. 843-50.

75. Roy, M., W.S. Pear, and J.C. Aster, *The multifaceted role of Notch in cancer.* Curr Opin Genet Dev, 2007. **17**(1): p. 52-9.

76. Matsui, W.H., *Cancer stem cell signaling pathways.* Medicine (Baltimore), 2016. **95**(1 Suppl 1): p. S8-S19.

77. Crick, F.H., *On protein synthesis.* Symp Soc Exp Biol, 1958. **12**: p. 138-63.

78. Brenner, S., F. Jacob, and M. Meselson, *An unstable intermediate carrying information from genes to ribosomes for protein synthesis.* Nature, 1961. **190**: p. 576-581.

79. Moore, M.J., *From birth to death: the complex lives of eukaryotic mRNAs.* Science, 2005. **309**(5740): p. 1514-8.

80. Gerstberger, S., M. Hafner, and T. Tuschl, *A census of human RNA-binding proteins.* Nat Rev Genet, 2014. **15**(12): p. 829-45.

81. Glisovic, T., et al., *RNA-binding proteins and post-transcriptional gene regulation.* FEBS Lett, 2008. **582**(14): p. 1977-86.

82. Hattori, A., K. Buac, and T. Ito, *Regulation of Stem Cell Self-Renewal and Oncogenesis by RNA-Binding Proteins.* Adv Exp Med Biol, 2016. **907**: p. 153-88.

83. Braude, P., et al., *Post-transcriptional control in the early mouse embryo.* Nature, 1979. **282**(5734): p. 102-5.

84. Yartseva, V. and A.J. Giraldez, *The Maternal-to-Zygotic Transition During Vertebrate Development: A Model for Reprogramming.* Curr Top Dev Biol, 2015. **113**: p. 191-232.

85. Ye, J. and R. Blelloch, *Regulation of pluripotency by RNA binding proteins.* Cell Stem Cell, 2014. **15**(3): p. 271-80.

86. Weil, T.T., *Post-transcriptional regulation of early embryogenesis.* F1000Prime Rep, 2015. **7**: p. 31.

87. Audic, Y. and R.S. Hartley, *Post-transcriptional regulation in cancer.* Biol Cell, 2004. **96**(7): p. 479-98.

88. Lu, R., et al., *Systems-level dynamic analyses of fate change in murine embryonic stem cells.* Nature, 2009. **462**(7271): p. 358-62.

89. Sampath, P., et al., *A hierarchical network controls protein translation during murine embryonic stem cell self-renewal and differentiation.* Cell Stem Cell, 2008. **2**(5): p. 448-60.

90. Benevento, M., et al., *Proteome adaptation in cell reprogramming proceeds via distinct transcriptional networks.* Nat Commun, 2014. **5**: p. 5613.

91. Lundberg, E., et al., *Defining the transcriptome and proteome in three functionally different human cell lines.* Mol Syst Biol, 2010. **6**: p. 450.

92. Schwanhausser, B., et al., *Global quantification of mammalian gene expression control.* Nature, 2011. **473**(7347): p. 337-42.

93. Vogel, C., et al., *Sequence signatures and mRNA concentration can explain two-thirds of protein abundance variation in a human cell line.* Mol Syst Biol, 2010. **6**: p. 400.

94. Ingolia, N.T., *Ribosome profiling: new views of translation, from single codons to genome scale.* Nat Rev Genet, 2014. **15**(3): p. 205-13.

95. Hershey, J.W., N. Sonenberg, and M.B. Mathews, *Principles of translational control: an overview.* Cold Spring Harb Perspect Biol, 2012. **4**(12).

96. Jackson, R.J., C.U. Hellen, and T.V. Pestova, *The mechanism of eukaryotic translation initiation and principles of its regulation.* Nat Rev Mol Cell Biol, 2010. **11**(2): p. 113-27.

97. Kong, J. and P. Lasko, *Translational control in cellular and developmental processes.* Nat Rev Genet, 2012. **13**(6): p. 383-94.

98. Cho, P.F., et al., *A new paradigm for translational control: inhibition via 5'-3' mRNA tethering by Bicoid and the eIF4E cognate 4EHP.* Cell, 2005. **121**(3): p. 411-23.

99. Rosettani, P., et al., *Structures of the human eIF4E homologous protein, h4EHP, in its m7GTP-bound and unliganded forms.* J Mol Biol, 2007. **368**(3): p. 691-705.

100. Weill, L., et al., *Translational control by changes in poly(A) tail length: recycling mRNAs.* Nat Struct Mol Biol, 2012. **19**(6): p. 577-85.

101. Truitt, M.L. and D. Ruggero, *New frontiers in translational control of the cancer genome.* Nat Rev Cancer, 2016. **16**(5): p. 288-304.

102. Kronja, I., et al., *Widespread changes in the posttranscriptional landscape at the Drosophila oocyte-to-embryo transition.* Cell Rep, 2014. **7**(5): p. 1495-508.

103. Langley, A.R., et al., *New insights into the maternal to zygotic transition.* Development, 2014. **141**(20): p. 3834-41.

104. Latham, K.E., et al., *Quantitative analysis of protein synthesis in mouse embryos. I. Extensive reprogramming at the one- and two-cell stages.* Development, 1991. **112**(4): p. 921-32.

105. Ingolia, N.T., L.F. Lareau, and J.S. Weissman, *Ribosome profiling of mouse embryonic stem cells reveals the complexity and dynamics of mammalian proteomes.* Cell, 2011. **147**(4): p. 789-802.

106. Blanco, S., et al., *Stem cell function and stress response are controlled by protein synthesis.* Nature, 2016. **534**(7607): p. 335-40.

107. Buszczak, M., R.A. Signer, and S.J. Morrison, *Cellular differences in protein synthesis regulate tissue homeostasis.* Cell, 2014. **159**(2): p. 242-51.

108. Signer, R.A., et al., *Haematopoietic stem cells require a highly regulated protein synthesis rate.* Nature, 2014. **509**(7498): p. 49-54.

109. Ruggero, D., *Translational control in cancer etiology.* Cold Spring Harb Perspect Biol, 2013. **5**(2).

110. Gani, R., *The nucleoli of cultured human lymphocytes. I. Nucleolar morphology in relation to transformation and the DNA cycle.* Exp Cell Res, 1976. **97**(2): p. 249-58.

111. Ruggero, D. and P.P. Pandolfi, *Does the ribosome translate cancer?* Nat Rev Cancer, 2003. **3**(3): p. 179-92.

112. Furic, L., et al., *eIF4E phosphorylation promotes tumorigenesis and is associated with prostate cancer progression.* Proc Natl Acad Sci U S A, 2010. **107**(32): p. 14134-9.

113. Hsieh, A.C., et al., *Genetic dissection of the oncogenic mTOR pathway reveals druggable addiction to translational control via 4EBP-eIF4E.* Cancer Cell, 2010. **17**(3): p. 249-61.

114. Miluzio, A., et al., *Impairment of cytoplasmic eIF6 activity restricts lymphomagenesis and tumor progression without affecting normal growth.* Cancer Cell, 2011. **19**(6): p. 765-75.

115. Truitt, M.L., et al., *Differential Requirements for eIF4E Dose in Normal Development and Cancer.* Cell, 2015. **162**(1): p. 59-71.

116. Barna, M., et al., *Suppression of Myc oncogenic activity by ribosomal protein haploinsufficiency.* Nature, 2008. **456**(7224): p. 971-5.

117. Narla, A. and B.L. Ebert, *Ribosomopathies: human disorders of ribosome dysfunction.* Blood, 2010. **115**(16): p. 3196-205.

118. Hsieh, A.C., et al., *The translational landscape of mTOR signalling steers cancer initiation and metastasis.* Nature, 2012. **485**(7396): p. 55-61.

119. Wolfe, A.L., et al., *RNA G-quadruplexes cause eIF4A-dependent oncogene translation in cancer.* Nature, 2014. **513**(7516): p. 65-70.

120. Wurth, L. and F. Gebauer, *RNA-binding proteins, multifaceted translational regulators in cancer.* Biochim Biophys Acta, 2015. **1849**(7): p. 881-6.

121. Schoenberg, D.R. and L.E. Maquat, *Regulation of cytoplasmic mRNA decay.* Nat Rev Genet, 2012. **13**(4): p. 246-59.

122. Garneau, N.L., J. Wilusz, and C.J. Wilusz, *The highways and byways of mRNA decay.* Nat Rev Mol Cell Biol, 2007. **8**(2): p. 113-26.

123. Houseley, J., J. LaCava, and D. Tollervey, *RNA-quality control by the exosome.* Nat Rev Mol Cell Biol, 2006. **7**(7): p. 529-39.

124. Nagarajan, V.K., et al., *XRN 5'-->3' exoribonucleases: structure, mechanisms and functions.* Biochim Biophys Acta, 2013. **1829**(6-7): p. 590-603.

125. Tomecki, R. and A. Dziembowski, *Novel endoribonucleases as central players in various pathways of eukaryotic RNA metabolism.* RNA, 2010. **16**(9): p. 1692-724.

126. Decker, C.J. and R. Parker, *P-bodies and stress granules: possible roles in the control of translation and mRNA degradation.* Cold Spring Harb Perspect Biol, 2012. **4**(9): p. a012286.

127. Chen, C.Y. and A.B. Shyu, *AU-rich elements: characterization and importance in mRNA degradation.* Trends Biochem Sci, 1995. **20**(11): p. 465-70.

128. Chen, C.Y., et al., *AU binding proteins recruit the exosome to degrade ARE-containing mRNAs.* Cell, 2001. **107**(4): p. 451-64.

129. Gherzi, R., et al., *A KH domain RNA binding protein, KSRP, promotes ARE-directed mRNA turnover by recruiting the degradation machinery.* Mol Cell, 2004. **14**(5): p. 571-83.

130. Lykke-Andersen, J. and E. Wagner, *Recruitment and activation of mRNA decay enzymes by two ARE-mediated decay activation domains in the proteins TTP and BRF-1.* Genes Dev, 2005. **19**(3): p. 351-61.

131. Moraes, K.C., C.J. Wilusz, and J. Wilusz, *CUG-BP binds to RNA substrates and recruits PARN deadenylase.* RNA, 2006. **12**(6): p. 1084-91.

132. Tran, H., et al., *Facilitation of mRNA deadenylation and decay by the exosome-bound, DExH protein RHAU.* Mol Cell, 2004. **13**(1): p. 101-11.

133. Bhattacharyya, S.N., et al., *Relief of microRNA-mediated translational repression in human cells subjected to stress.* Cell, 2006. **125**(6): p. 1111-24.

134. Lal, A., et al., *Concurrent versus individual binding of HuR and AUF1 to common labile target mRNAs.* EMBO J, 2004. **23**(15): p. 3092-102.

135. Linker, K., et al., *Involvement of KSRP in the post-transcriptional regulation of human iNOS expression-complex interplay of KSRP with TTP and HuR.* Nucleic Acids Res, 2005. **33**(15): p. 4813-27.

136. Chaudhury, A., P. Chander, and P.H. Howe, *Heterogeneous nuclear ribonucleoproteins (hnRNPs) in cellular processes: Focus on hnRNP E1's multifunctional regulatory roles.* RNA, 2010. **16**(8): p. 1449-62.

137. Miller, M.A. and W.M. Olivas, *Roles of Puf proteins in mRNA degradation and translation.* Wiley Interdiscip Rev RNA, 2011. **2**(4): p. 471-92.

138. Vlasova-St Louis, I. and P.R. Bohjanen, *Coordinate regulation of mRNA decay networks by GU-rich elements and CELF1.* Curr Opin Genet Dev, 2011. **21**(4): p. 444-51.

139. Alonso, C.R., *A complex 'mRNA degradation code' controls gene expression during animal development.* Trends Genet, 2012. **28**(2): p. 78-88.

140. Chen, Y.H. and J. Coller, *A Universal Code for mRNA Stability?* Trends Genet, 2016. **32**(11): p. 687-688.

141. Neff, A.T., et al., *Global analysis reveals multiple pathways for unique regulation of mRNA decay in induced pluripotent stem cells.* Genome Res, 2012. **22**(8): p. 1457-67.

142. Stumpo, D.J., et al., *Chorioallantoic fusion defects and embryonic lethality resulting from disruption of Zfp36L1, a gene encoding a CCCH tandem zinc finger protein of the Tristetraprolin family.* Mol Cell Biol, 2004. **24**(14): p. 6445-55.

143. Tan, F.E. and M.B. Elowitz, *Brf1 posttranscriptionally regulates pluripotency and differentiation responses downstream of Erk MAP kinase.* Proc Natl Acad Sci U S A, 2014. **111**(17): p. E1740-8.

144. Leeb, M., et al., *Genetic exploration of the exit from self-renewal using haploid embryonic stem cells.* Cell Stem Cell, 2014. **14**(3): p. 385-93.

145. Chang, H.M., et al., *Trim71 cooperates with microRNAs to repress Cdkn1a expression and promote embryonic stem cell proliferation.* Nat Commun, 2012. **3**: p. 923.

146. Loedige, I., et al., *The mammalian TRIM-NHL protein TRIM71/LIN-41 is a repressor of mRNA function.* Nucleic Acids Res, 2013. **41**(1): p. 518-32.

147. Worringer, K.A., et al., *The let-7/LIN-41 pathway regulates reprogramming to human induced pluripotent stem cells by controlling expression of prodifferentiation genes.* Cell Stem Cell, 2014. **14**(1): p. 40-52.

148. Dai, Q., et al., *Primordial dwarfism gene maintains Lin28 expression to safeguard embryonic stem cells from premature differentiation.* Cell Rep, 2014. **7**(3): p. 735-46.

149. Elatmani, H., et al., *The RNA-binding protein Unr prevents mouse embryonic stem cells differentiation toward the primitive endoderm lineage.* Stem Cells, 2011. **29**(10): p. 1504-16.

150. Briata, P., et al., *p38-dependent phosphorylation of the mRNA decay-promoting factor KSRP controls the stability of select myogenic transcripts.* Mol Cell, 2005. **20**(6): p. 891-903.

151. Chenette, D.M., et al., *Targeted mRNA Decay by RNA Binding Protein AUF1 Regulates Adult Muscle Stem Cell Fate, Promoting Skeletal Muscle Integrity.* Cell Rep, 2016. **16**(5): p. 1379-90.

152. Figueroa, A., et al., *Role of HuR in skeletal myogenesis through coordinate regulation of muscle differentiation genes.* Mol Cell Biol, 2003. **23**(14): p. 4991-5004.

153. Deschenes-Furry, J., N. Perrone-Bizzozero, and B.J. Jasmin, *The RNA-binding protein HuD: a regulator of neuronal differentiation, maintenance and plasticity.* Bioessays, 2006. **28**(8): p. 822-33.

154. Ratti, A., et al., *A role for the ELAV RNA-binding proteins in neural stem cells: stabilization of Msi1 mRNA.* J Cell Sci, 2006. **119**(Pt 7): p. 1442-52.

155. Benjamin, D. and C. Moroni, *mRNA stability and cancer: an emerging link?* Expert Opin Biol Ther, 2007. **7**(10): p. 1515-29.

156. Sanduja, S., et al., *The role of tristetraprolin in cancer and inflammation.* Front Biosci (Landmark Ed), 2012. **17**: p. 174-88.

157. Denkert, C., et al., *Expression of the ELAV-like protein HuR is associated with higher tumor grade and increased cyclooxygenase-2 expression in human breast carcinoma.* Clin Cancer Res, 2004. **10**(16): p. 5580-6.

158. Denkert, C., et al., *Overexpression of the embryonic-lethal abnormal vision-like protein HuR in ovarian carcinoma is a prognostic factor and is associated with increased cyclooxygenase 2 expression.* Cancer Res, 2004. **64**(1): p. 189-95.

159. Erkinheimo, T.L., et al., *Elevated cyclooxygenase-2 expression is associated with altered expression of p53 and SMAD4, amplification of HER-2/neu, and poor outcome in serous ovarian carcinoma.* Clin Cancer Res, 2004. **10**(2): p. 538-45.

160. Dixon, D.A., et al., *Altered expression of the mRNA stability factor HuR promotes cyclooxygenase-2 expression in colon cancer cells.* J Clin Invest, 2001. **108**(11): p. 1657-65.

161. Goodarzi, H., et al., *Metastasis-suppressor transcript destabilization through TARBP2 binding of mRNA hairpins.* Nature, 2014. **513**(7517): p. 256-60.

162. Clement, S.L., et al., *Phosphorylation of tristetraprolin by MK2 impairs AU-rich element mRNA decay by preventing deadenylase recruitment.* Mol Cell Biol, 2011. **31**(2): p. 256-66.

163. Marchese, F.P., et al., *MAPKAP kinase 2 blocks tristetraprolin-directed mRNA decay by inhibiting CAF1 deadenylase recruitment.* J Biol Chem, 2010. **285**(36): p. 27590-600.

164. Winzen, R., et al., *Functional analysis of KSRP interaction with the AU-rich element of interleukin-8 and identification of inflammatory mRNA targets.* Mol Cell Biol, 2007. **27**(23): p. 8388-400.

165. Frye, M. and S. Blanco, *Post-transcriptional modifications in development and stem cells.* Development, 2016. **143**(21): p. 3871-3881.

166. Zhao, B.S., I.A. Roundtree, and C. He, *Post-transcriptional gene regulation by mRNA modifications.* Nat Rev Mol Cell Biol, 2017. **18**(1): p. 31-42.

167. Bartel, D.P., *MicroRNAs: target recognition and regulatory functions.* Cell, 2009. **136**(2): p. 215-33.

168. Denli, A.M., et al., *Processing of primary microRNAs by the Microprocessor complex.* Nature, 2004. **432**(7014): p. 231-5.

169. Gregory, R.I., et al., *The Microprocessor complex mediates the genesis of microRNAs.* Nature, 2004. **432**(7014): p. 235-40.

170. Han, J., et al., *The Drosha-DGCR8 complex in primary microRNA processing.* Genes Dev, 2004. **18**(24): p. 3016-27.

171. Landthaler, M., A. Yalcin, and T. Tuschl, *The human DiGeorge syndrome critical region gene 8 and Its D. melanogaster homolog are required for miRNA biogenesis.* Curr Biol, 2004. **14**(23): p. 2162-7.

172. Lee, Y., et al., *The nuclear RNase III Drosha initiates microRNA processing.* Nature, 2003. **425**(6956): p. 415-9.

173. Bohnsack, M.T., K. Czaplinski, and D. Gorlich, *Exportin 5 is a RanGTP-dependent dsRNA-binding protein that mediates nuclear export of pre-miRNAs.* RNA, 2004. **10**(2): p. 185-91.

174. Lund, E., et al., *Nuclear export of microRNA precursors.* Science, 2004. **303**(5654): p. 95-8.

175. Yi, R., et al., *Exportin-5 mediates the nuclear export of pre-microRNAs and short hairpin RNAs.* Genes Dev, 2003. **17**(24): p. 3011-6.

176. Bernstein, E., et al., *Role for a bidentate ribonuclease in the initiation step of RNA interference.* Nature, 2001. **409**(6818): p. 363-6.

177. Park, J.E., et al., *Dicer recognizes the 5' end of RNA for efficient and accurate processing.* Nature, 2011. **475**(7355): p. 201-5.

178. Lee, H.Y. and J.A. Doudna, *TRBP alters human precursor microRNA processing in vitro.* RNA, 2012. **18**(11): p. 2012-9.

179. Kim, Y., et al., *Deletion of human tarbp2 reveals cellular microRNA targets and cell-cycle function of TRBP.* Cell Rep, 2014. **9**(3): p. 1061-74.

180. Chendrimada, T.P., et al., *TRBP recruits the Dicer complex to Ago2 for microRNA processing and gene silencing.* Nature, 2005. **436**(7051): p. 740-4.

181. Gregory, R.I., et al., *Human RISC couples microRNA biogenesis and posttranscriptional gene silencing.* Cell, 2005. **123**(4): p. 631-40.

182. Huntzinger, E. and E. Izaurralde, *Gene silencing by microRNAs: contributions of translational repression and mRNA decay.* Nat Rev Genet, 2011. **12**(2): p. 99-110.

183. Eulalio, A., I. Behm-Ansmant, and E. Izaurralde, *P bodies: at the crossroads of post-transcriptional pathways.* Nat Rev Mol Cell Biol, 2007. **8**(1): p. 9-22.

184. Liu, J., et al., *MicroRNA-dependent localization of targeted mRNAs to mammalian P-bodies.* Nat Cell Biol, 2005. **7**(7): p. 719-23.

185. Kozomara, A. and S. Griffiths-Jones, *miRBase: integrating microRNA annotation and deep-sequencing data.* Nucleic Acids Res, 2011. **39**(Database issue): p. D152-7.

186. Friedman, R.C., et al., *Most mammalian mRNAs are conserved targets of microRNAs.* Genome Res, 2009. **19**(1): p. 92-105.

187. Lewis, B.P., C.B. Burge, and D.P. Bartel, *Conserved seed pairing, often flanked by adenosines, indicates that thousands of human genes are microRNA targets.* Cell, 2005. **120**(1): p. 15-20.

188. Lee, R.C., R.L. Feinbaum, and V. Ambros, *The C. elegans heterochronic gene lin-4 encodes small RNAs with antisense complementarity to lin-14.* Cell, 1993. **75**(5): p. 843-54.

189. Wightman, B., I. Ha, and G. Ruvkun, *Posttranscriptional regulation of the heterochronic gene lin-14 by lin-4 mediates temporal pattern formation in C. elegans.* Cell, 1993. **75**(5): p. 855-62.

190. Alvarez-Garcia, I. and E.A. Miska, *MicroRNA functions in animal development and human disease.* Development, 2005. **132**(21): p. 4653-62.

191. Greve, T.S., R.L. Judson, and R. Blelloch, *microRNA control of mouse and human pluripotent stem cell behavior.* Annu Rev Cell Dev Biol, 2013. **29**: p. 213-39.

192. Bernstein, E., et al., *Dicer is essential for mouse development.* Nat Genet, 2003. **35**(3): p. 215-7.

193. Spruce, T., et al., *An early developmental role for miRNAs in the maintenance of extraembryonic stem cells in the mouse embryo.* Dev Cell, 2010. **19**(2): p. 207-19.

194. Suh, N., et al., *MicroRNA function is globally suppressed in mouse oocytes and early embryos.* Curr Biol, 2010. **20**(3): p. 271-7.

195. Kanellopoulou, C., et al., *Dicer-deficient mouse embryonic stem cells are defective in differentiation and centromeric silencing.* Genes Dev, 2005. **19**(4): p. 489-501.

196. Kumar, R.M., et al., *Deconstructing transcriptional heterogeneity in pluripotent stem cells.* Nature, 2014. **516**(7529): p. 56-61.

197. Wang, Y., et al., *DGCR8 is essential for microRNA biogenesis and silencing of embryonic stem cell self-renewal.* Nat Genet, 2007. **39**(3): p. 380-5.

198. Houbaviy, H.B., M.F. Murray, and P.A. Sharp, *Embryonic stem cell-specific MicroRNAs.* Dev Cell, 2003. **5**(2): p. 351-8.

199. Medeiros, L.A., et al., *Mir-290-295 deficiency in mice results in partially penetrant embryonic lethality and germ cell defects.* Proc Natl Acad Sci U S A, 2011. **108**(34): p. 14163-8.

200. Tang, F., et al., *Tracing the derivation of embryonic stem cells from the inner cell mass by single-cell RNA-Seq analysis.* Cell Stem Cell, 2010. **6**(5): p. 468-78.

201. Wang, Y., et al., *Embryonic stem cell-specific microRNAs regulate the G1-S transition and promote rapid proliferation.* Nat Genet, 2008. **40**(12): p. 1478-83.

202. Gurtan, A.M., et al., *Let-7 represses Nr6a1 and a mid-gestation developmental program in adult fibroblasts.* Genes Dev, 2013. **27**(8): p. 941-54.

203. Melton, C., R.L. Judson, and R. Blelloch, *Opposing microRNA families regulate self-renewal in mouse embryonic stem cells.* Nature, 2010. **463**(7281): p. 621-6.

204. Judson, R.L., et al., *Embryonic stem cell-specific microRNAs promote induced pluripotency.* Nat Biotechnol, 2009. **27**(5): p. 459-61.

205. Li, Z., et al., *Small RNA-mediated regulation of iPS cell generation.* EMBO J, 2011. **30**(5): p. 823-34.

206. Subramanyam, D., et al., *Multiple targets of miR-302 and miR-372 promote reprogramming of human fibroblasts to induced pluripotent stem cells.* Nat Biotechnol, 2011. **29**(5): p. 443-8.

207. Mathieu, J. and H. Ruohola-Baker, *Regulation of stem cell populations by microRNAs.* Adv Exp Med Biol, 2013. **786**: p. 329-51.

208. Miska, E.A., *How microRNAs control cell division, differentiation and death.* Curr Opin Genet Dev, 2005. **15**(5): p. 563-8.

209. Roush, S. and F.J. Slack, *The let-7 family of microRNAs.* Trends Cell Biol, 2008. **18**(10): p. 505-16.

210. Lin, S. and R.I. Gregory, *MicroRNA biogenesis pathways in cancer.* Nat Rev Cancer, 2015. **15**(6): p. 321-33.

211. Calin, G.A. and C.M. Croce, *MicroRNAs and chromosomal abnormalities in cancer cells.* Oncogene, 2006. **25**(46): p. 6202-10.

212. Lu, J., et al., *MicroRNA expression profiles classify human cancers.* Nature, 2005. **435**(7043): p. 834-8.

213. Volinia, S., et al., *A microRNA expression signature of human solid tumors defines cancer gene targets.* Proc Natl Acad Sci U S A, 2006. **103**(7): p. 2257-61.

214. Kumar, M.S., et al., *Impaired microRNA processing enhances cellular transformation and tumorigenesis.* Nat Genet, 2007. **39**(5): p. 673-7.

215. Karube, Y., et al., *Reduced expression of Dicer associated with poor prognosis in lung cancer patients.* Cancer Sci, 2005. **96**(2): p. 111-5.

216. Lin, R.J., et al., *microRNA signature and expression of Dicer and Drosha can predict prognosis and delineate risk groups in neuroblastoma.* Cancer Res, 2010. **70**(20): p. 7841-50.

217. Merritt, W.M., et al., *Dicer, Drosha, and outcomes in patients with ovarian cancer.* N Engl J Med, 2008. **359**(25): p. 2641-50.

218. Heravi-Moussavi, A., et al., *Recurrent somatic DICER1 mutations in nonepithelial ovarian cancers.* N Engl J Med, 2012. **366**(3): p. 234-42.

219. Hill, D.A., et al., *DICER1 mutations in familial pleuropulmonary blastoma.* Science, 2009. **325**(5943): p. 965.

220. Rakheja, D., et al., *Somatic mutations in DROSHA and DICER1 impair microRNA biogenesis through distinct mechanisms in Wilms tumours.* Nat Commun, 2014. **2**: p. 4802.

221. Slade, I., et al., *DICER1 syndrome: clarifying the diagnosis, clinical features and management implications of a pleiotropic tumour predisposition syndrome.* J Med Genet, 2011. **48**(4): p. 273-8.

222. Torrezan, G.T., et al., *Recurrent somatic mutation in DROSHA induces microRNA profile changes in Wilms tumour.* Nat Commun, 2014. **5**: p. 4039.

223. Walz, A.L., et al., *Recurrent DGCR8, DROSHA, and SIX homeodomain mutations in favorable histology Wilms tumors.* Cancer Cell, 2015. **27**(2): p. 286-97.

224. Wegert, J., et al., *Mutations in the SIX1/2 pathway and the DROSHA/DGCR8 miRNA microprocessor complex underlie high-risk blastemal type Wilms tumors.* Cancer Cell, 2015. **27**(2): p. 298-311.

225. Lee, Y.S. and A. Dutta, *MicroRNAs in cancer.* Annu Rev Pathol, 2009. **4**: p. 199-227.

226. He, L., et al., *A microRNA polycistron as a potential human oncogene.* Nature, 2005. **435**(7043): p. 828-33.

227. Calin, G.A., et al., *Frequent deletions and down-regulation of micro- RNA genes miR15 and miR16 at 13q14 in chronic lymphocytic leukemia.* Proc Natl Acad Sci U S A, 2002. **99**(24): p. 15524-9.

228. Boyerinas, B., et al., *The role of let-7 in cell differentiation and cancer.* Endocr Relat Cancer, 2010. **17**(1): p. F19-36.

229. Johnson, S.M., et al., *RAS is regulated by the let-7 microRNA family.* Cell, 2005. **120**(5): p. 635-47.

230. Kim, H.H., et al., *HuR recruits let-7/RISC to repress c-Myc expression.* Genes Dev, 2009. **23**(15): p. 1743-8.

231. Kumar, M.S., et al., *Suppression of non-small cell lung tumor development by the let-7 microRNA family.* Proc Natl Acad Sci U S A, 2008. **105**(10): p. 3903-8.

232. Yu, F., et al., *let-7 regulates self renewal and tumorigenicity of breast cancer cells.* Cell, 2007. **131**(6): p. 1109-23.

233. Ha, M. and V.N. Kim, *Regulation of microRNA biogenesis.* Nat Rev Mol Cell Biol, 2014. **15**(8): p. 509-24.

234. Tang, X., et al., *Glycogen synthase kinase 3 beta (GSK3beta) phosphorylates the RNAase III enzyme Drosha at S300 and S302.* PLoS One, 2011. **6**(6): p. e20391.

235. Tang, X., et al., *Phosphorylation of the RNase III enzyme Drosha at Serine300 or Serine302 is required for its nuclear localization.* Nucleic Acids Res, 2010. **38**(19): p. 6610-9.

236. Herbert, K.M., et al., *Phosphorylation of DGCR8 increases its intracellular stability and induces a progrowth miRNA profile.* Cell Rep, 2013. **5**(4): p. 1070-81.

237. Paroo, Z., et al., *Phosphorylation of the human microRNA-generating complex mediates MAPK/Erk signaling.* Cell, 2009. **139**(1): p. 112-22.

238. Horman, S.R., et al., *Akt-mediated phosphorylation of argonaute 2 downregulates cleavage and upregulates translational repression of MicroRNA targets.* Mol Cell, 2013. **50**(3): p. 356-67.

239. Shen, J., et al., *EGFR modulates microRNA maturation in response to hypoxia through phosphorylation of AGO2.* Nature, 2013. **497**(7449): p. 383-7.

240. Zeng, Y., et al., *Phosphorylation of Argonaute 2 at serine-387 facilitates its localization to processing bodies.* Biochem J, 2008. **413**(3): p. 429-36.

241. Hocine, S., R.H. Singer, and D. Grunwald, *RNA processing and export.* Cold Spring Harb Perspect Biol, 2010. **2**(12): p. a000752.

242. Keene, J.D., *RNA regulons: coordination of post-transcriptional events.* Nat Rev Genet, 2007. **8**(7): p. 533-43.

243. Ambros, V. and H.R. Horvitz, *Heterochronic mutants of the nematode Caenorhabditis elegans.* Science, 1984. **226**(4673): p. 409-16.

244. Moss, E.G., *Heterochronic genes and the nature of developmental time.* Curr Biol, 2007. **17**(11): p. R425-34.

245. Slack, F. and G. Ruvkun, *Heterochronic genes in development and evolution.* Biol Bull, 1998. **195**(3): p. 375-6.

246. Moss, E.G., R.C. Lee, and V. Ambros, *The cold shock domain protein LIN-28 controls developmental timing in C. elegans and is regulated by the lin-4 RNA.* Cell, 1997. **88**(5): p. 637-46.

247. Moss, E.G. and L. Tang, *Conservation of the heterochronic regulator Lin-28, its developmental expression and microRNA complementary sites.* Dev Biol, 2003. **258**(2): p. 432-42.

248. Yang, D.H. and E.G. Moss, *Temporally regulated expression of Lin-28 in diverse tissues of the developing mouse.* Gene Expr Patterns, 2003. **3**(6): p. 719-26.

249. Heo, I., et al., *Lin28 mediates the terminal uridylation of let-7 precursor MicroRNA.* Mol Cell, 2008. **32**(2): p. 276-84.

250. Newman, M.A., J.M. Thomson, and S.M. Hammond, *Lin-28 interaction with the Let-7 precursor loop mediates regulated microRNA processing.* RNA, 2008. **14**(8): p. 1539-49.

251. Rybak, A., et al., *A feedback loop comprising lin-28 and let-7 controls pre-let-7 maturation during neural stem-cell commitment.* Nat Cell Biol, 2008. **10**(8): p. 987-93.

252. Viswanathan, S.R., G.Q. Daley, and R.I. Gregory, *Selective blockade of microRNA processing by Lin28.* Science, 2008. **320**(5872): p. 97-100.

253. Bussing, I., F.J. Slack, and H. Grosshans, *let-7 microRNAs in development, stem cells and cancer.* Trends Mol Med, 2008. **14**(9): p. 400-9.

254. Viswanathan, S.R., et al., *Lin28 promotes transformation and is associated with advanced human malignancies.* Nat Genet, 2009. **41**(7): p. 843-8.

255. Piskounova, E., et al., *Lin28A and Lin28B inhibit let-7 microRNA biogenesis by distinct mechanisms.* Cell, 2011. **147**(5): p. 1066-79.

256. Piskounova, E., et al., *Determinants of microRNA processing inhibition by the developmentally regulated RNA-binding protein Lin28.* J Biol Chem, 2008. **283**(31): p. 21310-4.

257. Hagan, J.P., E. Piskounova, and R.I. Gregory, *Lin28 recruits the TUTase Zcchc11 to inhibit let-7 maturation in mouse embryonic stem cells.* Nat Struct Mol Biol, 2009. **16**(10): p. 1021-5.

258. Heo, I., et al., *Mono-uridylation of pre-microRNA as a key step in the biogenesis of group II let-7 microRNAs.* Cell, 2012. **151**(3): p. 521-32.

259. Heo, I., et al., *TUT4 in concert with Lin28 suppresses microRNA biogenesis through pre-microRNA uridylation.* Cell, 2009. **138**(4): p. 696-708.

260. Thornton, J.E., et al., *Lin28-mediated control of let-7 microRNA expression by alternative TUTases Zcchc11 (TUT4) and Zcchc6 (TUT7).* RNA, 2012. **18**(10): p. 1875-85.

261. Chang, H.M., et al., *A role for the Perlman syndrome exonuclease Dis3l2 in the Lin28-let-7 pathway.* Nature, 2013. **497**(7448): p. 244-8.

262. Ustianenko, D., et al., *Mammalian DIS3L2 exoribonuclease targets the uridylated precursors of let-7 miRNAs.* RNA, 2013. **19**(12): p. 1632-8.

263. Loughlin, F.E., et al., *Structural basis of pre-let-7 miRNA recognition by the zinc knuckles of pluripotency factor Lin28.* Nat Struct Mol Biol, 2011. **19**(1): p. 84-9.

264. Nam, Y., et al., *Molecular basis for interaction of let-7 microRNAs with Lin28.* Cell, 2011. **147**(5): p. 1080-91.

265. Cho, J., et al., *LIN28A is a suppressor of ER-associated translation in embryonic stem cells.* Cell, 2012. **151**(4): p. 765-77.

266. Graf, R., et al., *Identification of LIN28B-bound mRNAs reveals features of target recognition and regulation.* RNA Biol, 2013. **10**(7): p. 1146-59.

267. Stefani, G., et al., *A novel mechanism of LIN-28 regulation of let-7 microRNA expression revealed by in vivo HITS-CLIP in C. elegans.* RNA, 2015. **21**(5): p. 985-96.

268. Wilbert, M.L., et al., *LIN28 binds messenger RNAs at GGAGA motifs and regulates splicing factor abundance.* Mol Cell, 2012. **48**(2): p. 195-206.

269. Balzer, E. and E.G. Moss, *Localization of the developmental timing regulator Lin28 to mRNP complexes, P-bodies and stress granules.* RNA Biol, 2007. **4**(1): p. 16-25.

270. Guo, Y., et al., *Identification and characterization of lin-28 homolog B (LIN28B) in human hepatocellular carcinoma.* Gene, 2006. **384**: p. 51-61.

271. Hafner, M., et al., *Identification of mRNAs bound and regulated by human LIN28 proteins and molecular requirements for RNA recognition.* RNA, 2013. **19**(5): p. 613-26.

272. Kawahara, H., et al., *Musashi1 cooperates in abnormal cell lineage protein 28 (Lin28)-mediated let-7 family microRNA biogenesis in early neural differentiation.* J Biol Chem, 2011. **286**(18): p. 16121-30.

273. Kim, S.K., et al., *SET7/9 methylation of the pluripotency factor LIN28A is a nucleolar localization mechanism that blocks let-7 biogenesis in human ESCs.* Cell Stem Cell, 2014. **15**(6): p. 735-49.

274. Vogt, E.J., et al., *Importance of the pluripotency factor LIN28 in the mammalian nucleolus during early embryonic development.* Development, 2012. **139**(24): p. 4514-23.

275. Lehrbach, N.J., et al., *LIN-28 and the poly(U) polymerase PUP-2 regulate let-7 microRNA processing in Caenorhabditis elegans.* Nat Struct Mol Biol, 2009. **16**(10): p. 1016-20.

276. Van Wynsberghe, P.M., et al., *LIN-28 co-transcriptionally binds primary let-7 to regulate miRNA maturation in Caenorhabditis elegans.* Nat Struct Mol Biol, 2011. **18**(3): p. 302-8.

277. Suzuki, H.I., A. Katsura, and K. Miyazono, *A role of uridylation pathway for blockade of let-7 microRNA biogenesis by Lin28B.* Cancer Sci, 2015. **106**(9): p. 1174-81.

278. Triboulet, R., M. Pirouz, and R.I. Gregory, *A Single Let-7 MicroRNA Bypasses LIN28-Mediated Repression.* Cell Rep, 2015. **13**(2): p. 260-6.

279. Nowak, J.S., et al., *Lin28a regulates neuronal differentiation and controls miR-9 production.* Nat Commun, 2014. **5**: p. 3687.

280. Peters, D.T., et al., *Human Lin28 Forms a High-Affinity 1:1 Complex with the 106~363 Cluster miRNA miR-363.* Biochemistry, 2016. **55**(36): p. 5021-7.

281. Rau, F., et al., *Misregulation of miR-1 processing is associated with heart defects in myotonic dystrophy.* Nat Struct Mol Biol, 2011. **18**(7): p. 840-5.

282. Takashima, Y., et al., *Suppression of lethal-7b and miR-125a/b Maturation by Lin28b Enables Maintenance of Stem Cell Properties in Hepatoblasts.* Hepatology, 2016. **64**(1): p. 245-60.

283. Warrander, F., et al., *lin28 proteins promote expression of 17 approximately 92 family miRNAs during amphibian development.* Dev Dyn, 2016. **245**(1): p. 34-46.

284. Polesskaya, A., et al., *Lin-28 binds IGF-2 mRNA and participates in skeletal myogenesis by increasing translation efficiency.* Genes Dev, 2007. **21**(9): p. 1125-38.

285. Peng, S., et al., *Genome-wide studies reveal that Lin28 enhances the translation of genes important for growth and survival of human embryonic stem cells.* Stem Cells, 2011. **29**(3): p. 496-504.

286. Jin, J., et al., *Evidence that Lin28 stimulates translation by recruiting RNA helicase A to polysomes.* Nucleic Acids Res, 2011. **39**(9): p. 3724-34.

287. Qiu, C., et al., *Lin28-mediated post-transcriptional regulation of Oct4 expression in human embryonic stem cells.* Nucleic Acids Res, 2010. **38**(4): p. 1240-8.

288. Shyh-Chang, N., et al., *Lin28 enhances tissue repair by reprogramming cellular metabolism.* Cell, 2013. **155**(4): p. 778-92.

289. Xu, B. and Y. Huang, *Histone H2a mRNA interacts with Lin28 and contains a Lin28-dependent posttranscriptional regulatory element.* Nucleic Acids Res, 2009. **37**(13): p. 4256-63.

290. Zhang, J., et al., *LIN28 Regulates Stem Cell Metabolism and Conversion to Primed Pluripotency.* Cell Stem Cell, 2016. **19**(1): p. 66-80.

291. Lei, X.X., et al., *Determinants of mRNA recognition and translation regulation by Lin28.* Nucleic Acids Res, 2012. **40**(8): p. 3574-84.

292. Yang, J., et al., *LIN28A Modulates Splicing and Gene Expression Programs in Breast Cancer Cells.* Mol Cell Biol, 2015. **35**(18): p. 3225-43.

293. Zeng, Y., et al., *Lin28A Binds Active Promoters and Recruits Tet1 to Regulate Gene Expression.* Mol Cell, 2016. **61**(1): p. 153-60.

294. Tsialikas, J. and J. Romer-Seibert, *LIN28: roles and regulation in development and beyond.* Development, 2015. **142**(14): p. 2397-404.

295. Vadla, B., et al., *lin-28 controls the succession of cell fate choices via two distinct activities.* PLoS Genet, 2012. **8**(3): p. e1002588.

296. Euling, S. and V. Ambros, *Heterochronic genes control cell cycle progress and developmental competence of C. elegans vulva precursor cells.* Cell, 1996. **84**(5): p. 667-76.

297. Faas, L., et al., *Lin28 proteins are required for germ layer specification in Xenopus.* Development, 2013. **140**(5): p. 976-86.

298. Ouchi, Y., J. Yamamoto, and T. Iwamoto, *The heterochronic genes lin-28a and lin-28b play an essential and evolutionarily conserved role in early zebrafish development.* PLoS One, 2014. **9**(2): p. e88086.

299. Stratoulias, V., T.I. Heino, and F. Michon, *Lin-28 regulates oogenesis and muscle formation in Drosophila melanogaster.* PLoS One, 2014. **9**(6): p. e101141.

300. Shinoda, G., et al., *Lin28a regulates germ cell pool size and fertility.* Stem Cells, 2013. **31**(5): p. 1001-9.

301. West, J.A., et al., *A role for Lin28 in primordial germ-cell development and germ-cell malignancy.* Nature, 2009. **460**(7257): p. 909-13.

302. Wulczyn, F.G., et al., *Post-transcriptional regulation of the let-7 microRNA during neural cell specification.* FASEB J, 2007. **21**(2): p. 415-26.

303. Yang, M., et al., *Lin28 promotes the proliferative capacity of neural progenitor cells in brain development.* Development, 2015. **142**(9): p. 1616-27.

304. Balzer, E., et al., *LIN28 alters cell fate succession and acts independently of the let-7 microRNA during neurogliogenesis in vitro.* Development, 2010. **137**(6): p. 891-900.

305. Copley, M.R., et al., *The Lin28b-let-7-Hmga2 axis determines the higher self-renewal potential of fetal haematopoietic stem cells.* Nat Cell Biol, 2013. **15**(8): p. 916-25.

306. Lee, Y.T., et al., *LIN28B-mediated expression of fetal hemoglobin and production of fetal-like erythrocytes from adult human erythroblasts ex vivo.* Blood, 2013. **122**(6): p. 1034-41.

307. Oshima, M., et al., *Ezh2 regulates the Lin28/let-7 pathway to restrict activation of fetal gene signature in adult hematopoietic stem cells.* Exp Hematol, 2016. **44**(4): p. 282-96 e3.

308. Rowe, R.G., et al., *Developmental regulation of myeloerythroid progenitor function by the Lin28b-let-7-Hmga2 axis.* J Exp Med, 2016. **213**(8): p. 1497-512.

309. Wang, L.D., et al., *The role of Lin28b in myeloid and mast cell differentiation and mast cell malignancy.* Leukemia, 2015. **29**(6): p. 1320-30.

310. Yuan, J., et al., *Lin28b reprograms adult bone marrow hematopoietic progenitors to mediate fetal-like lymphopoiesis.* Science, 2012. **335**(6073): p. 1195-200.

311. Urbach, A., et al., *Lin28 sustains early renal progenitors and induces Wilms tumor.* Genes Dev, 2014. **28**(9): p. 971-82.

312. Shinoda, G., et al., *Fetal deficiency of lin28 programs life-long aberrations in growth and glucose metabolism.* Stem Cells, 2013. **31**(8): p. 1563-73.

313. Zhu, H., et al., *Lin28a transgenic mice manifest size and puberty phenotypes identified in human genetic association studies.* Nat Genet, 2010. **42**(7): p. 626-30.

314. Zhu, H., et al., *The Lin28/let-7 axis regulates glucose metabolism.* Cell, 2011. **147**(1): p. 81-94.

315. Corre, C., et al., *Sex-specific regulation of weight and puberty by the Lin28/let-7 axis.* J Endocrinol, 2016. **228**(3): p. 179-91.

316. Xu, B., K. Zhang, and Y. Huang, *Lin28 modulates cell growth and associates with a subset of cell cycle regulator mRNAs in mouse embryonic stem cells.* RNA, 2009. **15**(3): p. 357-61.

317. Parisi, S., et al., *Lin28 is induced in primed embryonic stem cells and regulates let-7-independent events.* FASEB J, 2017. **31**(3): p. 1046-1058.

318. Buganim, Y., et al., *Single-cell expression analyses during cellular reprogramming reveal an early stochastic and a late hierarchic phase.* Cell, 2012. **150**(6): p. 1209-22.

319. Golipour, A., et al., *A late transition in somatic cell reprogramming requires regulators distinct from the pluripotency network.* Cell Stem Cell, 2012. **11**(6): p. 769-82.

320. Hanna, J., et al., *Direct cell reprogramming is a stochastic process amenable to acceleration.* Nature, 2009. **462**(7273): p. 595-601.

321. Ramachandran, R., B.V. Fausett, and D. Goldman, *Ascl1a regulates Muller glia dedifferentiation and retinal regeneration through a Lin-28-dependent, let-7 microRNA signalling pathway.* Nat Cell Biol, 2010. **12**(11): p. 1101-7.

322. Zhou, J., S.B. Ng, and W.J. Chng, *LIN28/LIN28B: an emerging oncogenic driver in cancer stem cells.* Int J Biochem Cell Biol, 2013. **45**(5): p. 973-8.

323. Molenaar, J.J., et al., *LIN28B induces neuroblastoma and enhances MYCN levels via let-7 suppression.* Nat Genet, 2012. **44**(11): p. 1199-206.

324. Beachy, S.H., et al., *Enforced expression of Lin28b leads to impaired T-cell development, release of inflammatory cytokines, and peripheral T-cell lymphoma.* Blood, 2012. **120**(5): p. 1048-59.

325. Madison, B.B., et al., *LIN28B promotes growth and tumorigenesis of the intestinal epithelium via Let-7.* Genes Dev, 2013. **27**(20): p. 2233-45.

326. Tu, H.C., et al., *LIN28 cooperates with WNT signaling to drive invasive intestinal and colorectal adenocarcinoma in mice and humans.* Genes Dev, 2015. **29**(10): p. 1074-86.

327. Nguyen, L.H., et al., *Lin28b is sufficient to drive liver cancer and necessary for its maintenance in murine models.* Cancer Cell, 2014. **26**(2): p. 248-61.

328. Thornton, J.E. and R.I. Gregory, *How does Lin28 let-7 control development and disease?* Trends Cell Biol, 2012. **22**(9): p. 474-82.

329. Chen, C., et al., *IKKbeta Enforces a LIN28B/TCF7L2 Positive Feedback Loop That Promotes Cancer Cell Stemness and Metastasis.* Cancer Res, 2015. **75**(8): p. 1725-35.

330. Dangi-Garimella, S., et al., *Raf kinase inhibitory protein suppresses a metastasis signalling cascade involving LIN28 and let-7.* EMBO J, 2009. **28**(4): p. 347-58.

331. King, C.E., et al., *LIN28B promotes colon cancer progression and metastasis.* Cancer Res, 2011. **71**(12): p. 4260-8.

332. Kugel, S., et al., *SIRT6 Suppresses Pancreatic Cancer through Control of Lin28b.* Cell, 2016. **165**(6): p. 1401-15.

333. Liang, H., et al., *miR-26a suppresses EMT by disrupting the Lin28B/let-7d axis: potential cross-talks among miRNAs in IPF.* J Mol Med (Berl), 2016. **94**(6): p. 655-65.

334. Zhang, W.C., et al., *Glycine decarboxylase activity drives non-small cell lung cancer tumor-initiating cells and tumorigenesis.* Cell, 2012. **148**(1-2): p. 259-72.

335. Boyerinas, B., et al., *Identification of let-7-regulated oncofetal genes.* Cancer Res, 2008. **68**(8): p. 2587-91.

336. Johnson, C.D., et al., *The let-7 microRNA represses cell proliferation pathways in human cells.* Cancer Res, 2007. **67**(16): p. 7713-22.

337. Lee, Y.S. and A. Dutta, *The tumor suppressor microRNA let-7 represses the HMGA2 oncogene.* Genes Dev, 2007. **21**(9): p. 1025-30.

338. Mayr, C., M.T. Hemann, and D.P. Bartel, *Disrupting the pairing between let-7 and Hmga2 enhances oncogenic transformation.* Science, 2007. **315**(5818): p. 1576-9.

339. Powers, J.T., et al., *Multiple mechanisms disrupt the let-7 microRNA family in neuroblastoma.* Nature, 2016. **535**(7611): p. 246-51.

340. Sampson, V.B., et al., *MicroRNA let-7a down-regulates MYC and reverts MYC-induced growth in Burkitt lymphoma cells.* Cancer Res, 2007. **67**(20): p. 9762-70.

341. Thomson, J.M., et al., *Extensive post-transcriptional regulation of microRNAs and its implications for cancer.* Genes Dev, 2006. **20**(16): p. 2202-7.

342. Lightfoot, H.L., E.A. Miska, and S. Balasubramanian, *Identification of small molecule inhibitors of the Lin28-mediated blockage of pre-let-7g processing.* Org Biomol Chem, 2016. **14**(43): p. 10208-10216.

343. Lim, D., et al., *Discovery of a Small-Molecule Inhibitor of Protein-MicroRNA Interaction Using Binding Assay with a Site-Specifically Labeled Lin28.* J Am Chem Soc, 2016.

344. Lin, S. and R.I. Gregory, *Identification of small molecule inhibitors of Zcchc11 TUTase activity.* RNA Biol, 2015. **12**(8): p. 792-800.

345. Roos, M., et al., *A Small-Molecule Inhibitor of Lin28.* ACS Chem Biol, 2016. **11**(10): p. 2773-2781.

346. Li, X., et al., *MiR-181 mediates cell differentiation by interrupting the Lin28 and let-7 feedback circuit.* Cell Death Differ, 2012. **19**(3): p. 378-86.

347. Ma, X., et al., *Lin28/let-7 axis regulates aerobic glycolysis and cancer progression via PDK1.* Nat Commun, 2014. **5**: p. 5212.

348. Shyh-Chang, N., et al., *Human pluripotent stem cells decouple respiration from energy production.* EMBO J, 2011. **30**(24): p. 4851-2.

349. Frost, R.J. and E.N. Olson, *Control of glucose homeostasis and insulin sensitivity by the Let-7 family of microRNAs.* Proc Natl Acad Sci U S A, 2011. **108**(52): p. 21075-80.

350. Gonzales, K.A., et al., *Deterministic Restriction on Pluripotent State Dissolution by Cell-Cycle Pathways.* Cell, 2015. **162**(3): p. 564-79.

351. Shyh-Chang, N., G.Q. Daley, and L.C. Cantley, *Stem cell metabolism in tissue development and aging.* Development, 2013. **140**(12): p. 2535-47.

352. Gilbert, W.V., *Functional specialization of ribosomes?* Trends Biochem Sci, 2011. **36**(3): p. 127-32.

353. Xue, S. and M. Barna, *Specialized ribosomes: a new frontier in gene regulation and organismal biology.* Nat Rev Mol Cell Biol, 2012. **13**(6): p. 355-69.

354. Nguyen, L.H. and H. Zhu, *Lin28 and let-7 in cell metabolism and cancer.* Transl Pediatr, 2015. **4**(1): p. 4-11.

355. Antebi, A., J.G. Culotti, and E.M. Hedgecock, *daf-12 regulates developmental age and the dauer alternative in Caenorhabditis elegans.* Development, 1998. **125**(7): p. 1191-205.

356. Hammell, C.M., X. Karp, and V. Ambros, *A feedback circuit involving let-7-family miRNAs and DAF-12 integrates environmental signals and developmental timing in Caenorhabditis elegans.* Proc Natl Acad Sci U S A, 2009. **106**(44): p. 18668-73.

357. Morita, K. and M. Han, *Multiple mechanisms are involved in regulating the expression of the developmental timing regulator lin-28 in Caenorhabditis elegans.* EMBO J, 2006. **25**(24): p. 5794-804.

358. Bhat-Nakshatri, P., et al., *Estradiol-regulated microRNAs control estradiol response in breast cancer cells.* Nucleic Acids Res, 2009. **37**(14): p. 4850-61.

359. Gehrke, S., et al., *Pathogenic LRRK2 negatively regulates microRNA-mediated translational repression.* Nature, 2010. **466**(7306): p. 637-41.

360. Schulz, C., et al., *Leucine-rich repeat kinase 2 modulates retinoic acid-induced neuronal differentiation of murine embryonic stem cells.* PLoS One, 2011. **6**(6): p. e20820.

361. Marson, A., et al., *Connecting microRNA genes to the core transcriptional regulatory circuitry of embryonic stem cells.* Cell, 2008. **134**(3): p. 521-33.

362. Soufi, A., et al., *Pioneer transcription factors target partial DNA motifs on nucleosomes to initiate reprogramming.* Cell, 2015. **161**(3): p. 555-68.

363. Chang, T.C., et al., *Lin-28B transactivation is necessary for Myc-mediated let-7 repression and proliferation.* Proc Natl Acad Sci U S A, 2009. **106**(9): p. 3384-9.

364. Iliopoulos, D., H.A. Hirsch, and K. Struhl, *An epigenetic switch involving NF-kappaB, Lin28, Let-7 MicroRNA, and IL6 links inflammation to cell transformation.* Cell, 2009. **139**(4): p. 693-706.

365. Zhong, X., et al., *Identification of microRNAs regulating reprogramming factor LIN28 in embryonic stem cells and cancer cells.* J Biol Chem, 2010. **285**(53): p. 41961-71.

366. Kim, C.W., et al., *Ectopic over-expression of tristetraprolin in human cancer cells promotes biogenesis of let-7 by down-regulation of Lin28.* Nucleic Acids Res, 2012. **40**(9): p. 3856-69.

367. Herrera, R.A., K. Kiontke, and D.H. Fitch, *Makorin ortholog LEP-2 regulates LIN-28 stability to promote the juvenile-to-adult transition in Caenorhabditis elegans.* Development, 2016. **143**(5): p. 799-809.

368. Lee, S.H., et al., *The ubiquitin ligase human TRIM71 regulates let-7 microRNA biogenesis via modulation of Lin28B protein.* Biochim Biophys Acta, 2014. **1839**(5): p. 374-86.

369. Wang, L.X., et al., *Reversible acetylation of Lin28 mediated by PCAF and SIRT1.* Biochim Biophys Acta, 2014. **1843**(6): p. 1188-95.

370. Machnicka, M.A., et al., *MODOMICS: a database of RNA modification pathways--2013 update.* Nucleic Acids Res, 2013. **41**(Database issue): p. D262-7.

371. Saletore, Y., et al., *The birth of the Epitranscriptome: deciphering the function of RNA modifications.* Genome Biol, 2012. **13**(10): p. 175.

372. Chang, H., et al., *TAIL-seq: genome-wide determination of poly(A) tail length and 3' end modifications.* Mol Cell, 2014. **53**(6): p. 1044-52.

373. Norbury, C.J., *Cytoplasmic RNA: a case of the tail wagging the dog.* Nat Rev Mol Cell Biol, 2013. **14**(10): p. 643-53.

374. Scheer, H., et al., *Uridylation Earmarks mRNAs for Degradation... and More.* Trends Genet, 2016. **32**(10): p. 607-19.

375. Martin, G. and W. Keller, *RNA-specific ribonucleotidyl transferases.* RNA, 2007. **13**(11): p. 1834-49.

376. Tomecki, R., et al., *Identification of a novel human nuclear-encoded mitochondrial poly(A) polymerase.* Nucleic Acids Res, 2004. **32**(20): p. 6001-14.

377. Wang, L., et al., *A regulatory cytoplasmic poly(A) polymerase in Caenorhabditis elegans.* Nature, 2002. **419**(6904): p. 312-6.

378. Kwak, J.E. and M. Wickens, *A family of poly(U) polymerases.* RNA, 2007. **13**(6): p. 860-7.

379. Rissland, O.S., A. Mikulasova, and C.J. Norbury, *Efficient RNA polyuridylation by noncanonical poly(A) polymerases.* Mol Cell Biol, 2007. **27**(10): p. 3612-24.

380. Calabretta, S. and S. Richard, *Emerging Roles of Disordered Sequences in RNA-Binding Proteins.* Trends Biochem Sci, 2015. **40**(11): p. 662-72.

381. Lunde, B.M., C. Moore, and G. Varani, *RNA-binding proteins: modular design for efficient function.* Nat Rev Mol Cell Biol, 2007. **8**(6): p. 479-90.

382. Aravind, L. and E.V. Koonin, *DNA polymerase beta-like nucleotidyltransferase superfamily: identification of three new families, classification and evolutionary history.* Nucleic Acids Res, 1999. **27**(7): p. 1609-18.

383. Shen, B. and H.M. Goodman, *Uridine addition after microRNA-directed cleavage.* Science, 2004. **306**(5698): p. 997.

384. Xu, K., et al., *MicroRNA-mediated target mRNA cleavage and 3'-uridylation in human cells.* Sci Rep, 2016. **6**: p. 30242.

385. Ren, G., et al., *Methylation protects microRNAs from an AGO1-associated activity that uridylates 5' RNA fragments generated by AGO1 cleavage.* Proc Natl Acad Sci U S A, 2014. **111**(17): p. 6365-70.

386. Marzluff, W.F., E.J. Wagner, and R.J. Duronio, *Metabolism and regulation of canonical histone mRNAs: life without a poly(A) tail.* Nat Rev Genet, 2008. **9**(11): p. 843-54.

387. Tan, D., et al., *Structure of histone mRNA stem-loop, human stem-loop binding protein, and 3'hExo ternary complex.* Science, 2013. **339**(6117): p. 318-21.

388. Meeks-Wagner, D. and L.H. Hartwell, *Normal stoichiometry of histone dimer sets is necessary for high fidelity of mitotic chromosome transmission.* Cell, 1986. **44**(1): p. 43-52.

389. Mullen, T.E. and W.F. Marzluff, *Degradation of histone mRNA requires oligouridylation followed by decapping and simultaneous degradation of the mRNA both 5' to 3' and 3' to 5'.* Genes Dev, 2008. **22**(1): p. 50-65.

390. Hoefig, K.P., et al., *Eri1 degrades the stem-loop of oligouridylated histone mRNAs to induce replication-dependent decay.* Nat Struct Mol Biol, 2013. **20**(1): p. 73-81.

391. Slevin, M.K., et al., *Deep sequencing shows multiple oligouridylations are required for 3' to 5' degradation of histone mRNAs on polyribosomes.* Mol Cell, 2014. **53**(6): p. 1020-30.

392. Lyons, S.M., et al., *The C-terminal extension of Lsm4 interacts directly with the 3′ end of the histone mRNP and is required for efficient histone mRNA degradation.* RNA, 2014. **20**(1): p. 88-102.

393. Su, W., et al., *mRNAs containing the histone 3′ stem-loop are degraded primarily by decapping mediated by oligouridylation of the 3′ end.* RNA, 2013. **19**(1): p. 1-16.

394. Welch, J.D., et al., *EnD-Seq and AppEnD: sequencing 3′ ends to identify nontemplated tails and degradation intermediates.* RNA, 2015. **21**(7): p. 1375-89.

395. Schmidt, M.J., S. West, and C.J. Norbury, *The human cytoplasmic RNA terminal U-transferase ZCCHC11 targets histone mRNAs for degradation.* RNA, 2011. **17**(1): p. 39-44.

396. Lackey, P.E., J.D. Welch, and W.F. Marzluff, *TUT7 catalyzes the uridylation of the 3′ end for rapid degradation of histone mRNA.* RNA, 2016. **22**(11): p. 1673-1688.

397. Morozov, I.Y., et al., *mRNA 3′ tagging is induced by nonsense-mediated decay and promotes ribosome dissociation.* Mol Cell Biol, 2012. **32**(13): p. 2585-95.

398. Morozov, I.Y., et al., *CUCU modification of mRNA promotes decapping and transcript degradation in Aspergillus nidulans.* Mol Cell Biol, 2010. **30**(2): p. 460-9.

399. Rissland, O.S. and C.J. Norbury, *Decapping is preceded by 3′ uridylation in a novel pathway of bulk mRNA turnover.* Nat Struct Mol Biol, 2009. **16**(6): p. 616-23.

400. Sement, F.M., et al., *Uridylation prevents 3′ trimming of oligoadenylated mRNAs.* Nucleic Acids Res, 2013. **41**(14): p. 7115-27.

401. Lim, J., et al., *Uridylation by TUT4 and TUT7 marks mRNA for degradation.* Cell, 2014. **159**(6): p. 1365-76.

402. Faehnle, C.R., J. Walleshauser, and L. Joshua-Tor, *Mechanism of Dis3l2 substrate recognition in the Lin28-let-7 pathway.* Nature, 2014. **514**(7521): p. 252-6.

403. Lubas, M., et al., *Exonuclease hDIS3L2 specifies an exosome-independent 3′-5′ degradation pathway of human cytoplasmic mRNA.* EMBO J, 2013. **32**(13): p. 1855-68.

404. Malecki, M., et al., *The exoribonuclease Dis3L2 defines a novel eukaryotic RNA degradation pathway.* EMBO J, 2013. **32**(13): p. 1842-54.

405. Thomas, M.P., et al., *Apoptosis Triggers Specific, Rapid, and Global mRNA Decay with 3' Uridylated Intermediates Degraded by DIS3L2.* Cell Rep, 2015. **11**(7): p. 1079-89.

406. Zuber, H., et al., *Uridylation and PABP Cooperate to Repair mRNA Deadenylated Ends in Arabidopsis.* Cell Rep, 2016. **14**(11): p. 2707-17.

407. Aphasizheva, I., et al., *Pentatricopeptide repeat proteins stimulate mRNA adenylation/uridylation to activate mitochondrial translation in trypanosomes.* Mol Cell, 2011. **42**(1): p. 106-17.

408. Lapointe, C.P. and M. Wickens, *The nucleic acid-binding domain and translational repression activity of a Xenopus terminal uridylyl transferase.* J Biol Chem, 2013. **288**(28): p. 20723-33.

409. Ochi, H. and K. Chiba, *Hormonal stimulation of starfish oocytes induces partial degradation of the 3' termini of cyclin B mRNAs with oligo(U) tails, followed by poly(A) elongation.* RNA, 2016. **22**(6): p. 822-9.

410. Ameres, S.L. and P.D. Zamore, *Diversifying microRNA sequence and function.* Nat Rev Mol Cell Biol, 2013. **14**(8): p. 475-88.

411. Kim, B., et al., *TUT7 controls the fate of precursor microRNAs by using three different uridylation mechanisms.* EMBO J, 2015. **34**(13): p. 1801-15.

412. Yeom, K.H., et al., *Single-molecule approach to immunoprecipitated protein complexes: insights into miRNA uridylation.* EMBO Rep, 2011. **12**(7): p. 690-6.

413. Newman, M.A., V. Mani, and S.M. Hammond, *Deep sequencing of microRNA precursors reveals extensive 3' end modification.* RNA, 2011. **17**(10): p. 1795-803.

414. Bortolamiol-Becet, D., et al., *Selective Suppression of the Splicing-Mediated MicroRNA Pathway by the Terminal Uridyltransferase Tailor.* Mol Cell, 2015. **59**(2): p. 217-28.

415. Reimao-Pinto, M.M., et al., *Uridylation of RNA Hairpins by Tailor Confines the Emergence of MicroRNAs in Drosophila.* Mol Cell, 2015. **59**(2): p. 203-16.

416. Liu, X., et al., *A MicroRNA precursor surveillance system in quality control of MicroRNA synthesis.* Mol Cell, 2014. **55**(6): p. 868-79.

417. Li, J., et al., *Methylation protects miRNAs and siRNAs from a 3'-end uridylation activity in Arabidopsis.* Curr Biol, 2005. **15**(16): p. 1501-7.

418. Tu, B., et al., *Distinct and cooperative activities of HESO1 and URT1 nucleotidyl transferases in microRNA turnover in Arabidopsis.* PLoS Genet, 2015. **11**(4): p. e1005119.

419. Wang, X., et al., *Synergistic and independent actions of multiple terminal nucleotidyl transferases in the 3' tailing of small RNAs in Arabidopsis.* PLoS Genet, 2015. **11**(4): p. e1005091.

420. Zhao, Y., et al., *The Arabidopsis nucleotidyl transferase HESO1 uridylates unmethylated small RNAs to trigger their degradation.* Curr Biol, 2012. **22**(8): p. 689-94.

421. Dolken, L., et al., *Mouse cytomegalovirus microRNAs dominate the cellular small RNA profile during lytic infection and show features of posttranscriptional regulation.* J Virol, 2007. **81**(24): p. 13771-82.

422. Ibrahim, F., et al., *Uridylation of mature miRNAs and siRNAs by the MUT68 nucleotidyltransferase promotes their degradation in Chlamydomonas.* Proc Natl Acad Sci U S A, 2010. **107**(8): p. 3906-11.

423. Burroughs, A.M., et al., *A comprehensive survey of 3' animal miRNA modification events and a possible role for 3' adenylation in modulating miRNA targeting effectiveness.* Genome Res, 2010. **20**(10): p. 1398-410.

424. Jones, M.R., et al., *Zcchc11 uridylates mature miRNAs to enhance neonatal IGF-1 expression, growth, and survival.* PLoS Genet, 2012. **8**(11): p. e1003105.

425. Jones, M.R., et al., *Zcchc11-dependent uridylation of microRNA directs cytokine expression.* Nat Cell Biol, 2009. **11**(9): p. 1157-63.

426. Thornton, J.E., et al., *Selective microRNA uridylation by Zcchc6 (TUT7) and Zcchc11 (TUT4).* Nucleic Acids Res, 2014. **42**(18): p. 11777-91.

427. Wyman, S.K., et al., *Post-transcriptional generation of miRNA variants by multiple nucleotidyl transferases contributes to miRNA transcriptome complexity.* Genome Res, 2011. **21**(9): p. 1450-61.

428. Ameres, S.L., et al., *Target RNA-directed trimming and tailing of small silencing RNAs.* Science, 2010. **328**(5985): p. 1534-9.

429. Baccarini, A., et al., *Kinetic analysis reveals the fate of a microRNA following target regulation in mammalian cells.* Curr Biol, 2011. **21**(5): p. 369-76.

430. Haas, G., et al., *Identification of factors involved in target RNA-directed microRNA degradation.* Nucleic Acids Res, 2016. **44**(6): p. 2873-87.

431. Read, R.L., et al., *Cytoplasmic poly(A) polymerases mediate cellular responses to S phase arrest.* Proc Natl Acad Sci U S A, 2002. **99**(19): p. 12079-84.

432. Rissland, O.S. and C.J. Norbury, *The Cid1 poly(U) polymerase.* Biochim Biophys Acta, 2008. **1779**(4): p. 286-94.

433. Wang, S.W., et al., *Cid1, a fission yeast protein required for S-M checkpoint control when DNA polymerase delta or epsilon is inactivated.* Mol Cell Biol, 2000. **20**(9): p. 3234-44.

434. Blahna, M.T., et al., *Terminal uridyltransferase enzyme Zcchc11 promotes cell proliferation independent of its uridyltransferase activity.* J Biol Chem, 2011. **286**(49): p. 42381-9.

435. Astuti, D., et al., *Germline mutations in DIS3L2 cause the Perlman syndrome of overgrowth and Wilms tumor susceptibility.* Nat Genet, 2012. **44**(3): p. 277-84.

436. Pirouz, M., et al., *Dis3l2-Mediated Decay Is a Quality Control Pathway for Noncoding RNAs.* Cell Rep, 2016. **16**(7): p. 1861-73.

437. Ustianenko, D., et al., *TUT-DIS3L2 is a mammalian surveillance pathway for aberrant structured non-coding RNAs.* EMBO J, 2016. **35**(20): p. 2179-2191.

438. Zhou, X., et al., *RdRP-synthesized antisense ribosomal siRNAs silence pre-rRNA via the nuclear RNAi pathway.* Nat Struct Mol Biol, 2017. **24**(3): p. 258-269.

439. Fu, X., et al., *miR-26a enhances miRNA biogenesis by targeting Lin28B and Zcchc11 to suppress tumor growth and metastasis.* Oncogene, 2014. **33**(34): p. 4296-306.

440. Lin, C.J., et al., *Characterization of a TUTase/RNase complex required for Drosophila gametogenesis.* RNA, 2017. **23**(3): p. 284-296.

441. Tsanov, K.M. and G.Q. Daley, *Signaling through RNA-binding proteins as a cell fate regulatory mechanism.* Cell Cycle, 2017: p. 0.

442. Ng, H.H. and M.A. Surani, *The transcriptional and signalling networks of pluripotency.* Nat Cell Biol, 2011. **13**(5): p. 490-6.

443. Kunath, T., et al., *FGF stimulation of the Erk1/2 signalling cascade triggers transition of pluripotent embryonic stem cells from self-renewal to lineage commitment.* Development, 2007. **134**(16): p. 2895-902.

444. Rigbolt, K.T., et al., *System-wide temporal characterization of the proteome and phosphoproteome of human embryonic stem cell differentiation.* Sci Signal, 2011. **4**(164): p. rs3.

445. Van Hoof, D., et al., *Phosphorylation dynamics during early differentiation of human embryonic stem cells.* Cell Stem Cell, 2009. **5**(2): p. 214-26.

446. Mansour, S.J., et al., *Transformation of mammalian cells by constitutively active MAP kinase kinase.* Science, 1994. **265**(5174): p. 966-70.

447. Cai, N., et al., *Post-translational modulation of pluripotency.* J Mol Cell Biol, 2012. **4**(4): p. 262-5.

448. Kwon, S.C., et al., *The RNA-binding protein repertoire of embryonic stem cells.* Nat Struct Mol Biol, 2013. **20**(9): p. 1122-30.

449. Morgenstern, J.P. and H. Land, *Advanced mammalian gene transfer: high titre retroviral vectors with multiple drug selection markers and a complementary helper-free packaging cell line.* Nucleic Acids Res, 1990. **18**(12): p. 3587-96.

450. Eggan, K., et al., *Hybrid vigor, fetal overgrowth, and viability of mice derived by nuclear cloning and tetraploid embryo complementation.* Proc Natl Acad Sci U S A, 2001. **98**(11): p. 6209-14.

451. Khandelia, P., K. Yap, and E.V. Makeyev, *Streamlined platform for short hairpin RNA interference and transgenesis in cultured mammalian cells.* Proc Natl Acad Sci U S A, 2011. **108**(31): p. 12799-804.

452. Villen, J. and S.P. Gygi, *The SCX/IMAC enrichment approach for global phosphorylation analysis by mass spectrometry.* Nat Protoc, 2008. **3**(10): p. 1630-8.

453. Beausoleil, S.A., et al., *A probability-based approach for high-throughput protein phosphorylation analysis and site localization.* Nat Biotechnol, 2006. **24**(10): p. 1285-92.

454. Trapnell, C., et al., *Differential gene and transcript expression analysis of RNA-seq experiments with TopHat and Cufflinks.* Nat Protoc, 2012. **7**(3): p. 562-78.

455. Anders, S., P.T. Pyl, and W. Huber, *HTSeq--a Python framework to work with high-throughput sequencing data.* Bioinformatics, 2015. **31**(2): p. 166-9.

456. Tsanov, K.M., et al., *LIN28 phosphorylation by MAPK/ERK couples signalling to the post-transcriptional control of pluripotency.* Nat Cell Biol, 2017. **19**(1): p. 60-67.

457. Bradner, J.E., D. Hnisz, and R.A. Young, *Transcriptional Addiction in Cancer.* Cell, 2017. **168**(4): p. 629-643.

458. Khabar, K.S., *Hallmarks of cancer and AU-rich elements.* Wiley Interdiscip Rev RNA, 2017. **8**(1).

459. Lindeboom, R.G., F. Supek, and B. Lehner, *The rules and impact of nonsense-mediated mRNA decay in human cancers.* Nat Genet, 2016. **48**(10): p. 1112-8.

460. Cummins, J.M., et al., *The colorectal microRNAome.* Proc Natl Acad Sci U S A, 2006. **103**(10): p. 3687-92.

461. Blau, H.M., C.P. Chiu, and C. Webster, *Cytoplasmic activation of human nuclear genes in stable heterocaryons.* Cell, 1983. **32**(4): p. 1171-80.

462. Beard, C., et al., *Efficient method to generate single-copy transgenic mice by site-specific integration in embryonic stem cells.* Genesis, 2006. **44**(1): p. 23-8.

463. Ran, F.A., et al., *Genome engineering using the CRISPR-Cas9 system.* Nat Protoc, 2013. **8**(11): p. 2281-308.

464. Sanjana, N.E., O. Shalem, and F. Zhang, *Improved vectors and genome-wide libraries for CRISPR screening.* Nat Methods, 2014. **11**(8): p. 783-4.

465. Reya, T., et al., *A role for Wnt signalling in self-renewal of haematopoietic stem cells.* Nature, 2003. **423**(6938): p. 409-14.

466. Shalem, O., et al., *Genome-scale CRISPR-Cas9 knockout screening in human cells.* Science, 2014. **343**(6166): p. 84-7.

467. Osborne, J.K., et al., *NeuroD1 regulates survival and migration of neuroendocrine lung carcinomas via signaling molecules TrkB and NCAM.* Proc Natl Acad Sci U S A, 2013. **110**(16): p. 6524-9.

468. Huang da, W., B.T. Sherman, and R.A. Lempicki, *Bioinformatics enrichment tools: paths toward the comprehensive functional analysis of large gene lists.* Nucleic Acids Res, 2009. **37**(1): p. 1-13.

469. Huang da, W., B.T. Sherman, and R.A. Lempicki, *Systematic and integrative analysis of large gene lists using DAVID bioinformatics resources.* Nat Protoc, 2009. **4**(1): p. 44-57.

470. Perrimon, N., C. Pitsouli, and B.Z. Shilo, *Signaling mechanisms controlling cell fate and embryonic patterning.* Cold Spring Harb Perspect Biol, 2012. **4**(8): p. a005975.

471. Meszaros, B., et al., *Degrons in cancer.* Sci Signal, 2017. **10**(470).

472. Garcia-Martinez, J., et al., *The cellular growth rate controls overall mRNA turnover, and modulates either transcription or degradation rates of particular gene regulons.* Nucleic Acids Res, 2016. **44**(8): p. 3643-58.

473. Yang, M. and K.H. Vousden, *Serine and one-carbon metabolism in cancer.* Nat Rev Cancer, 2016. **16**(10): p. 650-62.

474. Defoiche, J., et al., *Measurement of ribosomal RNA turnover in vivo by use of deuterium-labeled glucose.* Clin Chem, 2009. **55**(10): p. 1824-33.

475. Waalkes, T.P., S.R. Dinsmore, and J.E. Mrochek, *Urinary excretion by cancer patients of the nucleosides N-dimethylguanosine, 1-methylinosine, and pseudouridine.* J Natl Cancer Inst, 1973. **51**(1): p. 271-4.

476. Waalkes, T.P., et al., *The urinary excretion of nucleosides of ribonucleic acid by patients with advanced cancer.* Cancer, 1975. **36**(2): p. 390-8.

477. Adams, J., *The development of proteasome inhibitors as anticancer drugs.* Cancer Cell, 2004. **5**(5): p. 417-21.

478. Pritchard, D.M., et al., *Inhibition by uridine but not thymidine of p53-dependent intestinal apoptosis initiated by 5-fluorouracil: evidence for the involvement of RNA perturbation.* Proc Natl Acad Sci U S A, 1997. **94**(5): p. 1795-9.

479. Kammler, S., S. Lykke-Andersen, and T.H. Jensen, *The RNA exosome component hRrp6 is a target for 5-fluorouracil in human cells.* Mol Cancer Res, 2008. **6**(6): p. 990-5.

480. Silverstein, R.A., E. Gonzalez de Valdivia, and N. Visa, *The incorporation of 5-fluorouracil into RNA affects the ribonucleolytic activity of the exosome subunit Rrp6.* Mol Cancer Res, 2011. **9**(3): p. 332-40.

481. Herrero, A.B. and S. Moreno, *Lsm1 promotes genomic stability by controlling histone mRNA decay.* EMBO J, 2011. **30**(10): p. 2008-18.

482. Singh, R.K., et al., *Excess histone levels mediate cytotoxicity via multiple mechanisms.* Cell Cycle, 2010. **9**(20): p. 4236-44.

483. Batista, P.J., et al., *m(6)A RNA modification controls cell fate transition in mammalian embryonic stem cells.* Cell Stem Cell, 2014. **15**(6): p. 707-19.

484. Geula, S., et al., *Stem cells. m6A mRNA methylation facilitates resolution of naive pluripotency toward differentiation.* Science, 2015. **347**(6225): p. 1002-6.

485. Wang, Y., et al., *N6-methyladenosine modification destabilizes developmental regulators in embryonic stem cells.* Nat Cell Biol, 2014. **16**(2): p. 191-8.

486. Song, J., et al., *Uridylation and adenylation of RNAs.* Sci China Life Sci, 2015. **58**(11): p. 1057-66.

487. Wurtmann, E.J. and S.L. Wolin, *RNA under attack: cellular handling of RNA damage.* Crit Rev Biochem Mol Biol, 2009. **44**(1): p. 34-49.

488. Choudhury, N.R., et al., *Trim25 Is an RNA-Specific Activator of Lin28a/TuT4-Mediated Uridylation.* Cell Rep, 2014. **9**(4): p. 1265-72.